CHEMICAL REVIEWS

REVIEW

pubs.acs.org/CR

Core/Shell Nanoparticles: Classes, Properties, Synthesis Mechanisms, Characterization, and Applications

Rajib Ghosh Chaudhuri and Santanu Paria*

Department of Chemical Engineering, National Institute of Technology, Rourkela 769 008, Orissa, India

CONTENTS

1. INTRODUCTION

Nanomaterials have, by definition, one or more dimension in the nanometer scale ($\leq$100 nm) range and subsequently show novel properties from their bulk materials. The synthesis, characterization, and applications of nanoparticles are among the most important sections of the wide range of nanotechnology areas falling under the general "nanotechnology" umbrella. In recent years, nanoparticles have been the center of attention of researchers in the field as the transition from microparticles to nanoparticles was seen to lead to immense changes in the physical and chemical properties of a material. The most important characteristics, among many others, on a nanoscale are as follows: First, the small size of the particles, which leads to

Received: December 23, 2010
Published: December 28, 2011

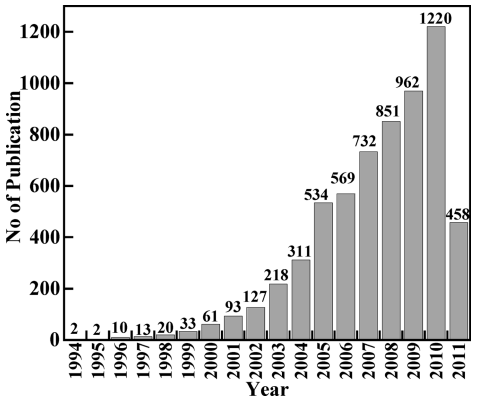

Figure 1. Publications per year for core/shell nanoparticles during the period 1994 to May 2011 (Data collected from SciFinder Scholar Database).

an increased surface area to volume ratio and as a result the domain where quantum effects predominate is entered. Second, the increasing surface area to volume ratio leads to an increase in the dominance of the surface atoms of the nanoparticle over those in its interior.

The synthesis of nanoparticles is a complex process and hence there is a wide range of techniques available for producing different kinds of nanoparticles. The result is that it is impossible to generalize all the synthesis techniques currently available. However, broadly these all techniques essentially fall into three categories: (i) condensation from vapor, (ii) synthesis by chemical reaction, and (iii) solid-state processes such as milling. By using the above-mentioned techniques, not only pure nanoparticles but also hybrid or coated nanoparticles (with hydrophilic or hydrophobic materials depending on the suitability of the applications) can be synthesized.

Initially researchers studied single nanoparticles because such particles have much better properties than the bulk materials. Later, in the late 1980s, researchers found that heterogeneous, composite or sandwich colloidal semiconductor particles have better efficiency than their corresponding single particles; in some cases they even develop some new properties.[1−3] More recently during the early 1990s, researchers synthesized concentric multilayer semiconductor nanoparticles with the view to improving the property of such semiconductor materials. Hence subsequently the terminology "core/shell" was adopted.[4−6] Furthermore, there has been a gradual increase in research activity because of the tremendous demand for more and more advanced materials fueled by the demands of modern technology. Simultaneously the advancement of characterization techniques has also greatly helped to establish the structures of these different core/shell nanostructures. A statistical data analysis is presented in Figure 1 to show the increasing trend of published research papers in this area. These were collected in May 2011 from "Scifinder Scholar" using the keyword "core/shell nanoparticle".

1.1. Different Shaped Nanoparticles

The advances in new synthesis techniques make it possible to synthesize not only the symmetrical (spherical) shape nanoparticles but also a variety of other shapes such as cube,[7−14] prism,[15,16] hexagon,[7,8,17−20] octahedron,[11,12] disk,[21] wire,[22−29] rod,[22,30−37] tube,[22,38−41] etc.

It is worth noting that most of the studies regarding different shaped nanoparticles are in fact recent. Just as for the simple

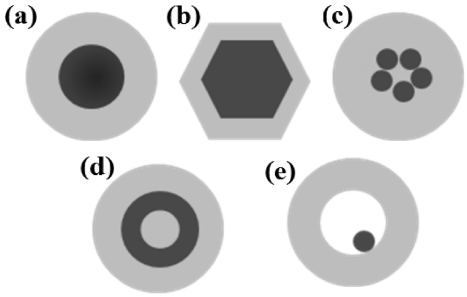

Figure 2. Different core/shell nanoparticles: (a) spherical core/shell nanoparticles; (b) hexagonal core/shell nanoparticles; (c) multiple small core materials coated by single shell material; (d) nanomatryushka material; (e) movable core within hollow shell material.

nonspherical nanoparticles, different shaped core/shell nanoparticles are also highly achievable as reported in some very recent articles.[42−46] The properties of nanoparticles are not only size dependent but are also linked with the actual shape. For example, certain properties of magnetic nanocrystals such as the blocking temperature, magnetic saturation, and permanent magnetization are all dependent on particle size, but the coercivity of the nanocrystals totally depends on the particle shape because of surface anisotropy effects.[9,47] Different shaped magnetic nanocrystals possess tremendous potential in helping our fundamental understanding of not only magnetism but also technological applications in the field such as high-density information storage.[9] Other nanoparticle physical and chemical properties such as catalytic activity and selectivity,[12,48−50] electrical[51,52] and optical properties,[53,54] and melting point[55] are also all highly shape-dependent. In addition, other properties such as sensitivity to surface-enhanced Raman scattering (SERS) and the plasmon resonance features of gold or silver particles also depend on the particle morphology.[56]

1.2. Classes of Core/Shell Nanoparticles

Nanoparticles can be categorized based on single or multiple materials into simple and core/shell or composite nanoparticles. In general, simple nanoparticles are made from a single material; whereas, as the name implies, composite and core/shell particles are composed of two or more materials. The core/shell type nanoparticles can be broadly defined as comprising a core (inner material) and a shell (outer layer material). These can consist of a wide range of different combinations in close interaction, including inorganic/inorganic, inorganic/organic, organic/inorganic, and organic/organic materials. The choice of shell material of the core/shell nanoparticle is generally strongly dependent on the end application and use.

Different classes of core/shell nanoparticles are shown schematically in Figure 2. Concentric spherical core/shell nanoparticles are the most common (Figure 2a) where a simple spherical core particle is completely coated by a shell of a different material. Different shaped core/shell nanoparticles have also given rise to immense research interest because of their different novel properties. Different shaped core/shell nanoparticles are generally formed when a core is nonspherical as shown in Figure 2b. Multiple core core/shell particles are formed when a single shell material is coated onto many small core particles together as shown in Figure 2c. Concentric nanoshells of alternative coating of dielectric core and metal shell material onto each other (A/B/A type) are shown in Figure 2d. Here nanoscale dielectric spacer

layers separate the concentric metallic layers These types of particles are also known as multilayered metallodielectric nanostructures or nanomatryushka and are mainly important for their plasmonic properties.[57−60] It is also possible to synthesize a moveable core particle within a uniformed hollow shell particle (Figure 2e) after a bilayer coating of the core material and just removing the first layer by using a suitable technique.

1.3. Approaches for Core/Shell Nanoparticle Synthesis

Approches for nanomaterial synthesis can be broadly divided into two categories: "top-down" and "bottom-up". The "top-down" approach often uses traditional workshop or microfabrication methods where externally controlled tools are used to cut, mill, and shape materials into the desired shape and order. For example, the most common techniques are lithographic techniques (e.g., UV, electron or ion beam, scanning probe, optical near field),[61−63] laser-beam processing,[64] and mechanical techniques (e.g., machining, grinding, and polishing).[65−68] "Bottom-up" approaches, on the other hand, exploit the chemical properties of the molecules to cause them to self-assemble into some useful conformation. The most common bottom-up approaches are chemical synthesis, chemical vapor deposition, laser-induced assembly (i.e., laser tapping), self-assembly, colloidal aggregation, film deposition and growth,[69−71] etc. Currently neither the top-down nor bottom-up approach is superior; each has its advantages and disadvantages. However, the bottom-up approach can produce much smaller sized particles and has the potential to be more cost-effective in the future because of the advantages of absolute precision, complete control over the process, and minimum energy loss compared with that of a top-down approach. Where the synthesis of core/shell nanoparticles is concerned, since ultimate control is required for achieving a uniform coating of the shell materials during the particle formation, the bottom-up approach has proven more suitable. A combination of the two approaches can also be utilized, such as core particles synthesized by the top-down approach but then coated by a bottom-up approach in order to maintain uniform and precise shell thickness. To control the overall size and shell thickness precisely, instead of employing a bulk medium using a microemulsion is preferable because water droplets act as a template or nanoreactor.

1.4. Importance of Core/Shell Nanoparticles

Core/shell nanoparticles are gradually attracting more and more attention, since these nanoparticles have emerged at the frontier between materials chemistry and many other fields, such as electronics, biomedical, pharmaceutical, optics, and catalysis. Core/shell nanoparticles are highly functional materials with modified properties. Sometimes properties arising from either core or shell materials can be quite different. The properties can be modified by changing either the constituting materials or the core to shell ratio.[72] Because of the shell material coating, the properties of the core particle such as reactivity decrease or thermal stability can be modified, so that the overall particle stability and dispersibility of the core particle increases. Ultimately, particles show distinctive properties of the different materials employed together. This is especially true of the inherent ability to manipulate the surface functions to meet the diverse application requirements.[73,74] The purpose of the coating on the core particle are many fold, such as surface modification, the ability to increase the functionality, stability, and dispersibility, controlled release of the core, reduction in consumption of precious materials, and so on.

Current applications of different core/shell nanoparticles are summarized in a review article by Karele et al.[75] The individual reports from different researchers also demonstrates the fact that core/shell nanoparticles are widely used in different applications such as biomedical[76−79] and pharmaceutical applications,[74] catalysis,[73,80] electronics,[4,81,82] enhancing photoluminescence,[83−85] creating photonic crystals,[86] etc. In particular in the biomedical field, the majority of these particles are used for bioimaging,[78,87−93] controlled drug release,[93,94] targeted drug delivery,[78,90,93−95] cell labeling,[78,96,97] and tissue engineering applications.[94,98]

In addition to the improved material properties, core/shell materials are also important from an economic point of view. A precious material can be coated over an inexpensive material to reduce the consumption of the precious material compared with making the same sized pure material. Core/shell nanoparticles are also used as a template for the preparation of hollow particles after removing the core either by dissolution or calcination. Nano- and microsized hollow particles are used for different purposes such as microvessels, catalytic supports,[99] adsorbents,[100] lightweight structural materials,[101,102] and thermal and electric insulators.[103]

1.5. Scope of This Review

Reviews play an important role in keeping interested parties up to date on the current state of the research in any academic field. This review aims to focus on the development of the five different aspects of core/shell nanoparticles. These are (i) classes, (ii) properties, (iii) synthesis mechanisms, (iv) characterization techniques, and (v) core/shell nanoparticle applications. Since core/shell nanoparticle synthesis and its applications are relevant emerging research areas in nanotechnology, over the last 2 decades different research groups have synthesized and studied the properties and applications of these different core/shell nanoparticles.

To date some researchers have also published some reviews as well as book chapters[104] in this field mainly highlighting some specific material properties such as Au/polymer,[105] polymer/silica,[106] silica/biomolecules,[107] organic/inorganic,[108] organic/organic,[74] organic coated core/shell,[109] magnetic,[90,110] semiconductor,[111,112] etc. or applications of some specific core/shell particles.[113] Finally, keeping in mind the importance of advanced materials in today's world, it is hoped that there is still a strong demand for an extensive review with updated literature on core/shell nanoparticles.

2. CLASSIFICATION OF CORE/SHELL NANOPARTICLES

There are large varieties of core/shell nanoparticles available so far with a wide range of applications. As a result, the classification of all the available core/shell nanoparticles, which depends on their industrial applications or is based on some other property, is a challanging task. In this review, we attempt to classify the core/shell nanoparticles depending on their material properties. In a broad sense, clearly the core or shell materials in a core/shell particle are either made of inorganic or organic materials. Depending on their material properties, the core/shell nanoparticles can be classified into four main different groups: (i) inorganic/inorganic; (ii) inorganic/organic; (iii) organic/inorganic; (iv) Organic/organic.

2.1. Inorganic/Inorganic Core/Shell Nanoparticles

Inorganic/inorganic core/shell nanoparticles are the most important class of all the different types of core/shell nanoparticles.

Table 1. Class 1 Inorganic/Inorganic (Silica) Core/Shell Nanoparticles and Class II Inorganic/Inorganic (Nonsilica) Core/Shell Nanoparticles[a]

	synthesis techniques and reagents used				
	core		shell		
core/shell	method	basic reagent	method	basic reagent	ref
Class I: Inorganic/Inorganic (Silica) Core/Shell Nanoparticles					
Metal Core					
Au/SiO_2	reduction by citric acid	$HAuCl_4$	sol−gel	TEOS	114,115
	reduction by $NaBH_4$	$HAuCl_4$	sol−gel	TEOS	116,117
	reduction by sodium citrate	$HAuCl_4$	hydrolysis	Na_2SiO_3	118,119
		gold sol	sol−gel	TEOS	120
	reduction by sodium citrate	$HAuCl_4$		SiO_2	121
	reduction by sodium citrate	$HAuCl_4$	hydrolysis	TEOS	122
Ag/SiO_2	reduction by N_2H_4	$AgNO_3$	Stöber method	TEOS	123
	reduction by $NaBH_4$	$AgClO_4$	hydrolysis	Na_2SiO_3	124
	reduction by glycol	$AgNO_3$	sol−gel	TEOS	115
	reduction by sodium oleate.	$AgNO_3$	Stöber method	TEOS	125
Ni/SiO_2	WEE	Ni wire	Stöber method	TEOS	126
Ni/SiO_2	reduction by citric acid	$NiCl_2 \cdot 6H_2O$	Stöber method	TEOS	127
Fe/SiO_2		Fe powder	Stöber method	TEOS	128
Fe/SiO_2		Fe powder		SiO_2 powder	129
Co/SiO_2	cryogenic melting method	Co metal	Stöber method	TEOS	130
	hydrolysis	$CoCl_2$, PEG	control hydrolysis	Na_2SiO_3	131
$FeNi/SiO_2$	cryogenic melting method	Fe, Ni metal	Stöber method	TEOS	130
Metal Oxide Core					
Fe_3O_4/SiO_2	wet chemical reaction	$FeCl_3$, N_2H_4	sol−gel	TEOS	132
	wet chemical reaction	$FeCl_3$, $FeSO_4$	hydrolysis	Na_2SiO_3	133
	wet chemical reaction	$FeCl_3$, $FeSO_4$,		commercial SiO_2	134
	TD	$Fe(C_5H_7O_2)_3$	sol−gel	TEOS	135
	chemical reaction in microemulsion	$FeCl_3$, $FeSO_4$,	sol−gel reaction in microemulsion	TEOS	136
ZnO/SiO_2	precipitation	$Zn(CH_3COO)_2$ $2H_2O$	hydrolysis	TEOS	137
Metal Chalcogenide and Metal Salt Core					
CdS/SiO_2	precipitation in microemulsion	$Cd(NO_3)_2$, $(NH_4)_2S$	sol−gel method in microemulsion	TEOS	138
	precipitation in microemulsion	$Cd(NO_3)_2$, $(NH_4)_2S$		silica	121
	precipitation in microemulsion	$Cd(NO_3)_2$, $(NH_4)_2S$	hydrolysis	MPTMS	139
AgI/SiO_2	precipitation	$AgClO_4$, KI	Stöber method	MPTMS	140
$CdTe/SiO_2$	precipitation	$Cd(ClO_4)_2$, NaHTe	hydrolysis	Na_2SiO_3	141
$CdSe/SiO_2$	precipitation	$Cd(ClO_4)_2$, *N*,*N*-dimethylselenourea	hydrolysis	Na_2SiO_3	141
$CdSe/CdS/SiO_2$	precipitation	$Cd(ClO_4)_2$, M *N*, *N*-dimethylselenourea	hydrolysis	Na_2SiO_3	141,142
$CdSe/ZnS/SiO_2$	precipitation	$(CH_3)_2Cd$, $(TMS)_2S$, $(TMS)_2Se$, TOPO	hydrolysis	(trihydroxysilyl)propyl methylphosphonate	143

dx.doi.org/10.1021/cr100449n |*Chem. Rev.* 2012, 112, 2373–2433

Table 1. Continued

	synthesis techniques and reagents used				
	core		shell		
core/shell	method	basic reagent	method	basic reagent	ref
$ZnS:Mn/SiO_2$	precipitation	$Zn(CH_3COO)_2$ $2H_2O$, $Mn(CH_3COO)_2$ $4H_2O$, Na_2S	sol−gel method in microemulsion	TEOS	144
$ZnS:Mn/SiO_2$		ZnS:Mn	alkaline hydrolysis	Na_2SiO_3	145
$CaCO_3/SiO_2$		$Ca(OH)_2$, CO_2	hydrolysis	Na_2SiO_3	145,146
$Gd_2O_3:Tm^{3+}/SiO_2$	hydrolysis with calcination	$Tm(NO_3)_3 \cdot 6H_2O$, $Gd(NO_3)_3 \cdot 6H_2O$	sol−gel method in microemulsion	TEOS	147
Yb^{3+}/SiO_2	hydrolysis with calcination	$Yb(NO_3)_3 \cdot 6H_2O$	sol−gel method in microemulsion	TEOS	147
$Zn_2SiO_4:Eu^{3+}/SiO_2$	hydrolysis with precipitation	$Zn(O_2C_2H_3)_2 \cdot 2H_2O$, $EuCl_3 \cdot 6H_2O$, TEOS	Pechini sol−gel process	TEOS	148
		Class II: Inorganic/Inorganic (Nonsilica) Core/Shell Nanoparticles			
		Metal Core			
Au/Ag	reduction by β-cyclodextrin	$HAuCl_4$	reduction by β-cyclodextrin	$AgNO_3$	149
Au/Co	reduction by sodium citrate	$HAuCl_4$	reduction by N_2H_4, H_2O	$CoCl_2$	150
Au/Pt	reduction by sodium citrate	$HAuCl_4$	electrochemical method	Pt metal	151
Au/Pt	reduction by sodium citrate	$HAuCl_4$	reduction by ascorbic acid	H_2PtCl_6	152,153
Au/Pd	reduction by sodium citrate	$HAuCl_4$	HCl treatment and reduction by ascorbic acid	$PdCl_2$	154
Au/Pd	reduction by CTAC	$HAuCl_4$	reduction by CTAC	K_2PdCl_4	155,156
Au/Pd	reduction by $NaBH_4$	$HAuCl_4$	reduction by $NaBH_4$	$PdCl_2$	157
Au/TiO_2	reduction by sodium citrate in the presence of PVP	$HAuCl_4$	reflux at high temperature	TBOT	158
Au/Fe_2O_3	reduction by $NaBH_4$	$HAuCl_4$	TD	$Fe(CO)_5$	159
Au/CdSe	reduction by N_2H_4, H_2O in microemulsion	$HAuCl_4$	reduction of by N_2H_4 in AOT microemulsion	$HAuCl_4$, $CdCl_2$, Se powder	160
Au/CuI	reduction by $NaBH_4$	$HAuCl_4$	electrochemical deposition with solid state precipitation	$CuSO_4$, H_2SO_4, KI	161
Au/CdS	reduction by $NaBH_4$	$HAuCl_4$	electrochemical deposition with solid state precipitation	$CdSO_4$, Na_2S	161
Au/C	reduction	$HAuCl_4$	TD	glucose	162
Ni/Ag	reduction by $NaBH_4$ in microemulsion	$Ni(NO_3)_2$	reduction by $NaBH_4$ in microemulsion	$AgNO_3$	163
Fe/Ag	reduction by $LiBEt_3H$	$FeCl_2$	reduction in organic media	$AgNO_3$	164
Ni/Pt	reduction by $NaBH_4$	$Ni(CH_3COO)_2$	reduction by $NaBH_4$ and N_2H_4	$H_2PtCl_4 \cdot 6H_2O$	165
Fe,Cu/ Au, Pt, Pd, Ag	reduction by vitamin C	$Fe(NO_3)_3 \cdot 9H_2O$, $CuCl_2$	reduction by vitamin C	$Na_2PtCl_6 \cdot 6H_2O$, $HAuCl_4 \cdot 3H_2O$, $AgNO_3$, $PdCl_2$	166
Co/Au, Pd, Pt, Cu	hydrothermal decomposition	$Co_2(CO)_8$	reduction transmetalation	Au precoursor $Pd(hfac)_2$, $Pt(hfac)_2$, $Cu(hfac)_2$	167

dx.doi.org/10.1021/cr100449n |*Chem. Rev.* 2012, 112, 2373–2433

Table 1. Continued

	synthesis techniques and reagents used				
	core		shell		
core/shell	method	basic reagent	method	basic reagent	ref
Fe/Pt	reduction by $NaBH_4$	$FeSO_4$	reduction transmetalation	K_2PtCl_4	168
Ag/C	reduction	$AgNO_3$	TD	glucose	169
Fe/C	reduction with CVD	Fe_3O_4		carbon	170
Fe/C	microwave treatment	ferrocene, silicon wafer	microwave treatment	ferrocene	171−173
Ni/C	TD	$Ni(C_5H_7O_2)_2$	TD	$Ni(C_5H_7O_2)_2$	172
Ag/Ag_2Se	reduction by sodium citrate	$AgNO_3$	TD with precipitation	KNCSe, $AgNO_3$,	174
Pd/PdO	SMAD method	Pd foil	partial oxidation in air	core Pd	175
Co/CdSe	high-temperature TD	$Co_2(CO)_8$	precipitation	$Cd(CH_3)_2$, Se	176
Cu/Cu_2O	WEE	Cu wire	oxidation	Cu	177
Au/CdS	reduction by sodium citrate.	$HAuCl_4$	precipitation	$Cd(NO_3)_2$, H_2S	85
FePt/CdS	TD with reduction	$Fe(CO)_5$, $Pt(C_5H_7O_2)_2$	precipitation	sulfur, $Cd(C_5H_7O_2)_2$	178
$Fe_{58}Pt_{42}/Fe_3O_4$	reduction with TD	$Pt(C_5H_7O_2)_2$, $Fe(CO)_5$	TD	$Fe(C_5H_7O_2)_3$, 1,2-hexadecanediol, oleic acid, oleylamine	179
Zn/ZnO		Zn powder	oxidation	Zn powder	180
		Nonmetallic Core			
C/Au	hydrothermal degradation	glucose	reduction	$HAuCl_4$	162
CNT/SnO_2		multiwalled CNTs	hydrolysis in acid media	$SnCl_2$	181
		Metal Oxide Core			
Fe_3O_4/Au	solvothermal method	$Fe(C_5H_7O_2)_3$, phenyl ether, OA, oleylamine	hydrolysis with TD	$Au(OOCCH_3)_3$, 1,2-hexadecanediol, OA, oleylamine	182
Fe_3O_4/Au	solvothermal method	$FeCl_3 \cdot 6H_2O$, sodium acrylate, CH_3COONa	reduction by $Na_3C_6H_5O_7$, $NaBH_4$.	$HAuCl_4$	183
Fe_3O_4/Au	wet chemical reaction	$FeCl_3$	reduction by $NaBH_4$	$HAuCl_4$	184
$Fe_3O_4/SiO_2/Al_2O_3$	wet chemical reaction	$FeCl_3$, $FeSO_4$	sol−gel method with precipitation	TEOS	133
$Fe_3O_4/SiO_2/TiO_2$	wet chemical reaction	$FeCl_3$, $FeSO_4$	sol−gel method	TEOS, TBOT	133
Fe_3O_4/TiO_2	wet chemical reaction	$FeCl_3 \cdot 6H_2O$, $FeCl_2 \cdot 4H_2O$	precipitation	$Ti(SO_4)_2$, $CO(NH_2)_2$	185
Fe_3O_4/C	hydrothermal reaction	$FeCl_3$	hydrothermal decomposition	organic polymer	186
Fe_xO_y/C	wet chemical reaction	$Fe(NO_3)_3 \cdot 6H_2O$	TD	glucose	187
ZnO/Ag		ZnO	photodegradation under UV light	$AgNO_3$	188
ZnO/Ag	hydrothermal reaction	$Zn(COOCH_3)_2$ $2H_2O$	TD with precipitation	$SnCl_2$, $AgNO_3$, triethanolamine	189
ZnO/TiO_2		commercial ZnO	sol−gel method	TBOT	190
Cu_2O/Au	reduction by N_2H_4	$Cu(NO_3)_2$	reduction by N_2H_4	$HAuCl_4$	191
SiO_2/Au		commercial SiO_2	TD	$Au(en_2)Cl_3$	192
$SiO_2/Zn_2SiO_4:Mn^{2+}$	modified Stöber method	TEOS	precipitation and annealing	$Zn(O_2C_2H_3)_2 \cdot 2H_2O$, $Mn(O_2C_2H_3)_2$	193
$SiO_2/Ca_{10}(PO_4)_6OH:Eu^{3+}$				$Ca(NO_3)_2 \cdot 4H_2O$, $EuCl_3 \cdot 6H_2O$, $(NH_4)_2HPO_4$	193
Fe_2O_3/Au	forced hydrolysis in KH_2PO_4 solution	$FeCl_3 \cdot 6H_2O$	reduction by formaldehyde	$HAuCl_4$	194

dx.doi.org/10.1021/cr100449n |*Chem. Rev.* 2012, 112, 2373–2433

Table 1. Continued

	synthesis techniques and reagents used				
	core		shell		
core/shell	method	basic reagent	method	basic reagent	ref
MgO/Fe_2O_3	modified aerogel/ hypercritical drying/ dehydration method	$Mg(OCH_3)_2$	TD	$Fe(C_5H_7O_2)_3$	195
CaO/Fe_2O_3		bulk CaO	TD	$Fe(C_5H_7O_2)_3$	195
$La_{2/3}Sr_{1/3}MnO_3$ (LSMO)/Au	sol−gel method	$Mn(CH_3COO)_2$ H_2O, diethylenetriaminepentaacetic acid	reduction by OA	$Au(OCOCH_3)_2$	196
		Metal Chalcogenide Core			
ZnS:Mn/ZnO	hydrothermal decomposition	$Zn(CH_3COO)_2$ $2H_2O$, $Mn(CH_3COO)_2 \cdot 4H_2O$, CH_3CSNH_2	alkaline hydrolysis	$Zn(NO_3)_2$	197
CdS/Ag	precipitation	$Cd(NO_3)_2$, Na_2S	precipitation followed by reduction by Na_2SO_3	$AgNO_3$, KBr, p(methylamino) phenol sulfide	5
		Inorganic (Semiconductor)/Inorganic (Nonsemiconductor) Core/Shell Nanoparticles			
$CdSe/SiO_2$	precipitation	$Cd(ClO_4)_2 \cdot 6H_2O$, NaHTe	hydrolysis	Na_2SiO_3	141
$CdTe/SiO_2$	precipitation with reflux	$Cd(ClO_4)_2$, NaHTe	hydrolysis	Na_2SiO_3	141
CdSe/ CdS/SiO_2,	precipitation with reflux	$Cd(ClO_4)_2 \cdot 6H_2O$, NaHTe	hydrolysis	Na_2SiO_3	141
CdSe/ CdS/SiO_2	precipitation with SILAR method	$Cd(CH_3)_2$, Se powder, TBP, $(TMS)_2S$	modified Stöber method	TEOS	142
$CdSe/ZnS/SiO_2$	precipitation	$Cd(CH_3)_2$, Se, TOP, $Zn(CH_3)_2$, $(TMS)_2S$	sol−gel method	(trihydroxysilyl)propyl methylphosphonate	143
CdS/SiO_2	coprecipitation	$Cd(NO_3)_2$, $(NH_4)_2S$	hydrolysis	MPTMS	139
CdS/SiO_2	precipitation in microemulsion	$Cd(NO_3)_2$, $(NH_4)_2S$	direct coating with core through coupling agent	APTMS, active silica	121
CdS/SiO_2	mixing of two microemulsions	$Cd(NO_3)_2$, $(NH_4)_2S$	sol−gel in microemulsion	TEOS	138
AgI/SiO_2	precipitation	$AgClO_4$, KI	modified Stöber method using NaOH as a catalyst	MPS	140
CdS/TiO_2	precipitation	$Cd(NO_3)_2 \cdot 4H_2O$, $Na_2S \cdot 9H_2O$,	sol−gel reaction	IPOT	198
ZnS/TiO_2	precipitation	$Na_2S \cdot 9H_2O$, $Zn(NO_3)_2$	sol−gel reaction	IPOT	198
$CdSe_xTe_{1-x}/$ ZnS/SiO_2		$CdSe_xTe_{1-x}$ coated ZnS	modified Stöber method using NaOH catalyst	MPS	199
		Inorganic (Semiconductor)/Inorganic (Semiconductor) Core/Shell			
CdSe/ZnS	precipitation in microemulsion	$Cd(ClO_4)_2$, $(Si(CH_3)_3)_2Se$	precipitation in microemulsion	$Zn(ClO_4)_2$, Na_2S	81
ZnS/CdSe	precipitation in microemulsion	$Zn(ClO_4)_2$, Na_2S	precipitation in microemulsion	$Cd(ClO_4)_2$, $(Si(CH_3)_3)_2Se$	81
CdS/PbS	precipitation	$Cd(NO_3)_2$, Na_2S, PVP	precipitation	$Pb(NO_3)_2$, Na_2S	200
CdS/CdSe	precipitation	$Cd(NO_3)_2$, H_2S, $(NaPO_3)_6$	precipitation	$Cd(NO_3)_2$, H_2Se, $(NaPO_3)_6$	201
CdS/HgS	precipitation	$CdCl_2$, $(NH_4)_2S$	reduction	$HgCl_2$, $(NH_4)_2S$	202
CdS/Ag_2S	precipitation in microemulsion	$Cd(NO_3)_2$,	reduction in microemulsion	$AgNO_3$, $(NH_4)_2S$	203,204
CdS/ZnS	precipitation in microemulsion	$Cd(OCOCH_3)_2$, $(NH_4)_2S$	SILAR method	$Zn(OCOCH_3)_2$, $(NH_4)_2S$	82
CdS/HgS/CdS	precipitation	$Cd(ClO_4)_2$, H_2S, sodium polyphosphate	SILAR method	$Hg(ClO_4)_2$, H_2S, $Cd(ClO_4)_2$	83

dx.doi.org/10.1021/cr100449n |*Chem. Rev.* 2012, 112, 2373–2433

Table 1. Continued

	synthesis techniques and reagents used				
	core		shell		
core/shell	method	basic reagent	method	basic reagent	ref
CdSe/CdS	precipitation	$Cd(NO_3)_2$, H_2Se, $(NaPO_3)_6$	precipitation	$Cd(NO_3)_2$, H_2S, $(NaPO_3)_6$	201
CdSe/CdS	precipitation	$Cd(ClO_4)_2$, *N*, *N*-dimethylselenourea, sodium citrate	SILAR method	thioacetamide, silicone oil	205
CdSe/CdS	precipitation	CdO, stearic acid, liquid paraffin, TBP-Se	high temperature ion exchange	TBP-S	206
CdSe/CdS	precipitation	$Cd(CH_3)_2$, Se powder, TBP	precipitation	$Cd(CH_3)_2$, $(TMS)_2S$	207
CdSe/ZnS	precipitation	$Cd(CH_3)_2$, Se, TOP	precipitation at high temperature	$Zn(CH_3)_2$, $(TMS)_2S$	208
CdSe/ZnS	precipitation with TD	$Cd(CH_3)_2$, TOPSe	precipitation at inert atmosphere	$Zn(C_2H_5)_2$, $(TMS)_2S$	209
CdSe/CdS	precipitation in microemulsion	$CdCl_2$, NaHSe,	precipitation in microemulsion	$CdCl_2$, Na_2S	210
CdSe/CdS/ZnS	precipitation	$Cd(CH_3COO)_2$, TOPSe, H_2S, HDA-TOPO-TOP	SILAR method	$Zn(C_2H_5)_2$, hexane, $(TMS)_2S$	211
CdSe/ZnSe/ZnS	precipitatiuon	$Cd(CH_3COO)_2$, $Zn(C_2H_5)_2$, TOPSe, HDA-TOPO-TOP	SILAR method	$Zn(C_2H_5)_2$, hexane, $(TMS)_2S$	211
CdSe/ZnSe	precipitation	Me_2Cd, TOPSe, TOP- TOPO	SILAR method	$Zn(C_2H_5)_2$, TOPSe	212
CdSe/ZnTe	reduction with precipitation	$CdCl_2 \cdot 2.5H_2O$, $NaBH_4$ and Na_2SeO_3	precipitation	$Zn(C_2H_5)_2$, TOPTe	213
CdTe/CdS	precipitation	NaHTe, $Cd(ClO_4)_2 \cdot 6H_2O$, thiols	precipitation	$Cd(ClO_4)_2 \cdot 6H_2O$, H_2S	214
CdTe/CdS	precipitation	$CdCl_2$, hydrogen telluride gas, thiol	precipitation	$CdCl_2$, GSH, thioacetamide (TAA)	215
CdTe/CdSe	precipitation	$CdCl_2 \cdot 2.5H_2O$, NaHTe	reduction with precipitation	$CdCl_2 \cdot 2.5H_2O$, $NaBH_4$ and Na_2SeO_3	213
CdTe/CdSe	reduction with precipitation	$CdCl_2 \cdot 2.5H_2O$, MPA, trisodium citrate dihydrate, Na_2TeO_3, $NaBH_4$	precipitation at high temperature	$CdCl_2$, MPA, $NaBH_4$	216
PbTe/CdSe	precipitation	$Pb(CH_3COO)_2$, OA, Te powder, TOP	precipitation reaction	$Cd(CH_3COO)_2$, OA	217
ZnSe/CdSe	precipitation in microemulsion	$Zn(ClO_4)_2$, BisTMS-Se	precipitation in microemulsion	$Cd(ClO_4)_2$, bisTMS-Se	4
CdS/Ag_2S	precipitation in microemulsion	$CdBr_2$, $(NH_4)_2S$	precipitation in microemulsion	$AgNO_3$, $(NH_4)_2S$	218
$Zn_{1-x}Cd_xSe$/ZnS	reduction with SILAR method	Se, $NaBH_4$, $Na_2S \cdot 9H_2O$, $CdCl_2 \cdot 2.5H_2O$, $Zn(CH_3COOH)_2 \cdot 2H_2O$	SILAR method	Na_2S	219
		Lanthanide Inorganic/Inorganic Core/Shell			
Au/SiO_2/Y_2O_3:Eu^{3+}	reduction, Stöber method	$HAuCl_4$, TEOS, PVP	direct coating at alkaline condition	Y_2O_3, Eu_2O_3, HNO_3	220
Fe_3O_4,γ-Fe_2O_3/ $NaYF_4$:Yb,Er	coprecipitation	$FeCl_2$, $FeCl_3$	coprecipitation	NaF, YCl_3, $YbCl_3$, $ErCl_3$, EDTA	221
SrS:Ce/ZnO	reduction precipitation	$SrSO_4$, $Na_2S_2O_3$, $(Ce)_2NO_3$, activated charcoal	oxidation	Zn powder	222
$CePO_4$:Tb/$LaPO_4$	coprecipitation	$CeCl_3 \cdot 7H_2O$, $TbCl_3 \cdot 6H_2O$, tributylphosphate	coprecipitation at high temperature in inert atmosphere	$LaCl_3 \cdot 7H_2O$, H_3PO_4	223
LaF_3/Eu	coprecipitation	NH_4F, $La(NO_3)_3 \cdot 6H_2O$	ion exchange method	$Eu(NO_3)_3 \cdot 6H_2O$	224
LnF_3:Eu^{3+}/ $La(NO_3)_3$	precipitation with doping	$Ln(NO_3)_3$, NH_4F, Eu^{3+} salt	self-deposition method	$La(NO_3)_3$	224−226

dx.doi.org/10.1021/cr100449n |*Chem. Rev.* 2012, 112, 2373–2433

Table 1. Continued

	synthesis techniques and reagents used				
	core		shell		
core/shell	method	basic reagent	method	basic reagent	ref
β-$NaYF_4$:Yb^{3+}, Er^{3+}/β-$NaYF_4$	precipitation	$(CF_3COO)Na$, $(CF_3COO)_3Y$, $(CF_3COO)_3Yb$, $(CF_3COO)Er$	precipitation with self-deposition	$(CF_3COO)Na$, $(CF_3COO)_3Y$	227
$LaPO_4$:Er/Yb	precipitation followed by doping of Er in microeemulsion, calcination	$La(NO_3)_3 \cdot 6H_2O$, H_3PO_4, $Er(NO_3)_3$	coprecipitation with calcination	$Y(NO_3)_3$	228
β-$NaYF_4$:Yb,Tm/ β-$NaYF_4$:Yb,Er	precipitation at alkaline condition	YCl_3, $YbCl_3$, $TmCl_3$, NH_4F	precipitation at alkaline condition	YCl_3, $YbCl_3$, $ErCl_3$	229
$LaF_3/Eu_{0.2}La_{0.8}F_3$	coprecipitation	$La(NO_3)_3$, fluorine/ADDP	coprecipitation	$Eu(NO_3)_3$, $La(NO_3)_3$	230
$LaPO_4$:Eu^{3+}/$LaPO_4$	doping in excess phosphate	$LaPO_4$, $EuPO_4$	self-coating	$LaPO_4$	231

[a] Abbreviations: MPS, 3-(mercaptopropyl)trimethoxy silane; TOPO, trioctylphosphine oxide; CTAC, cetyltrimethylammonium chloride; hfac, 1,1,1,5,5,5-hexafluoroacetylacetonate; SMAD, solvated metal atom dispersion; APTMS, (3-aminopropyl) trimethoxysilane; MPTMS, 3-(mercaptopropyl) trimethoxy silane; TBP, tributylphosphine; $(TMS)_2S$, bis-trimethylsilane sulfide; TOP, tri-*n*-octylphosphine; HDA-TOPO-TOP, hexadecylamine-tri-*n*-octylphosphine oxide-(tri-*n*-octylphosphine); TOP-TOPO, trioctylphosphine-trioctylphosphineoxide; MPA, 3-mercaptopropionic acid; bisTMS-Se, bis(trimethylsilyl) selenide; ADDP, ammonium di-*n*-octadecyldithiophosphate; WWE, wire electric explosion; PVP, polyvinylpyrrolidone; $Fe(C_5H_7O_2)_3$, iron(III) acetylacetonate; $Pt(C_5H_7O_2)_2$, platinum(II) acetylacetonate; $Cd(C_5H_7O_2)_2$, cadmium(II) acetylacetonate; $Na_3C_6H_5O_7$, trisodium citrate; $Ca(NO_3)_2 \cdot 4H_2O$, calcium nitrate tetrahydrate; $EuCl_3 \cdot 6H_2O$, europium chloride hexahydrate; $(NH_4)_2HPO_4$, ammonium hydrogen phosphate; IPOT, titanium isopropoxide or isopropyl orthotitanate; OA, oleic acid.

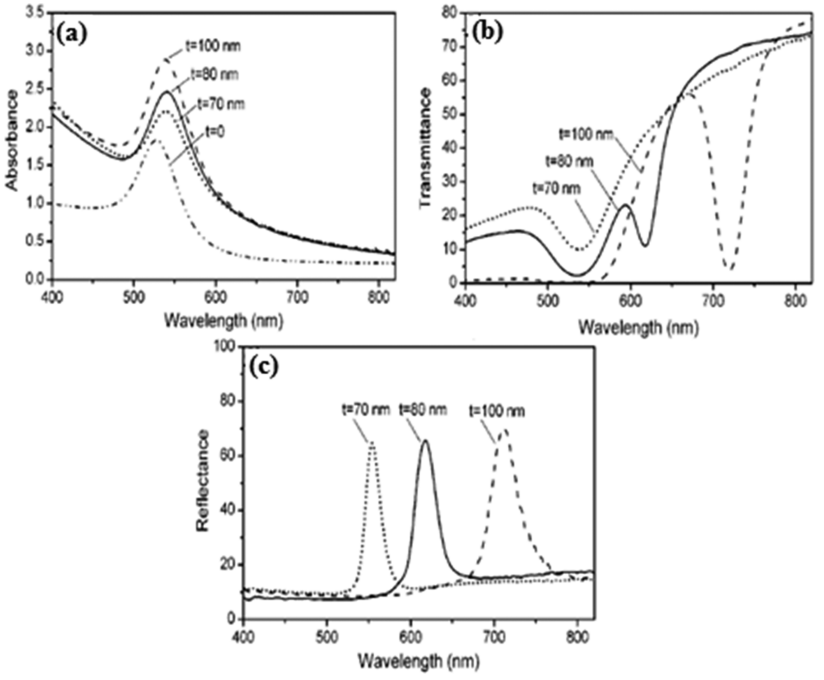

Figure 3. (a) UV−visible absorption spectra of aqueous dispersions containing Au/SiO_2 core/shell nanoparticles with different shell thicknesses (t). The gold cores are 50 nm in diameter for all samples. (b, c) Transmission and reflectance spectra taken from photonic crystals crystallized from Au/SiO_2 core/shell particles. The incident light was perpendicular to the (111) planes of these face-center-cubic crystalline lattices for all measurements. Reprinted with permission from ref 120. Copyright 2002 American Chemical Society.

These types of particles are widely used for the improvement of semiconductor efficiency, information storage, optoelectronics, catalysis, quantum dots, optical bioimaging, biological labeling, etc. Furthermore, of the different types of inorganic/inorganic nanoparticles, it can be seen that, in general, both the cores and shells are made of metal, metal oxide, other inorganic compounds, or silica. Depending on the nature of the shell material, core/shell particles can be broadly classified into two categories: either silica-containing ones or those comprised of any other inorganic material. The different inorganic/inorganic materials are listed in Table 1 according to their category.

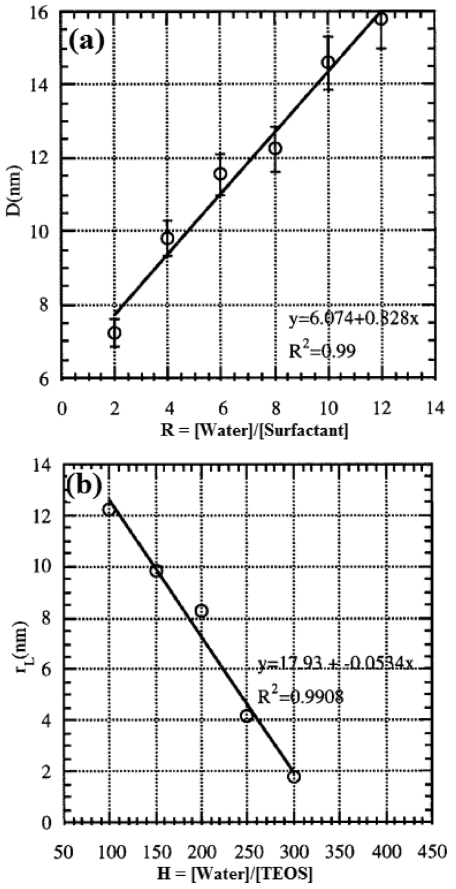

Figure 4. (a) Size of the Ag clusters with changing R ratio and (b) variations of the thicknesses of SiO_2 layers (r_L) as a function of H at $R = 4$ and X ([NH_4OH]/[TEOS]) = 1.
Reprinted with permission from ref 123. Copyright 1999 American Chemical Society.

2.1.1. Inorganic/Inorganic (Silica) Core/Shell Nanoparticles. The silica coating used on a core particle has several advantages. The most basic advantages of the silica coating compared with other inorganic (metal or metal oxide) or organic coatings are as follows: It reduces the bulk conductivity and increases the suspension stability of the core particles. In addition, silica is the most chemically inert material available; it can block the core surface without interfering in the redox reaction at the core surface. Silica coatings can also be used to modulate the position and intensity of the surface plasmon absorbance band since silica is optically transparent. As a result, chemical reactions at the core surface can be studied spectroscopically. Therefore, researchers have concentrated more on silica coatings on different inorganic core materials such as metals,[114,116−119,121,123,126,130,131,232−234] binary inorganic composites,[130,144,235] metal oxides,[132,134,135,236] and metal salts[121,139−142,146] than any other combination.

Among the possible metal cores, many researchers have studied the noble metals such as Au[114,116−119,121] and Ag[123−125] coated with silica. In addition, different metals such as Ni,[126] Co,[130,131] and Fe[128,129] and binary metal composites such as Fe−Ni[130,235] have also been studied. Silica-coated gold particles are synthesized using a slightly modified Stöber (or sol−gel) process in the presence of Au template as the core. Characterization techniques used for these particles include SEM, TEM, AFM, XPS, and UV spectroscopy.[114,116,118,120] According to the literature, by controlling the experimental parameters such as coating time, concentration of reactants, catalyst, and other precursors, the shell thickness from 20 to 100 nm can be controlled. The spectroscopic characterization of the core/shell particles show that with increasing shell thickness the intensity of the UV absorbance increases and the reflectance shifts toward the higher wavelength region as shown in Figure 3.[114,116,120] This method has been modified further in order to control the uniform thickness of the silica on the nanosilver (Ag) core particles.[124] Other researchers extended it further for coating onto Pt and CdS nanoparticles.[139] When the particles were synthesized in a microemulsion system, it was found that with the increasing molar ratio of water to surfactant (R = [water]/[surfactant]), the core size increases. Particle size distribution is also wide because of more intermicellar exchange (as shown in Figure 4a). The shell thickness also increases with R because of the increasing availability of water molecules for the hydrolysis of TEOS.[123] On the other hand, for a fixed R value, if the molar volume ratio of water to TEOS (H = [water]/[TEOS]) increases then the shell thickness decreases because of decreasing TEOS concentration (as shown in Figure 4b). Uniform sized spherical core/shell particles as shown in Figure 5 were obtained. Silver/silica particles can be used in fluorescence imaging, where the region of emission again depends on the thickness of the silica coating.[123] Cha et al.[125,232] synthesized silica-coated Ag core/shell nanoparticles from $AgNO_3$ using a different route. They used sodium oleate to form a siver−oleate complex and later decomposed the oleate complex by heating it at 300 °C for 2 h and then directly used it for coating silica, which in turn was synthesized from TEOS by a modified Stöber method.

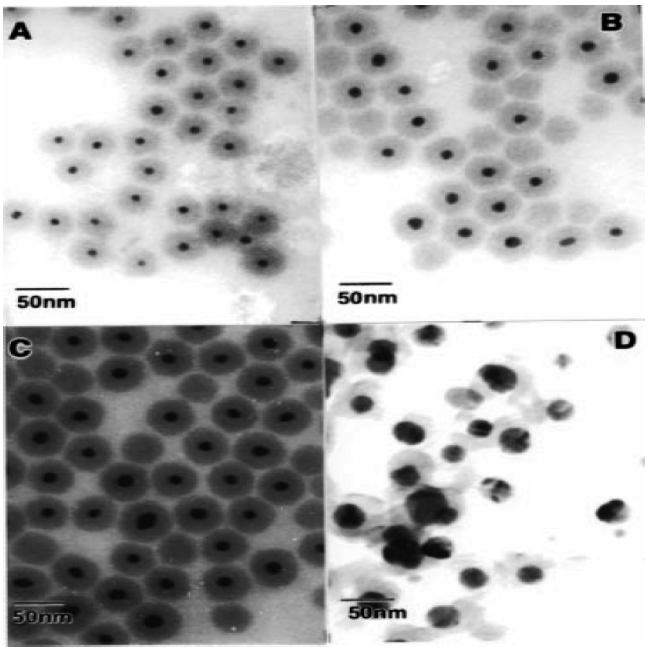

Figure 5. TEM micrographs of Ag/SiO_2 nanocomposites synthesized at $X = 1$ and $H = 100$ and at different water contents: (a) $R = 2$; (b) $R = 4$; (c) $R = 6$; (d) $R = 10$.
Reprinted with permission from ref 123. Copyright 1999 American Chemical Society.

The magnetic properties of other silica-coated cores, such as Fe, Ni, Co, Fe_3O_4, or a Fe−Ni alloy compound, were also studied in the presence of external magnetic fields.[130,131,134,235,237] The

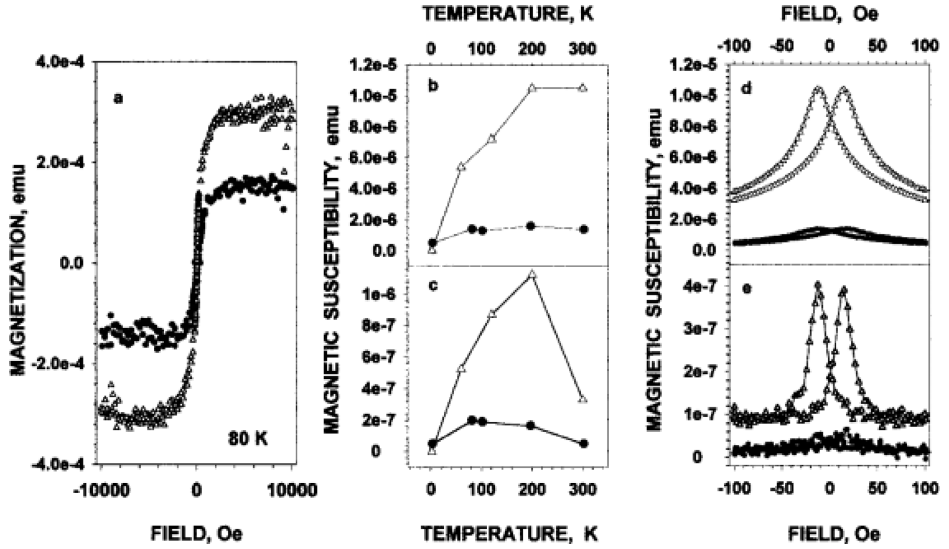

Figure 6. Magnetic properties of ten-layer LBL (layer by layer) films from silica-coated (●) and uncoated (△) magnetite: (a) hysteresis loops and (b,c) temperature and (d,e) magnetic field dependence of in-phase and out-of-phase parts of magnetic susceptibility.
Reprinted with permission from ref 134. Copyright 1999 Wiley-VCH.

saturation magnetization (M_S) of inert material-coated magnetic core/shell particles decreases compared with that of the naked uncoated magnetic particles, and this may be because of the intrinsic properties of the nanoparticle surface.[130,134,238,239] Magnetic nanoparticle synthesis using wet chemical processes in aqueous systems is easy, but there is the disadvantage of the difficulty of making a stable dispersion in such aqueous or related biological systems. Silica-coated magnetite particles, on the other hand, are well dispersed and more biocompatible when used for biological applications.[132,134−136] The hysteresis loop does not follow the same path as for naked magnetic particles when coated with an inert material (shown in Figure 6a). The temperature-dependent in-phase and out-of-phase magnetic susceptibility deceases because of a decrease in the magnetic anisotropic constant (K) in the presence of a silica coating on Fe_3O_4 nanoparticles (shown in Figure 6b,c). Similarly, the magnetic susceptibility decreases by almost 10 times in the presence of an applied external magnetic force (shown in Figure 6d,e). This may be because the surface atoms of the magnetic material are blocked.[134] Other nonmagnetic materials such as Mn with ZnS,[144,145] as well as metals,[132,135,136,240] are also used as core materials for silica coated core/shell particle synthesis.

2.1.2. Inorganic/Inorganic (Nonsilica) Core/Shell Nanoparticles. Apart from silica, various metals and metal oxides can also be used as shell materials. Similar to gold as the core material, core/shell particles with gold as the shell material have also been well studied by many researchers.[182,183,192,194,241,242] Gold coating on any particles enhances many physical properties,such as the chemical stability by protecting the core material from oxidation and corrosion, the biocompatibility, the bioaffinity through functionalization of amine/thiol terminal groups, and the optical properties.[182,192] Other shell metals such as Ni,[150] Co,[150] Pd,[154,156] Pt,[151,152,168,243] and Cu[244] are also important for some specific applications in the field of catalysis, solar energy absorption, permanent magnetic properties, etc. The surface-enhanced Raman scattering (SERS) activity of Pd metal is low compared with that of Au, Ag, or Cu. However, the SERS activity can be increased by choosing a suitable core such as Au. Again this activity decreases with the increasing thickness

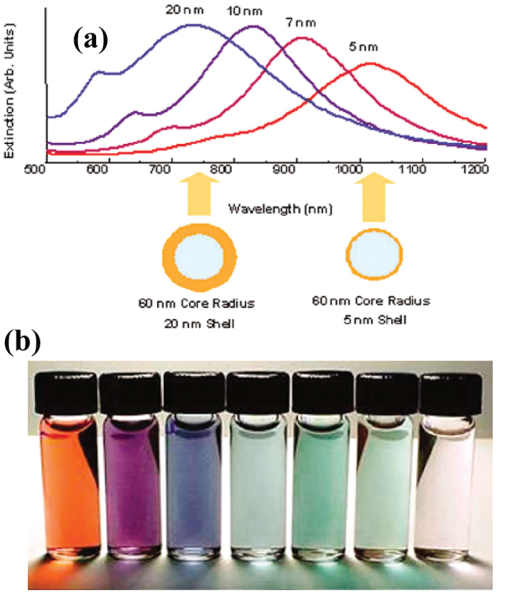

Figure 7. (a) Optical resonances of SiO_2/Au core nanoshells as a function of their core/shell ratio and (b) visual appearance of gold nanoshells with different thickness.
Reprinted with permission from ref 245. Copyright 2004 Adenine Press.

of the shell material.[152,154] Metal nanoshells have recently been developed as a new class of nanoparticles. They are composed of a dielectric core, possibly silica-coated, with a nanorange metallic layer, which is typically gold. Similar to the size-dependent color of pure gold nanoparticles, the optical response of gold nanoshells depends dramatically on the relative size of the core nanoparticle as well as the thickness of the gold shell.[245] By varying the relative core and shell thicknesses, the color of such gold nanoshells can be varied across a broad range of the optical spectrum spanning the visible and the near-infrared spectral regions as shown in Figure 7. The result is that the gold

Table 2. Electronic Band Gaps for Different Materials

material	symbol	band gap (eV)	ref
silicon	Si	1.11	248
germanium	Ge	0.67	248
silicon carbide	SiC	2.86	248
aluminum phosphide	AlP	2.45	248
aluminum arsenide	AlAs	2.16	248
aluminum antimonide	AlSb	1.6	248
gallium(III) nitride	GaN	3.4	248
gallium(III) phosphide	GaP	2.26	248
gallium(III) arsenide	GaAs	1.43	248
gallium antimonide	GaSb	0.7	248
gallium(II) sulfide	GaS	3.05	249
indium(III) nitride	InN	1.8	250
indium(III) phosphide	InP	1.35	248
indium(III) arsenide	InAs	0.36	248
zinc oxide	ZnO	3.37	251
zinc sulfide	ZnS	3.6	248
zinc selenide	ZnSe	2.7	248
zinc telluride	ZnTe	2.25	248
cadmium sulfide	CdS	2.42	248
cadmium selenide	CdSe	1.73	248
cadmium telluride	CdTe	1.49	252
lead(II) sulfide	PbS	0.37	248
lead(II) selenide	PbSe	0.26	253
lead(II) telluride	PbTe	0.31	254
copper(I) oxide	Cu_2O	1.2	255
silver bromide	AgBr	2.5	256
titanium dioxide	TiO_2	3.03 for rutile 3.18 for anatase	257

nanoshell may prove useful for biomedical imaging in future applications.

Pure magnetic nanoparticles have, however, some disadvantage for direct use in some specific areas. The main disadvantages are (i) the particles have a high tendency to aggregate, (ii) these particles can undergo rapid biodegradation when directly exposed to biological systems, and (iii) if the particles are not stable enough, the original particle structures may change in the presence of other external magnetic fields. As a result, magnetic nanoparticles with different inert inorganic coatings have gained in importance. These classes of nanoparticles are used as magnetic resonance imaging (MRI) contrast agents, in the magnetic separation of oligonucleotides, in other biocomponent applications, and finally as magnetically guided site-specific drug delivery systems.[182] More recently, biomagnetic nanoparticles where both core and shell have magnetic properties are being used for more advanced applications. This class of particles is mainly used to fabricate devices for novel nanomagnetic applications because it also allows a precise engineering of the magnetic properties by selectively tuning anisotropy, magnetization, and the dimensions of both core and shell. Some commonly studied systems are FePt/Fe_3Pt and FePt/Fe_3O_4.[179,246]

Core/shell nanoparticles are also used to enhance the adsorption capacity for environmental remediation applications. An example is the Fe_2O_3 coating on MgO and CaO nanoparticles, which can enhance the adsorption capability of toxic materials, such as SO_2 and H_2S, from the environment compared with that of pure MgO and CaO.[195,247]

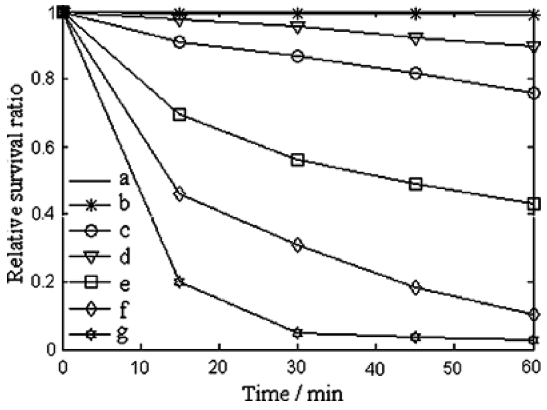

Figure 8. Relative viability of Hela cells in the presence of (a) only TiO_2 NPs, (b) only Fe_3O_4/TiO_2 core/shell NPs, (c) only ultraviolet irradiation, (d) only blue-light irradiation, (e) TiO_2 NPs and ultraviolet irradiation, (f) Fe_3O_4/TiO_2 core/shell NPs and blue-light irradiation, (g) external magnetic field, Fe_3O_4/TiO_2 core/shell NPs, and blue-light irradiation.
Reprinted with permission from ref 185. Copyright 2008 Elsevier Ltd.

2.1.3. Semiconductor Core/Shell Nanoparticles. Semiconductor nanoparticles are also known as quantum dots (QDs). One definition, describes a quantum dot as a semiconductor where excitons (electron and hole) are confined within all three spatial dimensions. The recommended band gap for semiconductor particles is normally greater than that for conductor materials but less than 4 eV, which are those normally found in insulating materials. In the early years of this research, pure group IVA (Si, Ge) elements were used as the semiconductor material, whereas later, compounds of different element groups, such as IIIA−VA, IIB−VIA, and IB−VIIA, also became popular as semiconductor materials. The lattice spacing of these different materials is almost the same with the only difference the fact that the bonds have a partially ionic character. This increases to a certain extent moving from left to right in the periodic table. Because of overlapping of the valence and conductance bands of two elements, the band gap also changes; either increasing or decreasing with respect to the pure semiconductor. The band gaps of some common semiconductor materials are given in Table 2. For the pure elements within a particular group, it can be seen that as we move from top to bottom the band gap decreases. Similarly, for the compounds of a particular element if other elements are changed in a group, the band gap gradually decreases while moving from top to bottom.

With respect to the core/shell nanoparticles discussed in this section, either both the core and shell are made of semiconductor materials or one is a semiconductor and the other is a nonsemiconductor material. So, depending on the material properties used the semiconductor core/shell nanoparticles can be classified as follows: (i) semiconductor/nonsemiconductor core/shell nanoparticles or (ii) semiconductor/semiconductor core/shell nanoparticles. Both types of particles are used for medical or bioimaging purposes,[88,89,91,92] enhancment of optical properties,[5,59,83−85,120,160,215,258−261] light-emitting devices,[262] nonlinear optics,[263,264] biological labeling,[96,97,265] improving the efficiency of either solar cells[266,267] or the storage capacity of electronics devices,[268] modern electronics field applications,[269,270] catalysis,[271] etc.

2.1.3.1. Semiconductor/Nonsemiconductor or Nonsemiconductor/Semiconductor Core/Shell Nanoparticles. Either the core or shell of this type of particles is made of a semiconductor material with the remaining layer either metal, metal oxide, silica, or any other inorganic material.[139,143,145,185,272] These semiconductor/nonsemiconductor core/shell nanoparticles are also important among the different inorganic/inorganic core/shell nanoparticles because of their suitability for more advanced applications in a wide range of fields extending from electronics to biomedical. Pure semiconductor nanoparticles or quantum dots are also represented in a new class of fluorescently labeled compounds with unique advantages compared with other fluorescent probes (organic dye or proteins).[273] These semiconductor materials are preferably used in photoluminescence (PL) applications, because the fluorescent emission spectra of these particles can be tuned by changing the particle size. As a result, a single wavelength light can be used for the simultaneous excitation of all the different sized quantum dots. The main advantage of these particles is the fact that they have dual properties. Among the different types of nonsemiconductor/semiconductor nanoparticles, the "magnetic core with semiconductor shell core/shell nanoparticles" are more versatile[185,272] because of their magnetic and fluorescence properties. The photocatalytic effect of magnetic core semiconductor shell particles is higher than that of pure semiconductor particles. He et al.[185] studied the photocatalytic effect of pure TiO_2 and Fe_2O_3/TiO_2 core/shell particles in malignant tumor therapy. They used cervical carcinoma Hela cells as a model for checking the efficacy of particles for apoptosis in the presence of different external driving forces (shown in Figure 8). The results show that the survival capacity of the tumor cells is minimal for core/shell particles in the presence of magnetic fields and blue light irradiation. They also studied the effect of particle concentration on apoptosis, and the results indicate that with increasing core/shell nanoparticle concentration, the efficiency increases. However, above a certain concentration the efficiency once again is reduced. This leads to the conclusion that an optimum particle concentration is required in order to achieve maximum efficiency.

2.1.3.2. Semiconductor/Semiconductor Core/Shell Nanoparticles. Over the past 2 decades, instead of using either a single semiconductor material or semiconductor/nonsemiconductor core/shell material, researchers have been using semiconductor/semiconductor core/shell materials to improve the efficiency and decrease the response time. Of particular interest is where both the core and shell are made of a semiconductor material or a semiconductor alloy.[81,83,111,201,203,211,217,274,275] These types of particles are used as either binary materials with core and shell or tertiary materials, that is, a core with a double shell coating. In most common core/shell quantum dots, the core and shell are mainly made of alloy materials. Apart from reviewing the relevant research papers, different aspects of the semiconductor/semiconductor core/shell materials have also been extensively reviewed by Reiss et al.[112] The main advantages of such particles are the fact that because they have an external coating of another semiconductor material, this increases optical activity and photooxidation stability.

Depending on their relative energy levels of the valence and conductance bands and the band gap of the core and shell materials, these semiconductor/semiconductor core/shell nanoparticles can also be classified into three different groups.

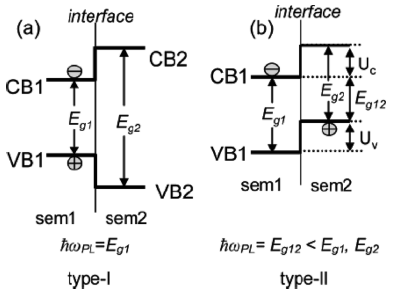

Figure 9. (a) Type I and (b) type II semiconductor/semiconductor core/shell materials. Sem1 = core material, Sem2 = shell material. Reprinted with permission from ref 276. Copyright 2007 American Chemical Society.

2.1.3.2.1. Shell Materials with Higher Band Gaps (Type I). In this category, the energy band gap of the shell material is wider than the band gap of the core material. The electrons and holes are confined within the core area because both the conduction and the valence band edges of the core are located within the energy gap of the shell.[276] As a result, the emission energy, $h_{\omega PL}$, is determined by the energy gap of the core material (E_{g1}). Figure 9a schematically shows this type I structure, where the conduction band of the shell is of higher energy (the higher band gap material) than that of the core. The valence band of the shell is also at a lower energy than that of core. This arrangement of energy levels is essential in order to confine electrons and holes within the core material. The shell is used to passivate the surface of the core with the goal of improving its overall optical properties. Another role of the shell is to separate the more optically active core surface from its surrounding environment. The wider band gap shell material increases the stability against photobleaching of the semiconductor core. However, the increasing thickness of the shell layer reduces the material surface activity of the core surface; as a result, quantum yield also reduces. With increasing shell layer thickness, a small red shift (5−10 nm) occurs for the UV−vis absorption spectra and the PL wavelength compared with that of uncoated core. These types of semiconductor particles especially those made from CdSe/CdS,[89,201,205−207,210,277] CdSe/ZnS,[208,209,278] or CdTe/CdS[215] materials, have been extensively studied by different research groups. Liu and Yu[215] studied the absorption and emission spectra of CdTe and CdS-coated CdTe nanoparticles and results showed that the absorption and emission peak positions are shifted to a higher wavelength with increasing reaction time (shown in Figure 10a,b). This is a result of the coating of CdS, the higher band gap material, on the lower band gap material, CdTe. In this case, the QY initially increases, but again with increasing reaction time, QY decreases because of the increase in shell thickness. The QYs of the core/shell nanoparticles depend on the pH of the reaction media as shown in Figure 10c. This may be because of the release of sulfur atoms from the organic sulfur supplier, glutathione (GSH), at higher pH values, which leads to a more uniform coating. In addition, Cd also reacts with GSH to form Cd-GSH or $Cd(GSH)_2$, which can prevent an increase in QY.

2.1.3.2.2. Shell Materials with Lower Band Gaps (Reverse Type I). This group is the reverse of the one discussed above. In this group, the narrower band gap shell material is grown over the wider band gap core material. In this case, both hole and electron charges are partially delocalized on the shell materials and emission wavelengths can be tuned by changing the thickness

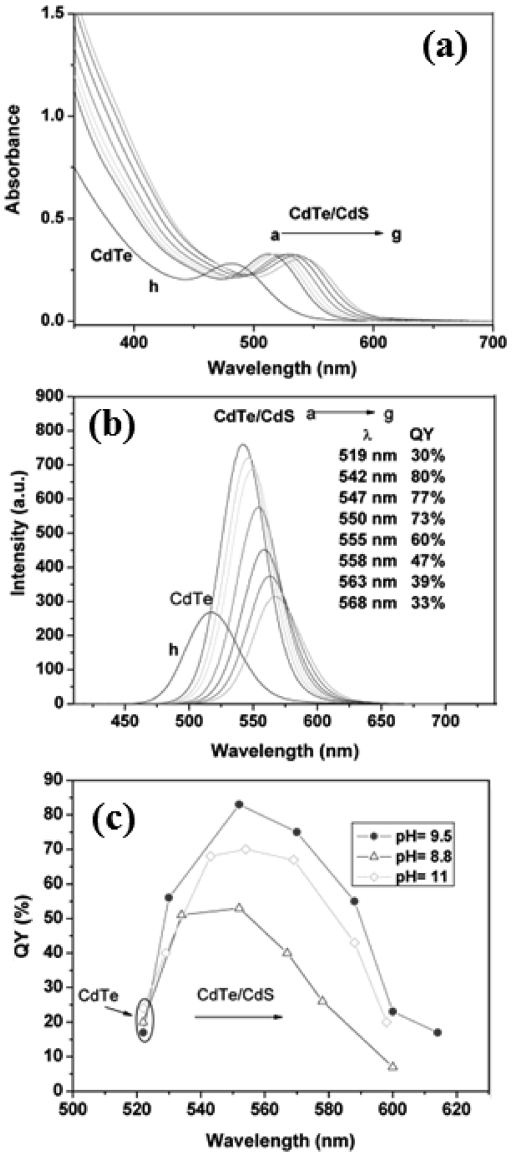

Figure 10. Typical temporal evolution of the (a) absorption and (b) corresponding emission spectra of thiopronin (TP)-capped CdTe and TP-capped CdTe/CdS QDs with thioacetamide (TAA) as the sulfur source. Curves a−g represents the (a) absorption and (b) corresponding emission spectra of CdTe/CdS QDs under reaction for 10 min, 30 min, 1 h, 2 h, 4 h, 7 h, and 10 h, respectively. Curve h represents the (a) absorption and (b) corresponding emission spectra of CdTe NCs. The excitation wavelength is at 400 nm. TheCdTe core template photoluminesce emission peaked at 518 nm. (c) QYs of the TP-capped CdTe and GSH-capped CdTe/CdS QDs as a function of PL peak position at different pH.
Reprinted with permission from ref 215. Copyright 2009 Elsevier Ltd.

of the shell. Within this category, the most extensively studied systems are CdS/CdSe[111,201,275] and ZnS/CdSe.[81] Here the types of particles have low quantum yields and higher resistance against photobleaching, whereas the quantum yield can be improved by coating another semiconductor material of a wider band gap. For example, the quantum yield (QY) of CdSe- coated CdS core/shell nanoparticles in aqueous media is 20%. Further coating with a higher band gap material (CdS) means the QY improves to 40%.[279]

2.1.3.2.3. Core, Shell Band Gap Staggered Type (Type II). The third group of this category is called type II. A type II QD, in contrast to type I, has both the valence and conduction bands of the core either lower or higher than those in the shell. As a result, one carrier is mostly confined to the core, while the other is mostly confined to the shell. Therefore, the energy gradient existing at the interfaces tends to spatially separate the electrons and holes on different sides of the heterojunction.[213,276] A schematic diagram of a type II QD is shown in Figure 9b. Because of the spatial separation of the electrons and holes, this type of QD is expected to have many novel properties, including longer exciton decay times than type I. For example, these structures can allow access to wavelengths that would otherwise be unavailable for a single material. In addition, type II nanocrystals are more suitable for photovoltaic or photoconduction applications because of the separation of charges in the lowest excited states. The energy gap in this type of material (E_{g12}) is determined by the energy separation between the conduction-band edge of one semiconductor and the valence band edge of the other semiconductor. E_{g12} can be related to the conduction (U_c) and valence (U_v) band energy offsets at the interface by the following equation:

$$E_{g12} = E_{g1} - U_v = E_{g2} - U_c \quad (1)$$

where E_{g1} and E_{g2} are the band gaps of semiconductors 1 and 2, respectively. In this case, emission is lower than the band gap of either semiconductor.

Here, since the effective band gap of the core/shell particle is lower compared with the corresponding pure core and shell materials, the possibility of manipulating the optical properties by tuning the shell thickness is easy for these types of particles. Therefore, the emission color is shifted toward spectral ranges[280] that are difficult to attain for other types of particles. Photoluminescence decay time of these types of particle is higher compared with type I semiconductor particles. Some common examples of these types of particles are CdTe/CdSe,[213,281−283] CdTe/CdS,[284] ZnTe/CdS,[285] PbTe/CdTe,[217] ZnTe/ZnSe,[280] CdSe/ZnSe,[4,212,213,286] PbSe/CdSe,[287] ZnSe/CdSe,[288] and CdS/ZnSe.[276] It can be observed that in most of these examples one component is aTe-based compound. In general, one problem associated with Te-containing compounds is a tendency toward oxidation, which in turn reduces chemical stability. Klimov and co-workers[288,289] synthesized core/shell nanocrystals (NCs) with a wide energy gap (E_g = 2.74 eV at 300 K) where the core semiconductor material (ZnSe) is surrounded by a shell of narrower energy gap (E_g = 1.73 eV at 300 K) material (CdSe). ZnSe/CdSe is a reverse type I core/shell nanoparticle, but according to their observations, the core to shell transition can be tuned by controlling the shell thickness. They observed that with increasing shell thickness the transition from type I (both electron and hole wave functions are distributed over the entire nanocore) to type II (electron and hole are spatially separated between the shell and the core, but there is a higher probability that the hole is found in the core than in the shell) and back to type I (both electron and hole primarily reside in the shell) (reverse type I, according to the convention adopted in this paper) localization regimes. Figure 11 shows an interesting example of a ZnSe/CdSe core/shell nanoparticle; here the type I or type II properties of the material depends on the shell thickness for a fixed core radius. This material also shows a high emission quantum yield (QY) of up to 80−90%.

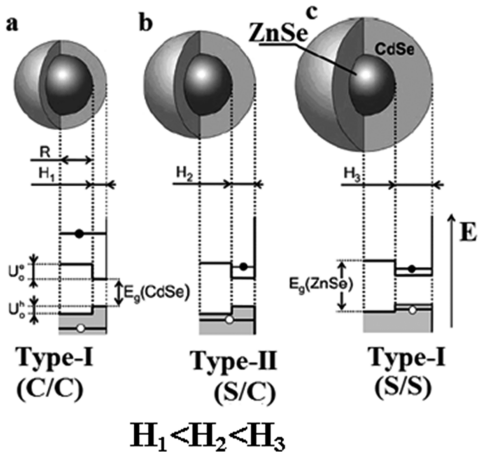

Figure 11. Three different localization regimes of ZnSe/CdSe QD in the case of a fixed core radius and different shell widths: (a) thin shell where both electron and hole wave functions are delocalized over the entire hetero-NC (reverse type I (C/C) regime); (b) intermediate shell where the hole wave function is still delocalized over the entire heterostructure, while the electron is confined primarily to the shell (type II (S/C) regime); (c) thick shell with both the electron and the hole localized mostly in the shell (type I (S/S) regime) (reverse type I, according to convention of this paper).
Reprinted with permission from ref 288. Copyright 2004 American Chemical Society.

The efficiency of semiconductor nanomaterials is mainly decided by two important parameters, namely, the quantum yield (QY) and the response time. The quantum yield is defined as the ratio of photons emitted being adsorbed by the semiconductor material. Normally, for single semiconductor particles synthesized in an aqueous phase, the quantum yield is very low but when the particular material is coated by a composite semiconductor material with a high energy band gap semiconducting material, the quantum yield increases.[207−209,211,271] As an example, the QY of naked core CdS nanocrystals is 3−6%, but after being coated with ZnS the core/shell CdS/ZnS nanocrystals show a QY of 20−30%.[290] For CS (core/shell) semiconductor particles, if the response time decreases, then the overall efficiency increases and the emission spectra shift toward the visible region; as a result, detection becomes easy. In general, CS semiconductor particles of type I and reverse type I have low quantum yields and in addition type II particles have low photo-oxidation stabilities. In order to improve these two properties, the CS particles are again coated with another semiconductor material to form a multilayer semiconductor material.

2.1.3.3. Core/Multishell Semiconductor Nanoparticles. The relative energy levels of VB and CB for multilayer heterogeneous semiconductor particles are schematically presented in Figure 12. The main advantages of multilayer semiconductor nanoparticles are higher quantum yield, higher photoluminescence efficiency, improved optical properties, increased half-life times of the semiconductor materials, easy detection of emission spectra because they are shifted toward higher wavelength in the visible range, photo-oxidation stability, improved appropriate electronic properties (band gap, band alignment), and finally better structural (lattice mismatch) properties than unlayered CS particles. One definition for the term lattice mismatch refers to "the situation where two materials having different lattice constants are brought together by deposition of one material on top

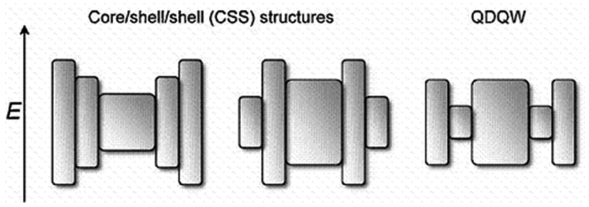

Figure 12. Schematic representation of the energy-level alignment in different CSS structures and in a QDQW system. The height of the rectangle represents the band gap energy, and their upper and lower edges correspond to the positions of the conduction and valence band edge, respectively, of the core (center) and shell materials.
Reprinted with permission from ref 112. Copyright 2009 Wiley-VCH.

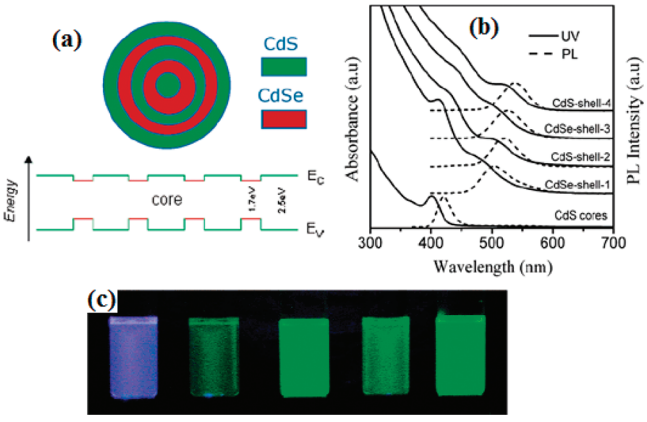

Figure 13. (a) Schematic diagram of an onion-like structure of alternate multifold CdS (1.7 eV)/CdSe (2.5 eV) structure and its corresponding energy diagram. (b) UV−vis absorption and PL spectra. (c) Corresponding luminescence image for the samples under UV lamp irradiation.
Reprinted with permission from ref 310. Copyright 2006 American Chemical Society.

of another".The advantage of lattice mismatch between the core and shell material is that the shell can grow to a significant thickness without losing its luminescence properties. Over the past few years, researchers have concentrated mainly on this type of particle because of their exciting applications. The concept of a multilayer semiconductor particle was first developed by Eychmüller et al.[291] Later the same group as well as many other research groups published in this area.[83,111,292−301] In multilayer QDs, such as core, double shell (CSS) materials, if a smaller band gap semiconductor material is embedded between a core and the outer shell of the material with the larger band gap, the particle is called a quantum dot quantum well (QDQW) (as shown in Figure 12). The selection of core and shell materials is carried out mainly taking into consideration the band gap as well as the lattice structure of the material used to form the CSS semiconductor particles. Some examples are CdSe/CdTe/ZnSe,[297] CdSe/CdS/$Zn_{0.5}Cd_{0.5}S$/ZnS,[299] $InAs_xP_{1-x}$/InP/ZnSe,[298] InAs/CdSe/ZnSe,[300] CdSe/HgTe/CdTe,[301] CdS/HgS/CdS,[83] CdSe/CdS/ZnS,[211] CdS/CdSe/CdS,[302] and CdSe/ZnS/CdSe.[279] The concept of the multishell semiconductor has been extensively documented by Dorfs and Eychmuller.[111] Alternate multilayered CdS/HgS/CdS is another example of a QDQW studied by many researchers.[83,291,303,304] The photo or optical stability of

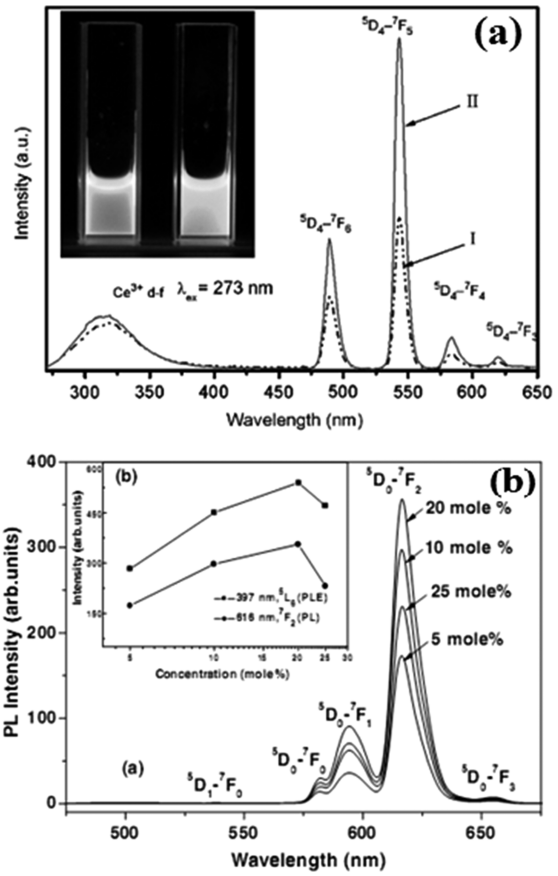

Figure 14. (a) Emission spectra of LaF_3:Ce^{3+}, Tb^{3+} NCs (I) and LaF_3:Ce^{3+}, Tb^{3+}/LaF_3 core/shell NCs (II); inset, photographs showing green fluorescence from these two samples. (b) The comparison of the room temperature photoluminescence (PL) and photoluminescence excitation (PLE) spectra of nanocrystalline TiO_2:Eu_x powders as a function of the amount of Eu.
(a) Reprinted with permission from ref 312. Copyright 2009 Elsevier Inc. (b) Reprinted with permission from ref 313. Copyright 2006 Elsevier Ltd.

this multilayered particle is comparable to that of CdS/HgS because of the further coating of the high band gap compound CdS. For the same reason, the quantum yield also increases. Here, since the particles of the low band gap compound HgS (ΔE = 2.1 eV) are sandwiched between the high band gap compound CdS (ΔE = 2.42 eV), the electrons are confined within the HgS layer and form a quantum well. Subsequently, different research groups studied similar multilayer quantum wells such as ZnS/CdS/ZnS[305] and CdS/CdSe/CdS.[306] The types of particles used in them were synthesized by SILAR (successive ionic layer adsorption and reaction) techniques.[299,307] The "reverse of QDQW", that is, a high band gap material sandwiched between low band gap semiconductor materials, has also been studied. In the case of CdSe/ZnS/CdSe,[279,308] with CSS type semiconductor particles, because of the higher band gap of the inner ZnS material, both the core and the outer CdSe layer emit two different wavelengths of light. This type of phenomena is used to generate white-light-emitting diodes (WLEDs) by multicolor emission within the range.[308,309] In their theoretical studies, Nizamoglu and Demir[308] showed spontaneous multicolor emission from multilayered heteronanocrystals

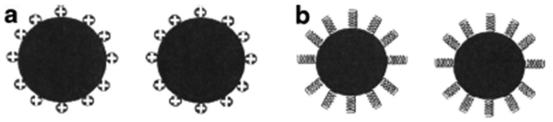

Figure 15. Particles stabilized by (a) the electrostatic layer and (b) steric repulsion.
Reprinted with permission from ref 78. Copyright 2008 American Chemical Society.

of onion-like (CdSe/ZnS)/CdSe/ZnS [(core)/shell/shell] structures (QDQW). The schematic diagram of an onion-like structure of alternate multifold CdS/CdSe structure as well as corresponding energy diagram, UV−vis and PL spectra, and luminescence image of the samples are shown in Figure 13a−c, respectively. As shown in the figure, the outermost shell plays an important role in PL QYs, and PL lifetimes of the core/multishell nanoparticles. In this specific case, the PL QY increases when the outmost shell is CdS; however, that with CdSe shell decreases dramatically.

2.1.4. Lanthanide Nanoparticles. Some of the problems associated with semiconductor QDs include oxidization and quenching, as well as toxicity to the human body, and this hinders their use in specific applications. The light emission effect of QDs also depends on size. Furthermore, at present, QDs are prohibitively expensive for most commercial applications. Other than semiconductor QD materials and organic light-emitting materials, lanthanide-doped dielectric nanoparticles, such as TiO_2:Eu^{3+}, $NaYF_4$:Yb,Er, and $LaPO_4$:Er,Yb, also have light emission effects. As a result, replacing QDs for biolabeling by rare earth-doped inorganic/inorganic core/shell particles is another option. Therefore, more recently researchers have been trying to dope rare earth materials onto dielectric materials for light emission purposes. Study of inorganic/inorganic core/shell nanoparticles with rare earth ions is currently an area of great research interest. Various research groups have also studied the optical properties and the stability of these types of particles.[220,221,223−225,227−230,311−314] The core of this type of particle is made of one or more of the lanthanide group elements, and the shell is made of silica or any other lanthanide group element. Some of the advantages of these particles are a high emission efficiency equivalent to the bulk materials, being easily dissolved in common solvents, and finally being able to attach onto polymeric matrices.[315] In addition, these types of particles are also fluorescently active, emit light in the visible range, which is easy to detect, are less toxic compared with semiconductor QD particles, and are water-soluble. Hence these are more suitable for biological applications. The doping of any lanthanide metal ion onto the base lanthanide salt also improves the photoluminescence intensity. Xi et al.[312] studied lanthanide core/shell nanoparticles where LaF_3 is the base material for both core and shell, but Ce^{3+}, Tb^{3+} doping on the core and coating with the same LaF_3 material was shown to improve the emission intensity at least 2-fold as shown in Figure 14 a.[312] The photoluminescence intensity also depends on the concentration of the doping materials. Normally, with increasing dopant concentration the PL intensity of the light also increases. For example, the doping of Eu onto TiO_2 with up to 20% Eu concentration, the PL intensity of the light first increases but then decreases on further increasing the concentration of Eu (as shown in Figure 14b).

Table 3. Class I, Magnetic Core/Organic Shell Nanoparticles (Class IA, Metal Core, and Class IB, Metal Oxide Core) and Class II Nonmagnetic Core/Organic Shell Nanoparticles (Class IIA, Metal Core, Class IIB, Metal Oxide Core, and Class IIC, Metal Salt and Metal Chalcogenide Core)[a]

	synthesis techniques and reagents used				
	core		shell		
core/shell	method	basic reagent	method	basic reagent	ref
Class I: Magnetic Core/Organic Shell Nanoparticles					
Class IA: Metal Core					
Fe/PIB	TD	$Fe(CO)_5$		PIB	325
Fe/PS	TD	$Fe(CO)_5$		PS	325
Fe/dextran	wet chemical reaction	$FeCl_3$		dextran	326,327
Class IB: Metal or Metalloid Oxide Core					
Fe_3O_4/PEG	coprecipitation	$FeCl_3$		PEG (mol wt. 4000)	77
Fe_3O_4/PEGMA	coprecipitation	$FeCl_3 \cdot 6H_2O$, $FeCl_2 \cdot 4H_2O$	RAFT	PEGMA	328
Fe_3O_4/PLA	coprecipitation	$FeCl_3 \cdot 6H_2O$, $FeCl_2 \cdot 4H_2O$	ring-opening polymerization	L-lactide	329
Fe_3O_4/PGMA/PS	coprecipitation	$FeCl_3$, $NaNO_2$	polymerization	GMA, EDMA	330
Fe_3O_4/MPEG	wet chemical reaction	$FeCl_3 \cdot 6H_2O$, $FeCl_2 \cdot 4H_2O$		MPEG (mol wt. 5000)	184
Fe_3O_4/starch				starch	
Fe_3O_4/PEO−PPO−PEO block polymer	reduction	$FeCl_3$		block polymer PEO−PPO−PEO	331
Fe_3O_4/poly(2-hydroxyethyl methacrylate)-*graft*-poly(ε-caprolactone)	hydrothermal degradation	$Fe(OCOCH_3)_3$	polymerization	pentamethyldiethylenetriamine	332
Fe_3O_4/PEG	wet chemical reaction	$FeCl_2 \cdot 4H_2O$, $FeCl_3 \cdot 6H_2O$		PEG-400	333
Fe_2O_3/polyorganosiloxane	coprecipitation	$FeCl_2$, $FeCl_3$	polycondensation	TMMS, DEDMS, ClBz-T	334
γ-Fe_2O_3/PEI+PEO−PGA	coprecipitation	$FeCl_2$, $FeCl_3$	SP	PEO−PGA	335
γ-Fe_2O_3/poly(2-MAOETIB)	precipitation	iron oxide, gelatin	EP	2-MAOETIB	336
iron oxide−SiO_2 composite/PS	Massart method with Stöber method	$FeCl_2$, $FeCl_3$, TEOS	polymerization	styrene	337
$CoFe_2O_4$/DTPA−CS	low-temperature solid-state method	$CoCl_2 \cdot 6H_2O$, $FeCl_3 \cdot 6H_2O$, NaCl	emulsion cross-linking polymerization	CS, DTPA	338
Class II: Nonmagnetic Core/Organic Shell Nanoparticles					
Class IIA: Metallic Core					
Au/aryl polyether	reduction	$HAuCl_4$	self-assembly	disulfide dendrons	339
Au/PSS and PDADMAC	reduction	$HAuCl_4$	layer by layer coating	PSS, PDADMAC	340
Au/organosilica	reduction	$HAuCl_4$	Stöber method	TEOS	341
Au/PSMA		gold sol	copolymerization	methacrylic acid, styrene	342
Ag/PS	reduction	$AgNO_3$	EP	styrene	105
Ag/TC	reduction	$AgNO_3$		TC	343
Ag/sulfonated polyaniline	reduction	$AgNO_3$		sulfonated polyaniline	169
Ag/PEG−HA hybrid nanogels	reduction	$AgNO_3$	precipitation polymerization	MEO_2MA, PEGDMA	344
Ag−Au/PEG−HA hybrid nanogels	galvanic replacement of Ag by Au in Ag/PEG−HA hybrid nanogels	$HAuCl_4$			
Class IIB: Metal or Metalloid Oxide Core					
ZrO_2/PMMA	alkaline hydrolysis in microemulsion	$ZrO(NO_3)_2$	EP	MMA	345
SiO_2/PMMA	Stöber method	TEOS	EP	MMA	346
SiO_2/PS	Stöber method	TEOS		PS	347
SiO_2/poly(3-aminophenylboronic acid)	Stöber method	TEOS	polymerization	APBA	348

dx.doi.org/10.1021/cr100449n |*Chem. Rev.* 2012, 112, 2373–2433

Table 3. Continued

	synthesis techniques and reagents used				
	core		shell		
core/shell	method	basic reagent	method	basic reagent	ref
SiO_2/PS	sol−gel	TEOS	DP	styrene	349
SiO_2/PS	Stöber method	TEOS	polymerization	styrene, MPTMS	350
SiO_2/chitosan		silica		commercial chitosan	351
TiO_2/PS2	sol−gel	TIP, TMAO	polymerization	styrene, PMDETA	352
TiO_2/PS	sol−gel	TIP, TMAO, OA	ligand exchange	PS2	352
Sb_2O_3/PMMA/PVC	polymerization	Sb_2O_3 and MMA		PVC	353
TiO_2−SiO_2/PMMA	hydrolysis	silicic acid, $TiCl_4$	polymerization	MMA	354
SnO_2/graphene	high temperature reflux	$SnCl_2$, H_2O, PEG	reduction	graphene oxide	355
	Class IIC: Metal Salt and Metal Chalcogenide Core				
$CaCO_3$/PS		$CaCO_3$	EP	styrene	356
CdS/thiol	precipitation	$CdSO_4$, H_2S		thiol	357
CdS/PMMA	high-temperature TD	Cd−oleylamine complexes, sulfur	DP	MMA	358
Mn-doped CdSe/ hexadecylamine	reduction with precipitation	$CdCl_2$, Se powder, $MnCl_2 \cdot 4H_2O$		hexadecylamine	359
ZnSe/ascorbic acid	reduction precipitation	$ZnCl_2$, Se powder		ascorbic acid	360

[a] Abbreviations: PIB, polyisobutylene; TD, thermal decomposition; RAFT, reversible addition−fragmentation polymerization; PEGDMA, poly(ethylene glycol) dimethacrylate; PSMA, polystyrene methacrylate; PEA, poly(ethylene amine); MAOETIB, 2-methacryloyloxyethyl(2,3,5-triiodobenzoate); PEO-PGA, poly(ethylene oxide)-*block*-poly(glutamic acid); PEO−PPO−PEO, poly(ethylene oxide)−poly(propylene oxide)−poly(ethylene oxide); TIP, titanium isopropoxide; TMAO. trimethylamine-*N*-oxide; MPTMS, methacryloxypropyltrimethoxysilane; APBA, 3-aminophenylboronic acid; MEO2MA, 2-(2-methoxyethoxy)ethyl methacrylate; PSS, poly(styrenesulfonate); PDADMAC, poly(diallyldimethylammonium chloride); GMA, glycidyl methacrylate; EDMA, ethylene glycol dimethacrylate; CVD, chemical vapor deposition; SP, suspension polymerization; PEGMA, poly(ethylene glycol) monomethacrylate; PLA, polylactide; PGMA/PS, poly(glycidyl methacrylate)/polystyrene; MPEG, methoxypoly(ethylene glycol); $CoFe_2O_4$, cobalt ferrite; DTPA, diethylenetriaminepentaacetic acid; CS, chitosan; TMMS, trimethoxymethylsilane; DEDMS, diethoxydimethylsilane; ClBz-T, (chloromethylphenyl)trimethoxysilane; TC, 3,3′-disulfopropyl-5,5′-dichlorothiacyanine sodium salt; PMDETA, pentamethyldiethylenetriamine; PS2, phosphonate-terminated polystyrene; OA, oleic acid.

Particles consisting of a magnetic core iron oxide coated with ytterbium (Yb) and erbium (Er) codoped with sodium yttrium fluoride ($NaYF_4$:Yb,Er) have both magnetic and high fluorescence properties, as well as good bioaffinity.[221] This type of nanoparticle shows high luminescence and has potential application in the field of electronics and bioimaging.[221,228,313]

2.2. Inorganic/Organic Core/Shell Nanoparticles

Inorganic/organic core/shell nanoparticles are made of metal, a metallic compound, metal oxide, or a silica core with a polymer shell or a shell of any other high density organic material. The advantages of the organic coating on the inorganic material are many fold. One example is the fact that the oxidation stability of the metal core is increased when otherwise the surface atoms of the metal core can be oxidized to the metal oxide in a normal environment.[316,317] In addition, they exhibit enhanced biocompatibility for bioapplications.[318−321] The polymer-coated inorganic materials have a broad spectrum of applications, ranging from catalysis to additives, pigments, paints, cosmetics, and inks.[322] In many applications, the particles are coated to stabilize them in the suspension media, and the stability of such a colloidal suspension depends mainly on the attractive and repulsive forces between the particles. There are four different types of forces: (i) van der Waals forces, (ii) induced short-range isotropic attractions, (iii) electrostatic repulsion, and (iv) steric repulsion. Depending on the synthesis media, the electrostatic and steric repulsion forces can be controlled (schematically shown in Figure 15) and hence the aggregation of the nanoparticles can be prevented.[78,323] For aqueous media electrostatic and for organic media steric repulsion forces predominate where particle stabilization is concerned. Therefore, in order to control these forces a uniform coating of a suitable material is essential. The topic of metal, semiconductor, or metal or metalloid oxide core nanoparticles with high density polymer or hyperbranched polymer shell coatings has been extensively reviewed by Advincula.[324] Depending on the material properties of the core particles, they can be broadly classified into two different groups: (i) magnetic/organic and (ii) nonmagnetic/organic core/shell nanoparticles. Different inorganic/organic core/shell nanoparticles are listed in Table 3 according to their classified category.

2.2.1. Magnetic/Organic Core/Shell Nanoparticles.

Magnetic nanoparticles with any polymer coating are used mainly for magnetic recording,[361] magnetic sealing,[362] electromagnetic shielding, MRI,[87,90,93,363,364] and especially in the biological field for specific drug targeting, magnetic cell separation, etc.[90,365−367] Magnetic core particle synthesis using wet chemical processes is very common[184,368−371] because of the advantages of obtaining good crystallinity and magnetization. The principal problem encountered is the formation of bigger size particles (order of micrometers). The stability of the magnetic nanoparticles under

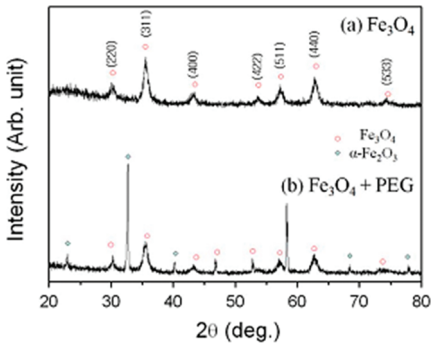

Figure 16. XRD pattern of naked Fe_3O_4 and PEG-coated Fe_3O_4. Reprinted with permission from ref 77. Copyright 2009 IEEE.

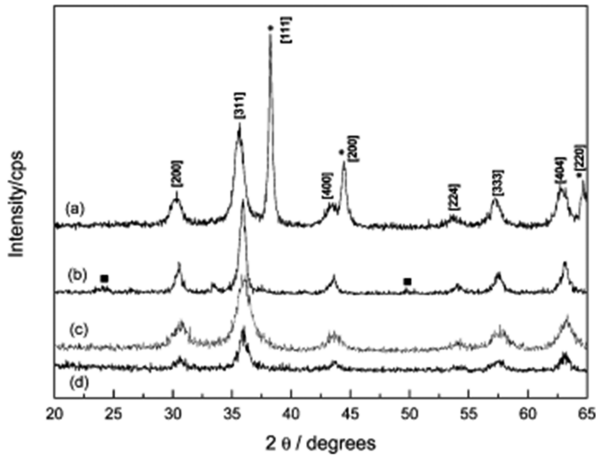

Figure 17. Powder X-ray diffraction patterns of (a) Au-coated, (b) MPEG-coated, (c) uncoated, and (d) starch-coated SPIONs: (∗) Au peaks; (■) MPEG peaks.
Reprinted with permission from ref 184. Copyright 2004 American Chemical Society.

an external high applied magnetic field is very important for *in vivo* biological application as well as in other fields. Therefore, in order to get a higher suspension stability of the particles by reducing the agglomeration, the magnetic nanoparticles are coated with different organic materials. Hydrophilic polymers[76,77,184,367] and polysaccharides[87,326,372−374] among others are very common. The stability of the magnetic nanoparticles has been extensively reviewed by Laurent et al.[78] Poly(ethylene glycol) (PEG) is a water-soluble biocompatible polymer, which has been studied by different researchers with a view to examining it as a magnetic particle coating because of its greater biocompatibility. Balakrishnan et al.[76] synthesized magnetic iron (Fe) core particles in aqueous media using the chemical reduction of $FeCl_2$ with sodium borohydride and coated with amine-terminated poly(ethylene glycol) (aPEG). They mainly studied the effects of the reactant concentration on particle size, crystallinity, and magnetic properties. According to their results, the particles become more amorphous with increasing reactant concentration. These types of particles can be used for the magnetic separation of biochemical compounds, cells, and also for controlled drug release within the body.[93] Both the crystalline structure and the composition of core magnetite nanoparticles can sometimes change during the coating process. As an example, magnetic Fe_3O_4 particles partially changed to α-Fe_2O_3 after applying a very thin surface coating of PEG outer shell (as shown in Figure 16).[77]

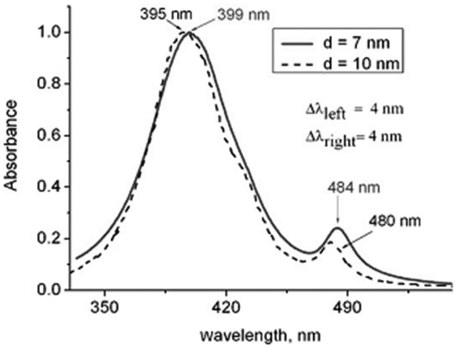

Figure 18. A comparison of the absorption spectra of Ag/TC core/shell nanoparticles in aqueous solutions, obtained for an average diameter of Ag core of 7 nm (solid line) and 10 nm (dotted line).
Reprinted with permission from ref 343. Copyright 2008 Elsevier Ltd.

Dextran, a polysaccharide polymer composed of exclusively *R*-D-glucopyranosyl units with varying degrees of chain length and branching, is also widely used as a shell coating.[326,372−376] Dextran is used as a polymeric shell because of its high biocompatibility. It in turn increases the biocompatibility of the magnetic nanoparticles to the extent that they can be used in *in vivo* applications. Side-chain-functionalized dextran coated ultrasmall superparamagnetic iron oxides (USPIO) show a prolonged blood residence time, which allows these USPIO particles to access the macrophages located in deep pathological tissues (such as lymph nodes, kidney, brain, osteoarticular tissues, etc.).[326,327] Dextran-coated Fe nanoparticles are also used for labeling red blood cells (RBC) in cell separation studies using high gradient magnetic chromatography (HGMC).[327]

Recently, a special interest on superparamagnetic iron oxide nanoparticles (SPIONs) has emerged because of their high biocompatibility and the fact they exhibit less residues. In fact the magnetic property of these particles vanishes after the removal of the external magnetic field.[77,376−382] As a result, the aggregation tendencies, because of interaction between the particles, are fewer and hence, particles can be more easily removed from the blood circulation system. At the same time, these particles are less toxic compared with other metal or metal oxide nanoparticles.[381,383] Mikhaylova et al.[184] synthesized SPIONs with three different biocompatible coatings: starch, methoxypoly(ethylene glycol) (MPEG), and gold (Au). According to them, the particle size does not change significantly on the shell material but the crystallinity strongly depends on the shell material. In the presence of a Au coating, the particles are more crystalline compared with those with an organic or even no coating. A comparison of two organic coatings reveals that the MPEG-coated particles are more crystalline than starch-coated particles (shown in Figure 17).

2.2.2. Nonmagnetic/Organic Core/Shell Nanoparticles.

These particular types of nanoparticles are equally important to organic-coated magnetic nanoparticles because of their wide range of applications. The nonmagnetic inorganic materials can be further subdivided into metal, metal oxide, and metal salt particles coated with different organic materials. These will now be discussed in the following sections.

2.2.2.1. Metal/Organic Core/Shell Nanoparticles. Different metal/organic composite particles play an important role in biological applications, since their surfaces are rich in functional groups can

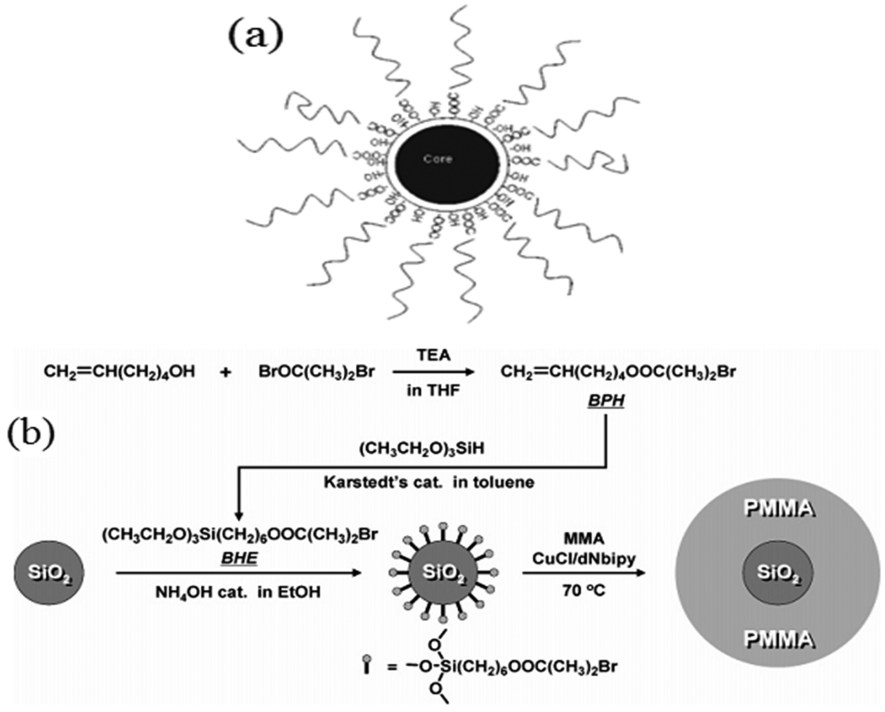

Figure 19. (a) A schematic view of the functionalized shell (Ag/Au)/ZrO_2/stearate core−shell nanocomposite. The core has a diameter of 15 nm and the ZrO_2 shell has a thickness of 3−4 nm. The zigzag chains in the figure correspond to the stearic acid chains. The presence of −OH groups between the chains is to indicate the presence of surface bound hydroxyl groups on ZrO_2. The chains do not interact with each other making a liquid-like assembly. Some of the chains may even be bent. (b) Schematic representation for the synthesis of polymer-coated silica particles by surface-initiated atom transfer radical polymerization.
(a) From ref 389, Reproduced by permission of The Royal Society of Chemistry. (b) Reprinted with permission from ref 399. Copyright 2005 American Chemical Society.

be easily tailored for bioconjugation purposes.[340,342,384] Nanoscale noble metals such as Au and Ag have attracted considerable attention because of their unique optical properties involving localized surface plasmon resonance.[385] The external field can create Raman scattering or surface fluorescence from nanoparticles consisting of Au or Ag core coated with the cyanide dye, the J-aggregate of 3,3′-disulfopropyl-5,5′-dichlorothiacyanine sodium salt (TC). These particles have been studied for potential applications as sensors and bioimaging materials.[343] The J-aggregate is a type of dye that has a specific absorption band that shifts to a longer wavelength with increasing sharpness (a higher absorption coefficient) when it aggregates under the influence of any external field such as a solvent or additive, and the emission occurs from this dye because of supramolecular self-organization with high intensity light. Results show that for a decrease in core size (10−7 nm) for core/shell nanoparticles, there is a red shift of 4 nm for both the absorbance peaks (shown in Figure 18). Au coated with polyaniline (PANI) is used as a biosensor for sensing the glucose in living systems.[386] Polymer-coated Au metal shows second harmonic generation (SHG) properties.[342] Second harmonic generation (SHG) is a nonlinear optical process in which a monochromatic light impinges on a surface lacking symmetry and can lead to the generation of light at a frequency twice that of the incident light (i.e., the second harmonic) and half the wavelength of the initial photons. They also studied the SHG properties of a chemically linked naphthyl styryl chromophore with polymer-coated gold particles and found an increase to 21% ± 9% compared with the polymer only compound.[342] A polymer-coated Ag nanocomposite material is utilized as a high-dielectric constant (K) polymer matrix in order to enhance the dielectric properties of such composite materials.[387,388]

2.2.2.2. Metal or Metalloid Oxide/Organic Core/Shell Nanoparticles. The formation of metal oxide nanoparticles using a chemical reaction is an easy task. However, maintaining the smaller sized particles in a dispersing media is difficult, because of their high tendency for growth and agglomeration. The best method for solving this problem is to coat the particles with a monolayer of polymer coating, which can be easily removed when required.[389] Organic materials coated with different metal oxides, especially transition metal oxides, are very important because of their excellent applications in the fields of catalysis,[390] optics,[391−393] controlled release,[394] material additives (filler),[395−398] and so on. A schematic presentation of organic monolayer coatings on inorganic core particles is shown in Figure 19a. The most common polymers used as organic coatings on silica cores are poly(methyl methacrylate) (PMMA),[346,354,399] polystyrene (PS),[347] poly(3-aminophenylboronic acid),[348] and poly(vinyl chloride) (PVC).[353] Polymer-coated silica nanoparticles increase colloidal stability and are broadly used in optical devices, sensors, catalysis, controlled release, material additives (fillers), and electrical devices. The schematic diagram of polymer coatings on silica cores is shown in Figure 19b.[347,348,400]

Natural polymers such as cellulose are used as a coating on TiO_2 nanoparticles to improve the pigment properties. Polystyrene-coated TiO_2 is used for the fabrication of higher capacitance (K) gate dielectric for flexible electronics applications.[352] Polymer-coated inorganic particles such as calcium phosphate find applications in dentistry as a brace material and filler.[401,402]

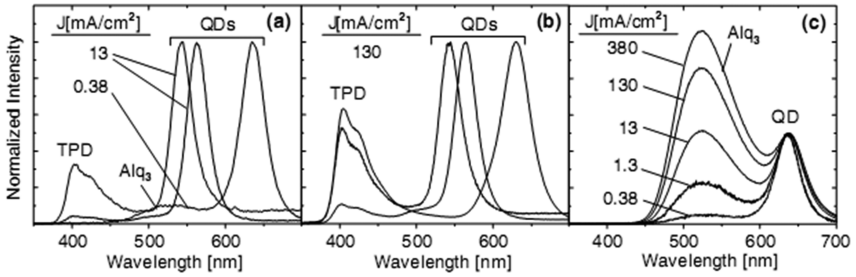

Figure 20. Typical normalized QD-LED electroluminescence spectra of three different sized CdSe QD samples measured at (a) low current levels (0.38−13 mA/cm^2), where most (>70% in all cases) of the emission is from the QDs in the device, with only small spectral contributions from either Alq_3 (when 3-(4-biphenylyl)-4-phenyl-5-*tert*-butylphenyl-1,2,4-triazole (TAZ) layer is omitted) or TPD (when TAZ layer is present), (b) moderate current levels (130 mA/cm^2), where two of the three spectra have a large fraction of EL from TPD, and (c) a progression of currents for a single device (from 0.38 to 380 mA/cm^2). Note that the devices emitting at 540 and 560 nm are the same in panels a and b. At low currents, a larger portion of the excitons are created within a Förster energy transfer radius of the QD monolayer. For all devices, 0.2% < photoluminescence quantum efficiency (η_{EL}) < 0.5%.
Reprinted with permission from Ref 404. Copyright 2003 Elsevier Ltd.

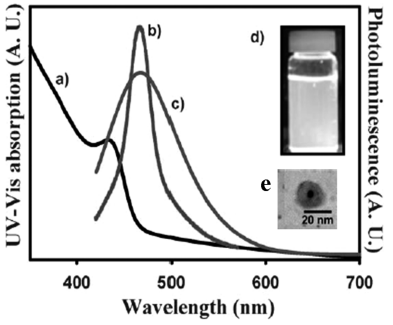

Figure 21. (a) UV−vis absorption of CdS core, (b) PL spectrum of CdS core, (c) PL spectrum of CdS/PMMA core/shell NPs, (d) emission photograph of CdS/PMMA core/shell NPs, and (e) a magnified TEM image of a single core/shell NP.
From ref 358, Reproduced by permission of The Royal Society of Chemistry.

Different inorganic metal oxides (Fe, Ti, Zr) coated with organic shell materials were also synthesized from their respective metal salts in TX-100 microemulsion systems.[345]

2.2.2.3. Metal Chalcogenide or Metal Salt/Organic Core/Shell Nanoparticles. Metal salts coated with conductive polymers such as polyaniline (PANI), polypyrole (PPy), and polythiophene (PTh) have attracted much interest for use in different applications in light-emitting devices,[403−405] electronic devices,[406,407] and chemical sensors[408] and as antistatic coatings.[409,410] However, commercialization of these particles is difficult because of the poor processability of these polymers. Polymer coatings on CdSe QDs improve the light-emitting properties compared with naked QDs. The contribution of the organic layer to the spectra is higher compared with QDs at higher current levels (shown in Figure 20).[404] On the other hand, a PMMA coating on CdS does not affect the optical properties of the core because of its transparency. In addition, it also protects the optical properties of the material from environmental disturbance.[358] Figure 21a shows a core particle with a UV−vis spectrum with a maximum absorption peak at 436 nm. The core particle exhibited a sharp emission peak at 467 nm, and there is blue shift (510 nm) evident after coating with the polymer. In addition, there is also no significant loss evident in quantum yield (∼12% to ∼8%) after polymer coating.

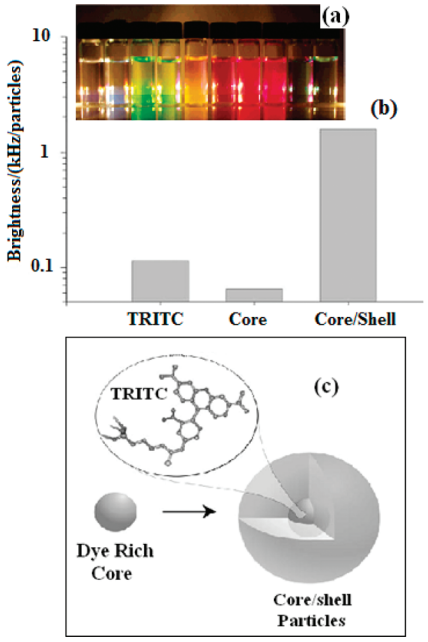

Figure 22. (a) Core/shell fluorescent silica nanoparticles using different dye species in the core including (left to right): AlexaFluor 350, *N*-(7-dimethylamino-4-methylcoumarin-3-yl)maleimide, AlexaFluor488, fluorescein isothiocyanate, tetramethylrhodamine isothiocyanate, AlexaFluor 555, AlexaFluor 568, Texas Red, AlexaFluor 680, and AlexaFluor 750, (b) a comparison of the brightness of free TRITC dye with same-sized C-dots and quantum dots in water at the same optical density, and (c) a schematic representation of the dye-rich core−shell architecture of the C-dot particles, in this case covalently incorporating the organic dye tetramethylrhodamine isothiocyanate (TRITC).
(a, b) Reprinted with permission from ref 452. Copyright 2005 American Chemical Society. (c) From ref 453, Reproduced by permission of The Royal Society of Chemistry.

Polymer-coated AgCl nanoparticles[408] are useful for sensor applications. Polymer-coated $CaCO_3$ shows improved mechanical properties as a filler material and is useful in different applications.[356,411] Polystyrene-coated $CaCO_3$ is widely used in the manufacture of paint, paper, rubber, plastics, etc. It was found that instead of pure $CaCO_3$, a poly(butylene tetraphthalate) (PBT) coating on stearic acid-modified $CaCO_3$ improves the

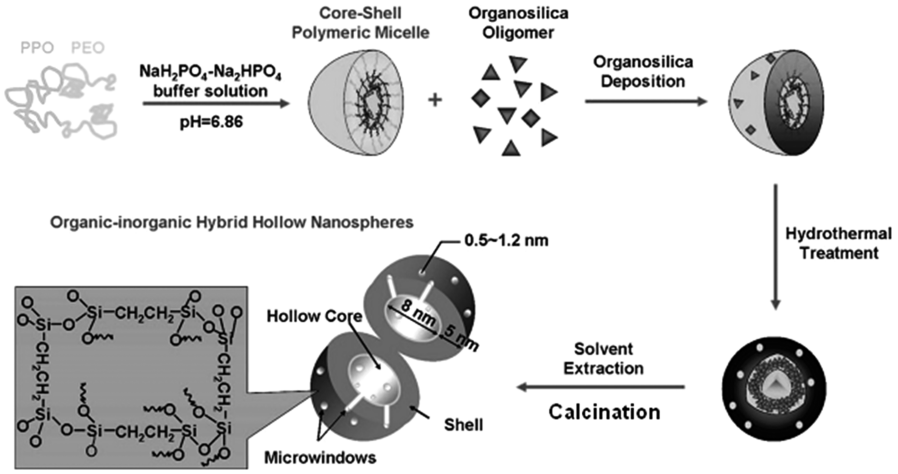

Figure 23. Schematic diagram of hollow nanoparticles synthesized using organic sacrificial core method. Reprinted with permission from ref 456. Copyright 2008 American Chemical Society.

mechanical, thermal, and structural properties of the $CaCO_3$. As an example, the tensile strength of stearic acid-modified $CaCO_3$ increases from 56 to 58.9 MPa because of the PBT coating; 80% weight fraction of the overall material.[412]

2.3. Organic/Inorganic Core/Shell Nanoparticles

Organic/inorganic core/shell nanoparticles are structurally just the reverse of the previous types describe above. The core of this particular class of core/shell nanoparticles is made of a polymer, such as polystyrene,[413−422] poly(ethylene oxide),[423,424] polyurethane,[80,425] poly(vinyl benzyl chloride),[426] poly(vinyl pyrrolidone),[427] dextrose,[428] surfactant,[429−432] and different copolymers, such as acrylonitrile−butadiene−styrene,[433] poly(styrene−acrylic acid),[434] and styrene−methyl methacrylate.[435] The shell can also be made from different materials, such as metals,[80,415,422,426] metal oxides,[413,419,424,427,428,435−440] metal chalcogenides,[434,441] or silica.[413,418,423,425,429,430,433,442−446] These types of particles, in general, have the dual properties of both the inorganic and organic materials.[447] The inorganic material, especially a metal oxide coating on an organic material, is beneficial in several respects, such as increased strength of the overall material,[448,449] resistance to oxidation, thermal and colloidal stability,[450] and abrasion resistance.[346,448,451] At the same time, these particles also show polymeric properties such as excellent optical properties, flexibility, and toughness, and in addition they can improve the brittleness of the inorganic particles.[418] Recently, this type of nanoparticle proved of great research interest because of their extensive applications in different fields of material science, including paints, magnetic fluids, catalysis, microelectronics, and biotechnology.[108] The noble metals such as gold and silver coated onto polymer materials increase the immobilization characteristics of protein; as a result these particles can be used in different areas of biotechnology, immunosensing, and biomedical applications.[80,344] Phadtare et al.[80] synthesized gold-coated polyurethane microsized core/shell particles for applications where biocatalytic activity was required in such applications as pepsin digestion. Organic/inorganic core/shell nanoparticles coated with a silica shell with fluorescent properties are very important in nanobiotechnology. The colors of the core/shell particles with different dye cores with silica shells are shown in the Figure 22a. C-dots fall into this category: they consist of dye/silica core/shell nanoparticles having a fluorescent brightness similar to quantum dots. Ow et al.[452] first reported the synthesis of different dye/silica core/shell nanoparticles in the size range 20−30 nm. The particular example of the tetramethylrhodamine isothiocyanate (TRITC) dye is shown in Figure 22b. It can be clearly seen that the brightness of the core is actually less than that of free TRITC, suggesting that the dense dye-rich core is heavily quenched compared with the free dye. Interestingly, after the coating of a dye-free silica shell onto the core, the brightness increases by a factor of 30. This enhancement is attributed to a change in the light emission properties of the organic dye because it is protected from the solvent by external silica coating.

Another interesting application of these types of particles is for the synthesis of hollow inorganic particles by using an organic material as the sacrificial core. The schematic diagram showing hollow nanoparticles synthesis by sacrificial organic core is shown in Figure 23. Many researchers have used different organic core materials for inorganic hollow particle synthesis.[80,413,414,420−422,426,434,435,454,455] A range of different organic/inorganic core/shell nanoparticles based on different core materials is listed in Table 4.

2.4. Organic/Organic Core/Shell Nanoparticles

In this category, both the core and shell particles are made of a polymer or another organic material. The different synthesis routes for different thermosensitive core/shell polymer nanoparticles have been reviewed by Ballauff and Lu.[463] These classes of particles are known as "smart particles" and have a wide range of applications in different fields, such as drug delivery,[464−466] biosensing,[467] chemical separation,[468] biomaterials,[469,470] and catalysis.[471−475] Different organic/organic core/shell nanoparticles that have been studied to date are listed in Table 5. The advantages of having a polymer coating on another polymer is to modify the physical properties of the overall material, such as toughness[476] or the glass transition temperature.[477,478] Depending on the intended application for the polymer/polymer type core/shell nanoparticles, they are chosen on the basis of their glass transition temperature (T_g). The glass transition temperature is an important characteristic of a polymer because below this temperature polymers are in what is called a "glassy state". When the temperature of the material crosses the glass transition temperature, the mechanical properties of the polymers change

Table 4. Organic/Inorganic Core/Shell Nanoparticles on the Basis of Different Core Materials[a]

	synthesis techniques and reagents used				
	core		shell		
core/shell	method	basic reagent	method	basic reagent	ref
PS/Cu, PS/Cu_2O	EP	styrene	hydrolysis with calcination	$Cu(NO_3)_2$	415
PS/Ag	DP	styrene	reduction	$Ag(NH_3)_2OH$, $SnCl_2$	422
PS/SiO_2	EP	styrene	sol−gel method	TMOS	421
		PS beads		SiO_2 sols	413
	cross-linking polymerization	styrene	Stöber method	TEOS	455
	EP	styrene	Stöber method	TEOS	420,457
	EP	styrene	Stöber method	TEOS	419
		PS beads	Stöber method	TEOS	438
PS/TiO_2		PS beads	alkaline hydrolysis	$TiCl_4$	413
	EP	styrene	sol−gel method	TBOT	416,421
PS/Fe_3O_4	EP	styrene	coprecipitation	$FeCl_2$, $2H_2O$	419
PS/Y compound	EP	styrene	reduction	$Y(NO_3)_3$	414
PS/ZnS		carboxylate modified PS (PS-CO_2)	coprecipitation	$Zn(CH_3COO)_2$	458
PS/Zr compound		PS beads	reduction	$Zr(SO_4)_2$	459
PU/SiO_2	polymerization or blending	PA, adipic acid, 1,4-butanediol, neopentyl glycol, 4-methyl-2-pentanone	Stöber method	TEOS	425
CU-dot/SiO_2		C-dots, polye thylene imine (PEI).	modified Stöber method	TEOS	443
PEG/Si/Al composite oxide		PEG	sol−gel	$Al(NO_3)_3$, TEOS	460
PEG/SiO_2		PEG (avg. M_w 18000−25000)	Stöber method	TEOS	444
PVBC/Pd	emulsion copolymerization	VBC, DVB	reduction	$PbCl_2$, HCOOH	426
PU/Au	DP	EHG, TDI, DBTDL	reduction	$HAuCl_4$	80
PVP/SiO_2		PVP (Avg. M_w. 40,000)	Stöber method	TEOS	444
CS-PAA/SiO_2		chitosan, polyacrylic acid	ion-exchange process	Na_2SiO_3, cation exchange resin (Amberlite 120)	445
Dextrose/TiO_2		dextrose	hydrolysis of TBOT	TBOT	428
PMMA/SiO_2	EP	MMA	Stöber method	TEOS	461
PS-MAA/SiO_2	EP	styrene, methyl acrylic acid	Stöber method	TEOS	457
		Surfactant			
CTAB/SiO_2		CTAB	Stöber method	TEOS $Na_2S_2O_3$,	430,442
CTAB/Ag_2S		CTAB	complex precipitation	$Na_2S_2O_3$, $AgNO_3$	431,432
SDS and TPAB/SiO_2		SDS, TPAB	Stöber method	TEOS	429
		Copolymer			
ABS/TiO_2	radical EP	acrylonitrile−butadiene, styrene	hydrolysis	$Ti(SO_4)_2$	427
PSAA/TiO_2	polycondensation	melamine, formaldehyde	hydrolysis	$TiO(SO_4)$	439
SMA/TiO_2	radical copolymerization	styrene, MMA	hydrolysis	TBOT	435
MF/SiO_2	EP	melamine, formaldehyde		nano-SiO_2 (commercial name Aerosil 200)	418
PS/TiO_2/SiO_2	DP	styrene, methyl acrylic acid	sol−gel	TBOT	462
PS/ZnS		PS	precipitation	$Zn(CH_3COO)_2$, $SC(NH_2)_2$	458

[a] Abbreviations: PS, polystyrene; PU, polyurethane; PMMA, poly(methyl methacrylate); MMA, methyl methacrylate; SMMA, styrene−methyl methacrylate (SMMA), ABS, acrylonitrile−butadiene−styrene; PSAA, poly(styrene−acrylic acid); PVBC, poly(vinyl benzyl chloride; PEG, poly-(ethylene glycol); PVP, polyvinylpyrrolidone; PA, phthalic anhydride; CS-PAA, chitosan−polyacrylic acid; TMOS, tetramethoxysilane; TEOS, tetraethoxysilane; TBOT, titanium tetrabutoxide or tetrabutoxide orthotitanate; TPAB, tetrapropylammonium bromide; CNT, carbon nanotube; MF, melamine formaldehyde; TPAB, tetrapropylammonium bromide; EHG, 2-ethyl 1,3-hexanediol; TDI, toluene diisocyanate; DBTDL, dibutyl tin dilaurate; VBC, 4-vinylbenzyl chloride; DVB, *p*-divinylbenzene; EP, emulsion polymerization; DP, dispersion polymerization; CTAB, cetyltrimethyl-ammonium bromide; $Na_2S_2O_3$, sodium thiosulfate; SDS, sodium dodecyl sulfate; TPAB, tetrapropylammonium bromide.

dx.doi.org/10.1021/cr100449n |*Chem. Rev.* 2012, 112, 2373–2433

Table 5. Organic/Organic Core/Shell Nanoparticles Based on Different Core Materials[a]

	synthesis techniques and reagents used				
	core		shell		
core/shell	method	basic reagent	method	basic reagent	ref
PS/NIPA	EP	styrene	seeded EP	NIPA	494
PS/PTBA	cross-linking polymerization	DIPB, styrene	free radical polymerization	TBA, EGDA	481
PS/styrene and MPS hybrid copolymer	EP	styrene	copolymerization	MPS, styrene	484
PLGA/DSPE-PEG-COOH		PLGA	self-coating of shell material	soybean lecithin, DSPE−PEG-COOH	482
PTBA/PS	free radical polymerization	TBA, EGDA	cross-linking free radical polymerization	DIPB, styrene	481
polyphenylene/PEO	chloromethylation with polymerization	dendrimer ($TdG_2(-10\ H)_{10}$), chloromethyloctylether, $SnCl_4$	anionic polymerization with nucleophilic substitution (Williamson reaction)	EO	468,495
perylenediimide Containing polyphenylene dendrimer/ PEO	copolymerization	EO, naphthalene pottasium	Williamson reaction	EO	468
poly(g-benzyl L-glutamate)/ PEO	polymerization	γ-BLG NCA		PEG	496
PNIPAM/DHEA		PNIPAM	cross-linking precipitation polymerization	PEG	496
PNIPAM/CMCS	EP	NIPAM, MBA, redox initiator APS and SPS		CMCS	497
TdG2/PS-PEO	chloromethylation with polymerization	dendrimer ($TdG_2(-10\ H)_{10}$), chloromethyloctylether, $SnCl_4$	Williamson reaction	PI, PEO	495
TdG2/PIP-PEO	chloromethylation with polymerization	dendrimer ($TdG_2(-10\ H)_{10}$), chloromethyloctylether, $SnCl_4$	Williamson reaction	PIP, PEO	495

[a] Abbreviations: NIPA, *N*-isopropylacrylamide; PNIPAM, poly(*N*-isopropylmethacrylamide); CMCS, carboxymethyl chitosan; MBA, *N*,*N*-methylenebisacrylamide; APS, ammonium persulfate; SPS, sodium pyrosulfite; DHEA, *N*,*N*′-(1,2-dihydroxyethylene)bisacrylamide; γ-BLG-NCA, γ-benzyl L-glutamate *N*-carboxyanhydride; PEO, poly(ethylene oxide); EO, ethylene oxide; PTBA, poly(*tert*-butyl acrylate); EGTA, ethylene glycol diacrylate; DIPB, 1,3-diisopropenyl benzene; PLGA, poly(D,L-lactic-*co*-glycolide); DSPE−PEG-COOH, 1,2-distearoyl-*sn*-glycero-3-phosphoethanolamine-*N*-carboxy(poly(ethylene glycol)); MPS, γ-methacryloyloxypro-pyltrimethoxysilane; DIPB, 1,3-diisopropenyl benzene; TBA, *tert*-butyl acrylate; TdG2, polyphenylene dendrimer; PEO, poly(ethylene oxide); PIP, polyisoprene.

from those of a glass (brittle) to a rubber (elastic) material. For example, a polymer coating on a polymer with a different T_g is used to modify latex-based paints.[479,480] A high T_g core material has the impact of improving the mechanical stability whereas a low T_g shell material improves the film-forming ability. Kirsch et al.[481] synthesized and characterized polystyrene/poly(*tert*-butyl acrylate) core/shell and inverse core/shell particles.

Polymer/polymer core/shell particles are also extensively used for controlled drug release applications in *in vivo* systems because of their good biodegradable and drug encapsulation property. Poly(D,L-lactic-*co*-glycolide) (PLGA) is a biodegradable organic polymer with a high capacity for encapsulating hydrophobic drugs. For example, 1,2-distearoyl-*sn*-glycero-3-phosphoethanolamine-*N*-carboxy(poly(ethylene glycol))2000 (DSPE−PEG-COOH)-coated PLGA core/shell particles were studied by Chan et al.[482] for use in controlled drug release in *in vivo* systems. They used soybean phosphatidylcholine or lecithin for the core surface modification with the shell DSPE−PEG-COOH mainly providing steric and electrostatic stabilization. The reaction scheme and results showing changing particle size with the molar ratio of lipid and PEG is shown in Figure 24. The authors mainly studied the stability factor of the core/shell particles and the drug release kinetics. They did this by changing various parameters for the *in vitro* system. According to their results, with increasing total lipid to polymer ratio, the drug release rate decreased significantly initially but after a long period of time, it then stayed almost the same. Polystyrene is the polymer of choice as core material for these types of particles.[481,483,484] The kinetics of PLGA/SPE−PEG-COOH core/shell particle formation by an emulsion polymerization method has also been studied by Ni et al.[484]

A blend of inorganic materials with the polymer was also found to increase the adhesion between the two polymers in the polymer/polymer core/shell nanoparticles; as a result, the mechanical properties improved. The addition of Sb_2O_3 nanoparticles as a blending agent during the synthesis of the PMMA core for the PMMA/PVC core/shell particles resulted in an enhancement of toughness and mechanical strength of the PVC.[353] The doping of the inorganic materials affects not only the properties of the polymer but also the properties of the inorganic materials.[474,475,485] The thermal sensitivity and catalytic activity of doped Ag metal on a shell material in a polystyrene

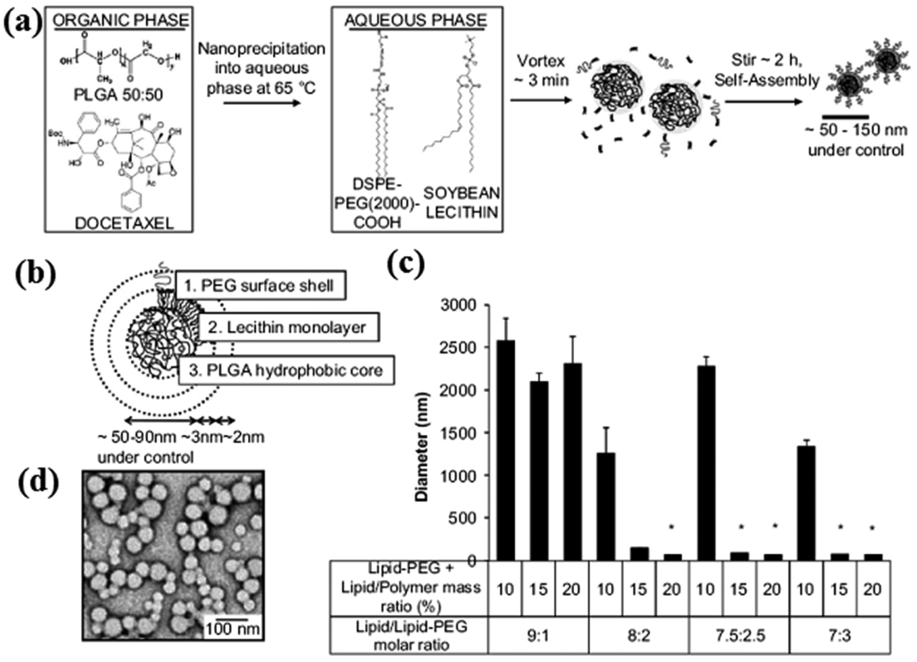

Figure 24. Synthesis of PLGA/lecithin/PEG core/shell NPs. (a) A schematic illustration showing the processes for preparing PLGA/lecithin/PEG NPs using a modified nanoprecipitation method. (b) The NPs are comprised of a hydrophobic poly(lactic-*co*-glycolic acid) (PLGA) core, a hydrophilic PEG shell, and a lecithin monolayer at the interface of the hydrophobic core and the hydrophilic shell. (c) By varying the parameters of total lipid/polymer mass ratio and lipid/lipid−PEG molar ratio, the NP size can be tuned in a physiological environment. The asterisk (∗) refers to optimal NP formulations. (d) A TEM image shows the core/shell structure of the NPs, which were negatively stained with uranyl acetate to enhance electron contrast between the polymers and the lipids.
Reprinted with permission from ref 482. Copyright 2009 Elsevier Ltd.

core and a poly(*N*-isopropylacrylamide) network cross-linked by *N*,*N*′-methylenebisacrylamide shell is much higher compare with normal Ag metal.[474,475]

Another interesting application of organic/organic core/shell nanoparticels is that with an organic dye (C-dot). C-dots coated with a polymer are promising as tools for sensing and imaging subcellular agents because they can be delivered into the cell cytoplasm. However, C-dots have physical properties that inhibit their free passage across the cell membrane. Generally, polyethyleneimine (PEI) is used to coat the C-dot particles because the PEI-coated C-dot particles act as an effective DNA delivery tool with a clear mechanism for achieving endosomal escape.[486] The results investigating the viability effects of C-dots, PEI, and PEI-coated C-dots on COS-7 cells in an *in vitro* study show that PEI alone affects COS-7 viability in concentrations above 50 μg/mL. However, C-dots and PEI-coated C-dots do not negatively affect cell viability over a range of concentrations 1−1000 μg/mL as shown in Figure 25a. Increased viability was found with increasing particle concentration. This could be attributed to the activation of the cells in the presence of the particles. They also studied the relative light-emitting capacity of the particles by varying the particle to DNA ratio for different coating materials (Results shown in Figure 25b). The results show that the transfection effect is maximum for a higher particle to DNA ratio for almost all the polymers compared with free DNA, except for eudragit EPO (EPO). The emitted light intensity is maximum for polyethyleneimine with a molecular weight of 25000 (MPEI).

In some cases, certain copolymers with functional groups undergo a cross-linking reaction with either core or shell to form stable spherical organic/organic core/shell nanoparticles. Several different shells cross-linked Knedel-like (SCK) core/shell nanoparticles with diameters between 5 and 100 nm were synthesized by Wooley.[487] The main advantages of these particles are that because they are nanostructured, they have a robust character, and the surface stability also changes with the environment conditions. The shell of these materials acts as a membrane that has a permeability to allow foreign materials to or out of the core. So, these type of materials can act as carrier materials and even mimic some biological systems and carry the designated material inside the cell. Generally this class of particle core is made of polystyrene;[488−490] but some other particles using block polymers are also available.[491−493]

2.5. Core/Multishell Nanoparticles

Among the core/multishell nanoparticles, bimetallics are very important. Rodríguez-González et al.[498] showed that for multishell bimetallic nanoparticles, the final shape depends on the selection of the core metal. For Au−Ag bimetallic multishell nanoparticles, the deposition of Ag on Au generates a pseudospherical geometry. However, deposition of Au on Ag leads to the preferential formation of polygonal particles with sharp facet intersections. The optical properties also change with the shell coating as shown in Figure 26. To begin, the gold colloid color was deep red; upon deposition of a silver shell, it turned yellow; a second gold shell led to a blue hue. Finally, after deposition of the second silver shell, an orange color was obtained. The optical plasmonic resonance of alternate multilayer core/shell particles of metal and dielectric material was studied by Radloff and Halas.[58] For this type of particle, because of the plasmon interaction of the internal and external metal layers, there will be a hybridization of the energy level metal plasmon bands to form symmetric and anitisymmetric plasmon resonances of

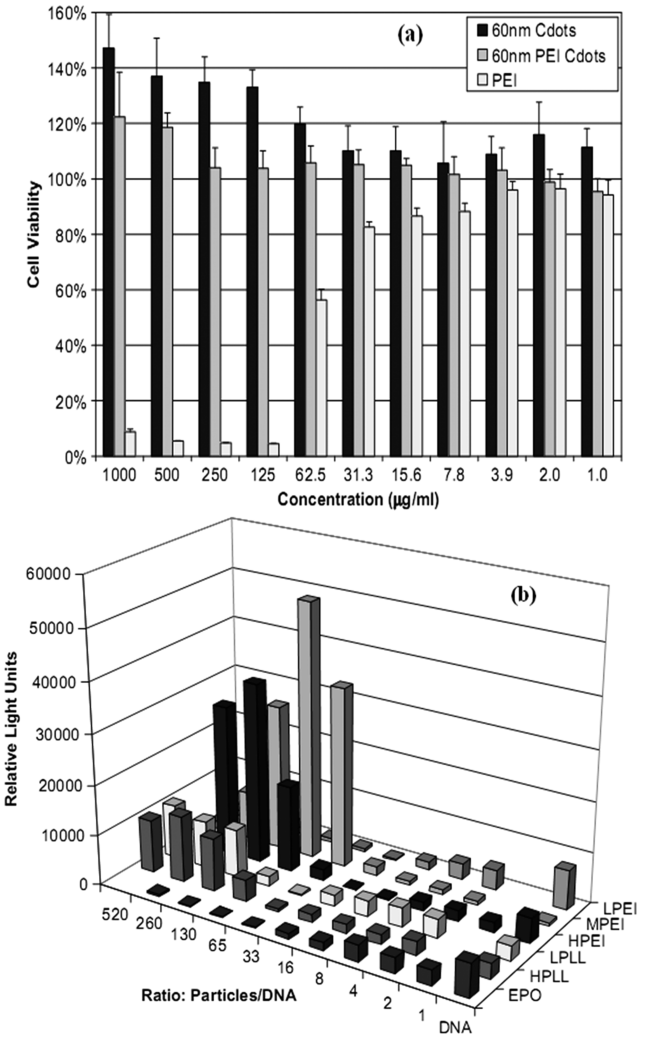

Figure 25. (a) Cell viability in the presence of PEI-coated C-dots. C-dots, PEI-coated C-dots, and free PEI were incubated with COS-7 cells, and the viability was analyzed after 24 h using the MTT cell proliferation assay kit (American Type Culture Collection) assay. (b) Transfection as measured by luciferase luminescence. C-dots coated with PEI MW 1800 (LPEI), PEI MW 25000 (MPEI), PEI MW 70000 (HPEI), poly-L-lysine low molecular weight (LPLL), poly-L-lysine high molecular weight (HPLL), and eudragit EPO (EPO) were complexed with DNA at the mass ratios indicated. DNA row indicates naked DNA with no polymer or particles.
Reprinted with permission from Ref 443. Copyright 2008 Elsevier Ltd.

different energies as shown in Figure 27. These plasmon resonance energies of the concentric multilayer nanoparticles can be calculated using the Mie scattering theory. When CdSe/ZnS core/shell QDs are coated with silica spheres, it improves their stability in biological buffers and biocompatibility in fluorescence imaging.[499] Silica-protected CdSe/ZnS QDs also act as stronger emitters with more consistent fluorescence intensity than naked core/shell nanocrystals. Organic coatings on inorganic core/shell nanoparticles change some properties; in particular, they increase solvent resistance and water dispersion capability. Inorganic core/shell nanoparticles Fe_3O_4/SiO_2 coated with poly(cyclotriphosphazene-*co*-4,4-sulfonyldiphenol) (PZS) have increased solvent resistance and water dispersion capability. The resulting high biocompatibility can be used directly for biological applications.[500]

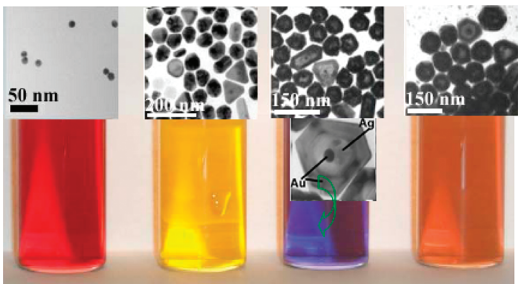

Figure 26. Color changes in colloidal dispersions of Au/Ag nanoparticles with increasing number of layers. Rodríguez-González, B.; Burrows, A.; Watanabe, M.; Kiely, C. J.; Liz-Marzán, L. M. *J. Mater. Chem.* **2005**, *15*, 1755, ref 498, Reproduced by permission of The Royal Society of Chemistry.

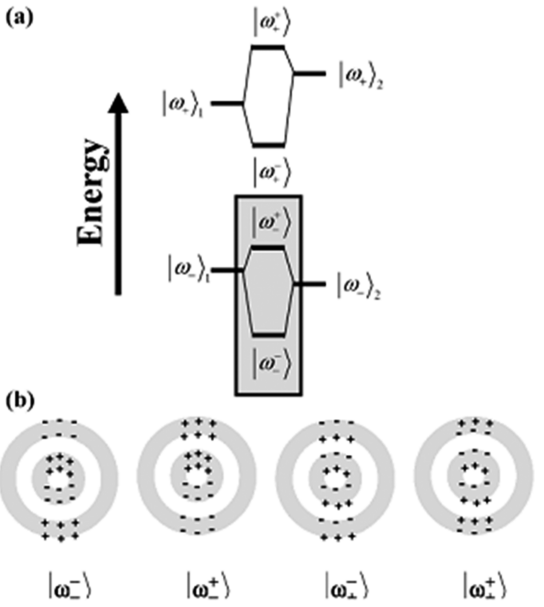

Figure 27. (a) Energy level diagram of the plasmon modes of a concentric nanoshell, depicted in terms of the "bonding" and "antibonding" modes of the inner and outer nanoshells of the composite nanostructure, and (b) induced polarizations of the concentric nanoshell modes.
Reprinted with permission from ref 58. Copyright 2004 American Chemical Society.

2.6. Movable Core/Hollow Shell Nanoparticles

Previous subsections of the nanoparticle classification show the evolution of different core/shell nanoparticles and their potential importance. This section summarizes the most recent developments with respect to an interesting type of nanoparticle. These have a movable core with a hollow shell, and they have several exciting applications. Different research groups have developed various techniques to synthesize inorganic movable cores with hollow shells. Some examples are Ag/polypyrrole—chitosan,[501] Ag/polystyrene,[502] Sn/carbon,[503] Au/C,[504] Au/silica,[505] Au/*p*BzMA,[506] SiO_2/TiO_2,[446] SiO_2/*p*(DVB-*co*-MAA),[507] α-Fe_2O_3/SnO_2,[508] Fe_3O_4/*p*(EGDMA-*co*-NVCz),[509] Au-functonalized *p*(EGDMA-*co*-MAA)/p(EGDMA-*co*-VPy)/PEGDMA,[510] and *p*(MAA-co-EGDMA)/PEGDMA.[511] The usual method for the synthesis of the movable core in a hollow shell nanoparticle is based on the "template assist route". In this method,

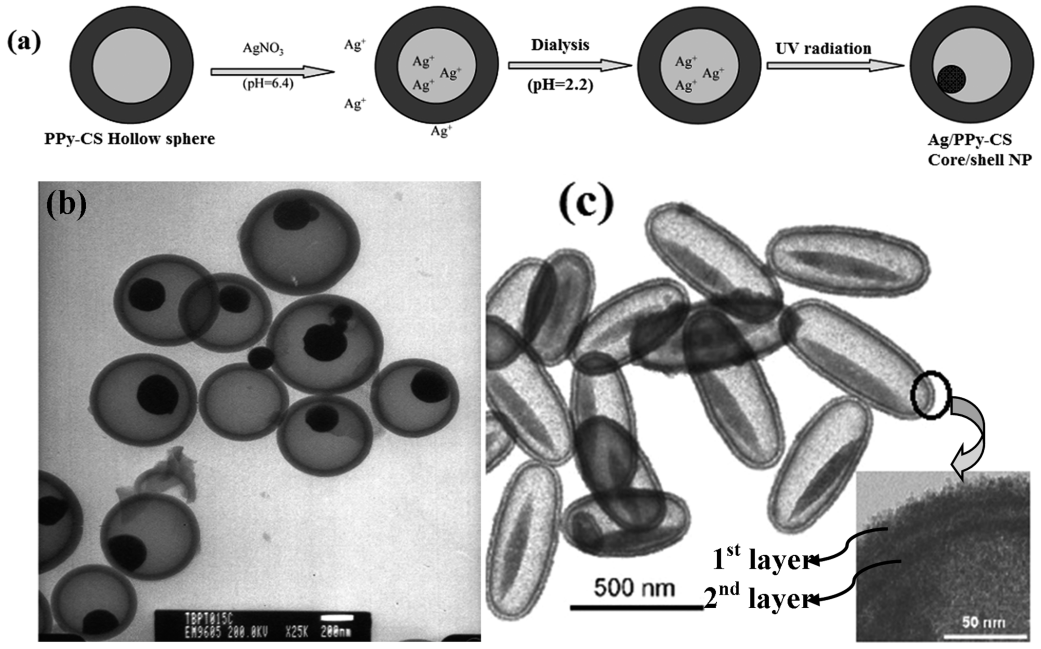

Figure 28. (a) Scheme of the procedure for the preparation of PPy−CS hollow nanoparticles containing movable Ag cores (Ag/PPy−CS). TEM images of the (b) movable Sn core in a hollow carbon shell nanoparticles and (c) double-walled SnO_2 nanococoons with movable a-Fe_2O_3 spindles. Inset figure shows the high resolution shell image.
(a) Reprinted with permission from ref 501. Copyright 2005 American Chemical Society. (b) Reprinted with permission from ref 503. Copyright 2003 American Chemical Society. (c) Reprinted with permission from ref 508. Copyright 2007 Wiley-VCH.

Table 6. Movable Core/Hollow Shell Nanoparticles Based on Different Core and Shell Materials[a]

core			shell				
type		material	type	material	sacrificial shell	removal technique	ref
inorganic	metal	Sn	inorganic	C	TBPT/RF	calcination	503
		Au		C	SiO_2	HF	504
		Au		SiO_2	C	calcination	505
	oxide	SiO_2		TiO_2	PS	calcination	446
		SiO_2		TiO_2	p(EGDMA-co-MAA)	calcination	512
		SiO_2		SnO_2	SiO_2	HF	514
		α-Fe_2O_3		SnO_2	SiO_2	HF	508
inorganic	metal	Au	organic	pBZMA	SiO_2	HF	506
		Ag		PS			502
		Ag		PPy-CS			501
	oxide	Fe_3O_4		p(EGDMA-*co*-NVCz)	SiO_2	HF	509
		SiO_2		*p*(DVB-co-MAA)	PMMA	C_2H_5OH	507
	metal chalcogenide	CdS		PS			513
organic	polymer	p(MAA-*co*-EGDMA)	organic	*p*EGDMA	SiO_2	HF	511
organic/inorganic	polymer/metal	Au-functionalized p(EGDMA-*co*-MAA)/p(EGDMA-*co*-VPy)	organic	*p*EGDMA	SiO_2	HF	510

[a] Abbreviations: PS, polystyrene; *p*(DVB-*co*-MAA), poly(divinylbenzene-*co*-methacrylic acid); *p*MMA, poly(methacrylic acid); *p*(MAA-*co*-EGDMA), poly(methacrylic acid-*co*-ethylene glycol dimethacrylate); *p*EGDMA, poly(ethylene glycol dimethacrylate); *p*(EGDMA-*co*-NVCz)), poly[(ethylene glycol dimethacrylate)-*co*-(*N*-vinylcarbazole)]; *p*(EGDMA-*co*-MAA), poly(ethylene glycol dimethacrylate-*co*-methacrylic acid); *p*BzMA, poly(benzyl methacrylate); *p*(EGDMA-*co*-MAA)/*p*(EGDMA-*co*-VPy), poly(ethylene glycol dimethacrylate-*co*-methacrylic acid)/poly(ethylene glycol dimethacrylate-*co*-vinylpyridine); TBPT/RF, tributylphenyltin/(resorcinol formaldehyde) core/shell nanoparticle; *p*Py-CS, polypyrrole−chitosan.

first core/double shell nanoparticles are synthesized, and then the middle shell is removed using a suitable technique such as dissolution[504,506−511] or calcination.[446,505,512] Of all the reported studies, two research groups have synthesized these particles using different novel routes. In one case (as shown in Figure 28), they avoided the formation of the middle sacrificial shell.[501,502,513] Liu et al.[502,513] synthesized the core particles inside a reverse microemulsion and then the polymer shell outside of the

reverse micelle (Figure 28a). Cheng et al. synthesized the porous hollow particles first, then the core inside the shell by UV radiation.[501] All the available literature regarding different movable cores inside hollow shell particles employing the removal techniques of the inner layer are summarized in Table 6. Generally the reported studies are for spherical shaped shells with thick shell walls. However, interestingly, Lou et al.[508] reported a double-walled ellipsoidal or cocoon shaped α-Fe_3O_4 movable core for SnO_2 hollow shell nanoparticles. These nonspherical hollow particles with movable magnetic cores may prove very useful in a range of new applications, such as magnetically separable photocatalysts and self-assembled photonic crystals with controlled bandgaps.

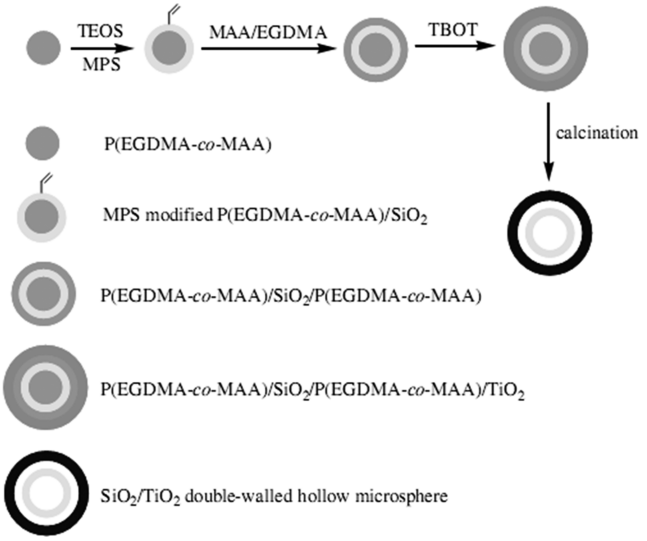

Figure 29. Procedure to synthesize monodisperse *p*(EGDMA-*co*-MAA)/SiO_2/*p*(EGDMA-*co*-MAA)/TiO_2 tetralayer microspheres and the corresponding hollow SiO_2/TiO_2 double-walled microspheres. Reprinted with permission from ref 512. Copyright 2010 Elsevier Ltd.

It is envisaged that the movable inorganic metal core material—functionalized polymer shell particles could be used in different applications, such as Sn/C particles for anodic material in lithium battery,[503] Au movable core/silica shells as good electrocatalysts for direct methanol fuel cells (DMFC),[505] and Au movable core/polymer shells as optical probes.[506] The TEM images of different shaped movable cores in hollow shells are shown in the Figure 28b,c.

Recently, hollow movable cores with hollow shells have also attracted attention.[512,514] Hollow SiO_2 movable cores in hollow TiO_2 shell particles were synthesized by multiple coating of successive organic layers on SiO_2 and TiO_2.[512] By use of this process, the core and shell of *p*(EGDMA-*co*-MAA) were removed by calcination, and the thickness of the organic and inorganic layer was controlled by the precise adjustment of the successive polymerization steps and the feed rate of the sol—gel precursor. The synthesis scheme of the movable hollow SiO_2 coated with TiO_2 is shown in Figure 29.

3. DIFFERENT SHAPED CORE/SHELL NANOPARTICLES

Other than the conventional spherical shaped core/shell nanoparticles, different shaped core/shell nanoparticles have proven equally important because of their potential applications especially in the fields of high-performance catalysis, nanoelectronics, and information storage units, as well as biological and biomedical sensors.[42,45,515,516] The different shaped core/shell nanoparticles available from the literature are summarized in Table 7. Generally, two different approaches are used for the synthesis of these different shaped core/shell nanoparticles. In the first approach, a soft or hard different shape template (core) is used to confine the physical shape.[43−46,189,243,516−520] In the second approach, a suitable capping agent, a block polymer or some other suitable reagent, is used to control the direction and dimension of the nanoparticle growth.[42,521,522]

In the first approach, a rigid core of a different shape is used as the template, and the shell material is deposited uniformly to give

Table 7. Different Shape Core/Shell Nanoparticles with Their Synthetic Approach

synthesis approach	type of core/shell	core shape	shape of core/shell	ref
soft or hard different	Au/Pt	rod	rod	243
shape template	Ag/Au	prism	prism	523
assist route	Ag/SiO_2	prism	triangular	524
	Fe/FeOOH-FeO	oval	oval	517
	Au/Ag	cube, truncated- octahedron, octahedron, twined hexagon, five-twinned decahedron, rod	cube, truncated- octahedron, octahedron, twined hexagon, five-twinned decahedron, rod	46
	Cu/Cu_2O	cubic, cuboctahedral, octahedral	cubic, cuboctahedral, octahedral	45
	Ni/NiO	cylindrical, hexagonal, ellipsoidal, polyhedral	cylindrical, hexagonal, ellipsoidal, polyhedral	519
	Au/Pt	octahedral, cubic	octahedral, cubic	44
	Ag/Au	hexagonal	hexagonal	520
	SiO_2/Ni	spherical	microflower	43
	ZnO/Ag	rod	rod	189
	Au/Ag	rod	dumbbell	516
	Cu_2O/Au	cubic	cubic, flowery	515
control directional growth	Au/Cu_2O	octahedral	cuboctahedral	525
		rod	pentagonal prism	
		plates	concave plate	
	Cu_2S/In_2S_3	spherical	matchstick-like, teardrop-like, pencil-like	42
	Au/Pd	spherical	flower	521

dx.doi.org/10.1021/cr100449n |*Chem. Rev.* 2012, 112, 2373–2433

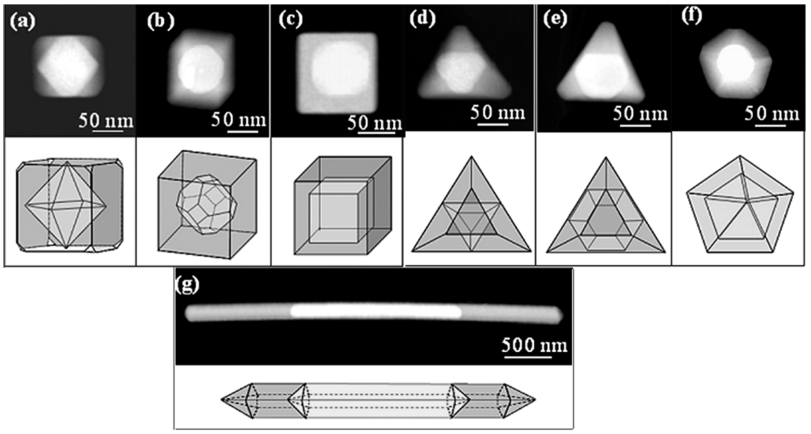

Figure 30. Scanning transmission electron microscope images using a high-angle annular dark field (HAADF)−STEM of the individual Au/Ag nanoparticles with various shapes and their evolution models from differently shaped Au cores: (a) from octahedral Au core to cubic Ag shell; (b) from truncated-octahedral Au core to cubic Ag shell; (c) from cubic Au core to cubic Ag shell; (d) from {111}-facet-dominated biangular Au core to {100}-facet-dominated biangular Ag shell; (e) from {111}-facet-dominated bihexagonal Au core to {100}-facet-dominated biangular Ag shell; (f) from five-twinned decahedral Au core to five-twinned decahedral Ag shell; (g) from Au nanorod core with five-twinned cross section to Ag nanorod shell with five-twinned cross section.
Reprinted with permission from ref 46. Copyright 2009 IOP Publishing Ltd.

similarly shaped core/shell nanoparticles. Generally, to achieve a template with a different shape, core particles are synthesized by changing the reaction parameters[44,45] and directly used for the coating as a template. The remaining step to form the different core/shell nanoparticles is the same as that used for the spherical core/shell nanoparticle formation. For example, three different shapes (cubic, cuboctahedral, and octahedral) for Cu/Cu_2O core/shell nanoparticles can be synthesized on a similarly shaped core by electrodeposition, without using any capping agent.[45] The different shaped core/shell nanoparticles based on the shape of the core particles are shown in Figure 30. It has been found that for the synthesis of different shaped bimetallic core/shell nanoparticles, both Au/Ag and Ag/Au core/shell nanoparticles were synthesized using their respectively shaped core.[46,526] Depending on the shape of the core particles, the coating efficiency of the shell materials also changes. It was found that the uniform coating efficiency decreases with shape distortion from spherical.[44] For the octahedral core/shell particles, the Pt shell is incompletely coated on the octahedral Au core particles, whereas spherical cores are completely coated with the shell material as shown in Figure 31a,c. In case of bimetallic core/shell nanoparticles, the shell is formed by a reduction−transmetalation process, and because of incomplete reduction of the salt by the core material, incomplete asymmetric coatings with different shaped core/shell nanoparticles are formed.[526] Even, for the soft template, the overall particle shape not only depends on the core shape but also on the shell thickness and the uniformity of the shell coating.[518] Dendrimers and polymers are generally used as the template in the soft core method. However, the mechanism of formation for organic/organic core/shell nanoparticles is different from inorganic particle synthesis. For organic particle synthesis, "grafting-onto" and "grafting-from" methods are used.[104,495] Star-shaped core/shell macromolecules are formed using these two methods. Generally, the "grafting-onto" method is used for the monolayer shell coating whereas, "grafting-from" is used for multilayer shell coatings. Various cubic and prism shape core/shell nanoparticles are shown in Figure 31b,d.

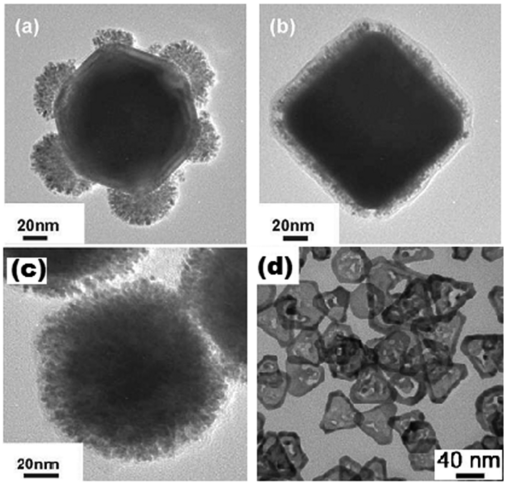

Figure 31. TEM images of (a) Au(oct)/Pt, (b) Au(cub)/Pt, (c) Au(sph)/Pt, and (d) Ag/Au core/shell nanoparticles with prism structure.
(a,b,c) Reprinted with permission from ref 44. Copyright 2010 Elsevier B. V. (d) Reprinted with permission from ref 523. Copyright 2010 Wiley-VCH.

The matchstick, tetradroplike, and pencil-like core/shell nanoparticles are formed from the Cu_2S spherical core by the addition of $In(acac)_3$ with constant heating at 200 °C as a result of the epitaxial growth of In_2S_3 semiconductor material with dodecanethiol capping agent. The self-assembly and the cross-linking of the polymer materials is another reason for the formation of different shaped core/shell nanoparticles.[522] Wang et al.[522] proposed a method for synthesizing different shaped nanoparticles.

Although many researchers have mentioned that nonspherical shaped core/shell nanoparticles may have different or even new properties than those with spherical shapes, comparative studies between spherical and nonspherical core/shell nanoparticles are rare. However, there are some reports available on the changing

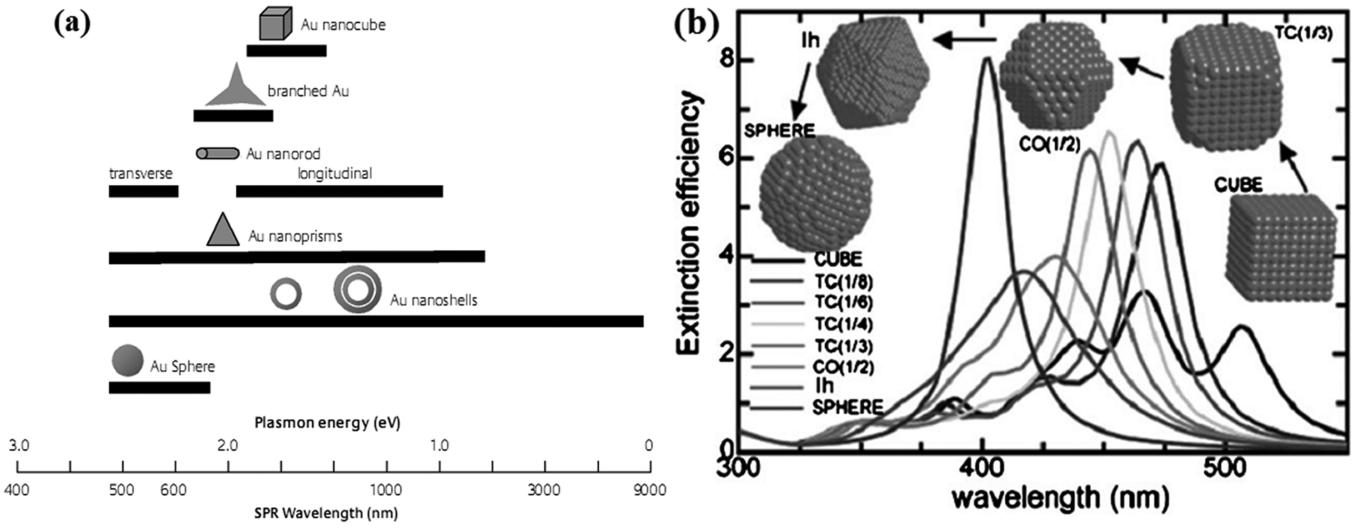

Figure 32. (a) Range of plasmon resonance of gold nanoparticles as a function of their morphology. (b) Extinction efficiencies as a function of the wavelength of the incident light of a silver cube, different truncated cubes, and a spherical nanoparticle.
(a) Reprinted with permission from ref 528. Copyright 2008 Springer. (b) Reprinted with permission from ref 530. Copyright 2007 American Chemical Society.

properties of simple nonspherical nanoparticles compared with spherical particles.[527−530] Sau et al.[527] extensively reviewed the properties and applications of nonspherical noble metal nanoparticles. Now, it seems fair enough to assume that similar changes in properties will also be exhibited for core/shell nanoparticles simply as a result of shape change. In the case of metallic nanoparticles, the catalytic properties improvement observed for nonspherical shapes may be attributed to the exposure of different crystallographic facets. The change in catalytic activity and selectivity of the nonspherical nanoparticles may be attributed to the introduction of a number of edges, corners, and faces over the spherical particles. As a specific example, Narayan and El-Sayed[529] have shown that the catalytic activity of platinum nanoparticles for the electron-transfer reaction between hexacyanoferrate(III) ions and thiosulfate ions followed the order: cubes < spheres < tetrahedra. Other studies also show anisotropic or nonspherical noble nanoparticles have better catalytic activity than the corresponding spherical ones in several applications such as fuel cells, waste treatment, bioprocessing, and many other specific chemical reactions.[527] Apart from their catalytic properties, the optical properties of nonspherical nanoparticles also vary dramatically with their physical dimensions. This is especially true for noble metals. The resonance frequency is tunable over a wide wavelength range from blue to near-infrared, and this enables one to set the surface plasmon resonance (SPR) to a wavelength or spectral region specific to a particular application by changing the shape as shown in Figure 32a.[528] The extinction efficiencies of the nobel metals also changes with the shape of the particles as shown in Figure 32b. As a result, these particles may have better biological applications because the resonance of the anisotropic gold nanoparticles can be positioned in the near-infrared region (800−1300 nm), where absorption by biomatter is low.[527,528]

4. TECHNIQUES, CLASSIFICATION, AND MECHANISM OF CORE/SHELL NANOPARTICLE SYNTHESIS

In general, core/shell nanoparticles are synthesized using a two-step process, first synthesis of core and second the synthesis of the shell. The synthesis techniques of core/shell nanoparticles can be classified into two types depending on the availability of core particles: (i) the core particles are synthesized and separately incorporated into the system with proper surface modification for coating the shell material;[176,192,413,424,531] (ii) the core particles are synthesized *in situ*, and this is followed by coating of the shell material.[80,182,532−534] In the first method, after the core particles are separately synthesized, purified by successive washings, and dried, they then undergo proper surface modification for coating the shell material in the reaction mixture for shell formation. In the second method, the core particles are first synthesized using suitable reactants in the presence of a growth inhibitor and or surface modifier; then after core formation is complete, more reactants are added to form the shell particle *in situ*.[150,182] Consequently shell material is selectively deposited on the modified core surface and core/shell particles are formed. The basic advantage of external core synthesis is the fact that core particles are available in pure form and hence there is less possibility of impurities on the core surface. Whereas, in *in situ* synthesis, the main problem is that some impurity from the reaction media may be trapped between the core and shell layer.

The most important step during synthesis of core/shell particles is to maintain uniform coating and to control the shell thickness. Some of the various synthetic methods for core/shell particles used by different research groups are precipitation,[535,536] polymerization,[93,106,537] microemulsion,[203,204,218] sol−gel condensation,[123,435] layer by layer adsorption techniques,[538,539] etc. Although several researchers have attempted to control the thickness and uniform coating of the shell using these methods, the methods are still not well established, and proper control is very difficult. The main difficulties are (i) agglomeration of core particles in the reaction media, (ii) preferential formation of separate particles of shell material rather than coating the core, (iii) incomplete coverage of the core surface, and (iv) control of the reaction rate. Usually, for core surface modification purposes, surface active agents[540] and polymers[123,322,540] are often used by different research groups. These surfactants or polymers can change the surface charge and selectivity of the core particles

Table 8. Standard Reduction Potentials of Different Metals[552]

reaction	standard electrode potential, E^0 (V)
$Zn^{2+} + 2e^- = Zn$	−0.7618
$Fe^{2+} + 2e^- = Fe$	−0.447
$Co^{2+} + 2e^- = Co$	−0.28
$Ni^{2+} + 2e^- = Ni$	−0.257
$2H^+ + 2e^- = H_2$	0.000
$Ag^+ + e^- = Ag$	0.7996
$Cu^+ + e^- = Cu$	0.521
$Cu^{2+} + 2e^- = Cu$	0.3419
$Pt^{2+} + 2e^- = Pt$	1.18
$Au^+ + e^- = Au$	1.692

so that the shell material can be selectively deposited onto the core surface to form uniform and completely coated core/shell particles.

As mentioned above, different methods are used for the synthesis of core/shell nanoparticles. Irrespective of core or shell particles, if only the material properties are taken into consideration, then particles can be broadly classified in two different groups, (i) inorganic and (ii) organic materials. Even so, some researchers have classified particles according to the different types of materials and methods employed.[74,75,94,104,106] In this section, we will attempt to briefly explain the mechanisms for the different methods with a view to improving the overall understanding because it is felt that this is an aspect that has not been properly emphasized in previously published reviews.

4.1. Synthesis of Inorganic Nanoparticles

A review of the literature clearly shows that the majority of reports are focused on inorganic materials rather than organics. Irrespective of core or shell particles, inorganic materials can be broadly classified into three different groups, (i) metal, (ii) metal or metalloid oxide, and (iii) metal chalcogenide and metal salt.

4.1.1. Synthesis of Metallic Nanoparticles. Metallic cores or shells of the core/shell nanoparticles are synthesized by the reduction of metal salts. For the synthesis of metallic nanoparticles, the synthesis media such as a microemulsion or aqueous phase, use of surfactants, and proper reducing agents all play a key role. The solution phase reduction mechanism is used for the synthesis of different metal nanoparticles, such as Au,[114,116,117,120,160,339,389,541] Ag,[123,124,343,389,542] Co,[533,543] Fe,[544,545] and Ni.[519,546−550] from their respective metal salts. The choice of reducing agent is very important for controlling the reaction rate as well as the particle size. Based on the reducing agent, the synthesis routes are classified into the following groups.

4.1.1.1. Reduction by Sodium Borohydride. The most commonly used reducing agents are sodium borohydride and hydrazine for the reduction of metal ions from their respective salts. Sodium borohydride was discovered by Schlesinger in 1942[551] and is an efficient water-soluble reducing agent used in both aqueous and organic media. Sodium borohydride has some distinct advantages for use as a reducing agent over other reducing agents: (i) it has low equivalent weight of 4.73 g/mol and 1 mol can supply eight electrons; (ii) it has high reducing power with a reducing potential −1.24 V vs standard hydrogen electrode (SHE) at pH 14, decreasing to 0.48 V at pH 0; (iii) it can reduce metal salts in either aqueous or nonaqueous media at any pH. Capping agents can also be used in this reducing media mainly for controlling the size of the particles as well as modifying the surface charge for incorporating a favorable shell coating.

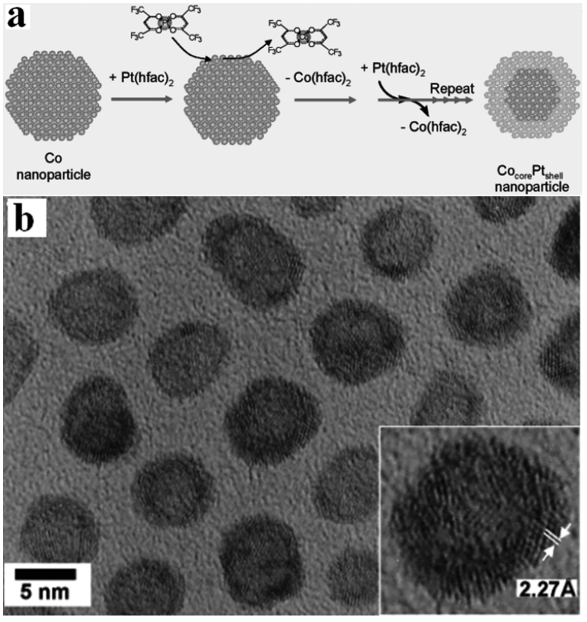

Figure 33. (a) Redox transmetalation processes for core/shell nanoparticle synthesis. During the reaction, the Pt^{2+} of $Pt(hfac)_2$ is reduced to Pt, while the surface Co atom of the Co nanoparticles is oxidized via hfac ligand migration to form $Co(hfac)_2$ as a reaction byproduct. Repeating cycles of this reaction result in core/shell bimetallic nanoparticles. (b) HRTEM images of 6.4 nm Co/Pt core/shell nanoparticles.
Reprinted with permission from ref 564. Copyright 2004 American Chemical Society.

The fundamental chemistry of reduction by borohydride can be explained in terms of electron transfer from borohydride to metal ion. Depending on the pH of the medium, the reduction mechanism of borohydride is different. At pH < 9.24, BO_3^{3-} is more stable compared with other anionic forms. The half cell reaction and reduction potential (E) can be written as

$$BH_4^- + 3H_2O = H_3BO_3 + 7H^+ + 8e^- \quad (2)$$

$$E = -0.481 - 0.0517\ \mathrm{pH} \quad (2a)$$

Under these pH conditions (<9.42), depending on the reduction potential, the metal ion is reduced to metal and hydrogen gas is generated. The general chemical reduction reaction of a bivalent metal ion by borohydride can be written as

$$BH_4^- + 4M^{2+} + 3H_2O = H_3BO_3 + 4M + 7H^+ \quad (3)$$

However, the overall reaction is a combination of reduction and hydrolysis of borohydride, which again depends on the reaction conditions, concentration of the reactants, mixing efficiency, and kinetics of the reactions. Finally, the total reaction can be represented as

$$BH_4^- + xM^{2+} + 3H_2O = H_3BO_3 + xM + (4-x)H_2 + (2x-1)H^+ \quad (4)$$

dx.doi.org/10.1021/cr100449n |Chem. Rev. 2012, 112, 2373–2433

For example, Fe metal synthesis by the sodium borohydride reduction of iron chloride can be written as[545]

$$4Fe^{3+} + 3BH_4^- + 9H_2O \rightarrow 4Fe^0 + 2H_2BO_3^- + 12H^+ + 6H_2 \quad (5)$$

However, at pH > 9.42, $B(OH)_4^-$ is more stable, and hence the reaction changes to

$$BH_4^- + 8OH^- = B(OH)_4^- + 4H_2O + 8e^- \quad (6)$$

$$E = -0.413 - 0.0591\ pH \quad (6a)$$

The borohydride ions also undergo acid-catalyzed hydrolysis according to the following reaction:

$$BH_4^- + H^+ + 3H_2O = H_3BO_3 + 4H_2 \quad (7)$$

Finally, in acidic or alkaline media borohydride ions release the electrons into the media and change to a more stable compound at that corresponding pH. The reduction of metal ion to metal takes place in the media depending on the reduction potential. The standard reduction electrode potentials of some common metal ions are given in the Table 8.[552]

4.1.1.2. Reduction by Hydrazine. Hydrazine is another common reducing agent for metal nanoparticle synthesis from the metal salt, and it is comparatively weaker than borohydride. The standard reduction potential of the hydrazinium ion ($N_2H_5^+$) is −0.23 ($N_2 + 5H^+ + 4e^- = N_2H_5^+$) in acidic medium, whereas in basic medium it is −1.23 ($N_2H_4 + 4OH^- = N_2 + 4H_2O + 4e^-$). Therefore, hydrazine is used for the synthesis of metals that have higher reduction potentials than hydrazine. Because the standard reduction potential of metals normally varies from −1 to any higher positive value, hydrazine is mainly used in alkaline medium and the maximum reduction efficiency of hydrazine is at pH > 11.[553] For example, the standard reduction potential of Ni^{2+} and $Ni(OH)_2$ are −0.257 and −0.72 V, both of which are greater than that of hydrazine in alkaline media. The overall reduction reaction of nickel salt to Ni metal by hydrazine can be written as

$$2Ni^{2+} + N_2H_4 + 4OH^- = 2Ni + N_2 + 4H_2O \quad (8)$$

Therefore, hydrazine is used for the synthesis of metals such as Ni,[547,554−556] Ag,[557] Cu,[558] and Pt[559] and bimetallic compounds such as Pd/Pt[560] and Pt/Ru.[561] The main advantage of using hydrazine is that the pH- and temperature-dependent reducing ability of hydrazine makes the reduction rate more easily controllable.

4.1.1.3. Reduction−Transmetalation. Other than the more common reduction techniques, metallic particles can also be synthesized by using a redox−transmetalation method. It is an advanced process compared with the conventional reduction techniques. In this method, initially the core material is synthesized by a common reduction process using any suitable reducing reagent. Then the metal salt is added to the solution without any additional reducing agent. When the metal salts come into contact with the core surface, they are reduced by the surface atoms of the metal core and deposited on the surface of the core. As a result, some portions of the metal core are oxidized to metal salt and diffuse through the shell layer into the bulk solution. A redox reaction can then spontaneously proceed under the favorable redox potentials between two metals. This technique has some advantages over normal reduction, such as (i) a conventional reducing agent is not required, (ii) shell formation is spontaneous without any separate reaction being required, (iii) self-nucleation of the shell metal can be avoided, and (iv) inhomogeneous growth of the shell can be prevented. However, the limitation of this method is that only those pairs of bimetallic core/shell nanoparticle are possible where the shell metal has a high reduction potential compared with the core material. This method has been efficiently used for the selective formation of bimetallic core/shell structures, some common examples of which are Ni/Au,[562] Co/Pt,[167,563,564] Ni/Ag,[550] Co/Au,[167] Co/Pd,[167] Co/Cu,[167] and Ag/Au.[565]

The reaction mechanism of bimetallic Ni/Au core/shell particle formation by reduction-transmetalation reaction can be written as

$$\text{Core formation}: Ni^{2+} + 2e^- = Ni \quad (9)$$

$$\text{Shell formation}: 3Ni + 2AuCl_4^- = 3Ni^{2+} + 2Au + 8Cl^- \quad (10)$$

The schematic mechanism of Co/Pt core/shell particle formation by the reduction−transmetalation method is shown in Figure 33a and the HRTEM image of Co/Pt particles is shown in Figure 33b. According to Park et al.,[564] 6.3 nm Co nanoparticles were used as the core and the salt $Pt(hfac)_2$ (hfac = hexafluoroacetylacetonate) was used for shell formation on the core surface in the presence of dodecyl isocyanide as a capping material in a nonane solvent media. Because of the higher reduction potential of Pt compared with Co metal, during the reaction, Pt^{2+} is reduced to Pt and deposited on the core surface. Simultaneously the core surface atoms (Co) are oxidized to Co^{2+} to form $Co(hfac)_2$.

4.1.1.4. Thermal Decomposition of Organometallic Compounds. High-temperature thermal decomposition of organometallic compounds is another suitable method for the synthesis of metal nanoparticles especially for core particle synthesis. In this method, organometallic compounds are decomposed to metals at high temperature in the presence of a surfactant in nonaqueous media but in the absence of water and oxygen. The surfactant acts as a dispersing agent for controlling the particle size. A simple example of this method is the synthesis of cobalt from a octacarbonyldicobalt complex.[167,176,566] In the presence of a surfactant molecule, $Co_2(CO)_8$ is decomposed to Co metal at 500 °C. Organic surfactant molecules act as a dispersing and stabilizing agent. Adsorbed surfactant on the cobalt core surface can be removed by successive washings using anhydrous methanol and storage either in toluene or benzene. Freshly synthesized Co metal is highly reactive toward oxidation; therefore, contact with air or water should be avoided. Otherwise the surface layers of the cobalt will be oxidized to cobalt oxide. The thermal decomposition of $Co_2(CO)_8$ at 500 °C can be stoichiometrically written as

$$Co_2(CO)_8 \rightarrow 2Co + 8CO \quad (11)$$

The metal carbonyls are highly toxic and relatively more expensive. Therefore, in order to improve the method, octacarbonyldicobalt is replaced by another organometallic precursor such as the Co(η^3-C_8H_{13}) (η^4-C_8H_{12}),[567] [bis(salicylidene) cobalt(II)]−oleylamine complex.[568] By using the thermal decomposition method with an organometallic precursor of another metal such as Cu from copper oxalate,[317] [bis(salicylidiminato)copper(II)] $[Cu(sal)_2]$,[569] Au from gold acetate $[Au(OCOCH_3)_3]$,[182] and Ni from nickel acetate

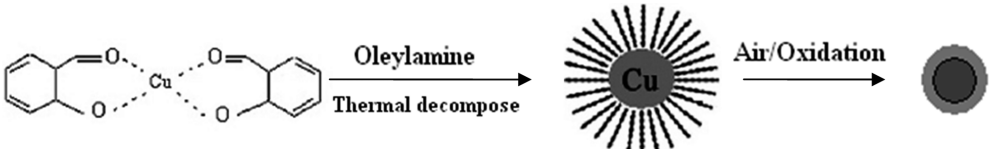

Figure 34. Schematic diagram for Cu/Cu_2O core/shell nanoparticle synthesis using the thermal decomposition of a metal organic complex. Reaction scheme adapted from ref 569.

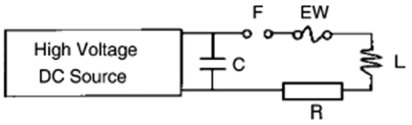

Figure 35. Schematic diagram of wire electric explosion (C, capacitor group; F, plasma switch; L, inductor; R, resistance of circuit; EW, exploding wire).
Reprinted with permission from ref 126. Copyright 2005 Elsevier B. V.

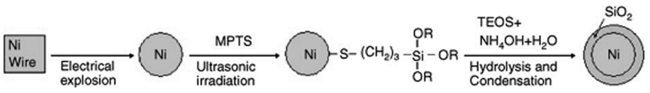

Figure 36. Schematic diagram used to prepare Ni/SiO_2 core/shell nanoparticles using WEE.
Reprinted with permission from ref 126. Copyright 2005 Elsevier B. V.

$[Ni(OCOCH_3)_2\ 4H_2O]$[545] have all been synthesized. In the presence of a stabilizing agent, the mechanism of particle formation is the same as octacarbonyldicobalt complex decomposition. However, the main advantage of using another organic complex is that the process requires a lower temperature (~250 °C) compared with the metal carbonyl complex (500 °C). After separation of the metal, several washings with anhydrous alcohol are required to remove the stabilizing agent before coating with the required shell materials.

This technique is more useful for the synthesis of metal/metal oxide core/shell nanoparticles from the same metal compound. There is no additional step required for the synthesis of the shell. After removal of the stabilizing agent from the core surface, surface atoms are oxidized to the corresponding metal oxide by atmospheric oxidation. A schematic diagram of Cu/Cu_2O core/shell nanoparticle formation by this technique is given in Figure 34.

4.1.1.5. Wire Electrical Explosion. Compared with all the other previously mentioned methods, metal nanoparticle synthesis by the wire electrical explosion (WEE) technique follows a totally different mechanism. In this method, a high voltage is applied through a thin wire in an inert gas atmosphere in a high-pressure closed chamber. Under these conditions, a strong pulse current with a high current density is passed through the wire so that the wire becomes overheated and evaporates very quickly. The result is that different sized metal nanoparticles are formed within that closed chamber because of the sudden explosion with a shock wave. In this process, the time required for thermal expansion is as short as several tens of microseconds. This process is not used conventionally for common industrial purposes, because it is not only very expensive but also impossible to use explicitly for different metals. It is mainly useful for those metals of high electrical conductivity that are easily available in the thin wire form. After particle formation, the particles should be collected carefully and kept in a closed vessel to prevent atmospheric oxidation. According to the available literature, this method is only used for the synthesis of metals such as Ni,[126] Al,[570,571] and Cu;[177] core/shell alloys such as Cu/Zn[572] or Ti/Ni,[237] and martensite stainless steel (MSS) (with alloy composition 72.1% Fe, 18.7% Cr, 6.7% Ni, 1.4% Mn, 0.8% Si, and 0.03% C).[573] The schematic diagram of the electrical explosion setup for Ni metal synthesis is given in Figure 35. This circuit is used in a closed chamber and a high-density strong pulse current is passed through metal wire (EW). As a result of the sudden heating, the wire starts to melt, and through condensation of the liquid metal, different sized nanoparticles are formed.

According to Fu et al.,[126] core Ni nanoparticles can be synthesized by using the WEE technique in a closed chamber with 0.25 MPa pressure by applying a DC voltage of 34 kV with a current density of 107 A/cm^2 through a Ni wire of 0.33 mm diameter and 7.5 cm in length. But there are some problems associated with this technique. After complete particle formation, they are separated and must be carefully stored in a closed vessel or in any anhydrous solvent to prevent the oxidation of the surface atoms. This technique is also used for the synthesis of bimetallic core/shells or metallic alloy formation. With respect to bimetallic core/shell nanoparticle synthesis, only those combinations that have a higher difference in saturation vapor pressure at a fixed temperature are possible. In this case, the particles having low saturation vapor pressure will form the core and the others form the shell after complete solidification of the core material. The core particles can also be coated in a separate step.[126] After separation of the core particles, a silica shell is coated in a nonaqueous media from TEOS (as shown in Figure 36).

4.1.2. Synthesis of Oxide (Metal and Metalloid) Nanoparticles. Metal or metalloid oxides are another important class of compounds that have been extensively synthesized over the past decade as a core or shell in core/shell nanoparticles. The synthesis of the metal oxide can be classified into two different categories depending on the mode of transformation: (i) gas−solid and (ii) liquid−solid transformations.[574] Among the gas−solid transformations, chemical vapor deposition (CVD) and pulse laser deposition (PLD) are the most common techniques. In general, liquid−solid transformation is the more common transformation mode for metal oxide synthesis either as a core or as a shell than the gas−solid transformation. Among the different liquid−solid transformation methods, the sol−gel and coprecipitation techniques are more acceptable methods for the synthesis of these metal or metalloid oxide nanoparticles. Silicon and titanium oxides are preferentially synthesized by the sol−gel method. However, coprecipitation techniques are mainly used for all the different types of oxides especially those metals from the hydroxide precipitate in alkaline pH. Other than these two, there are also other methods for metal oxide formation, and these will now be discussed.

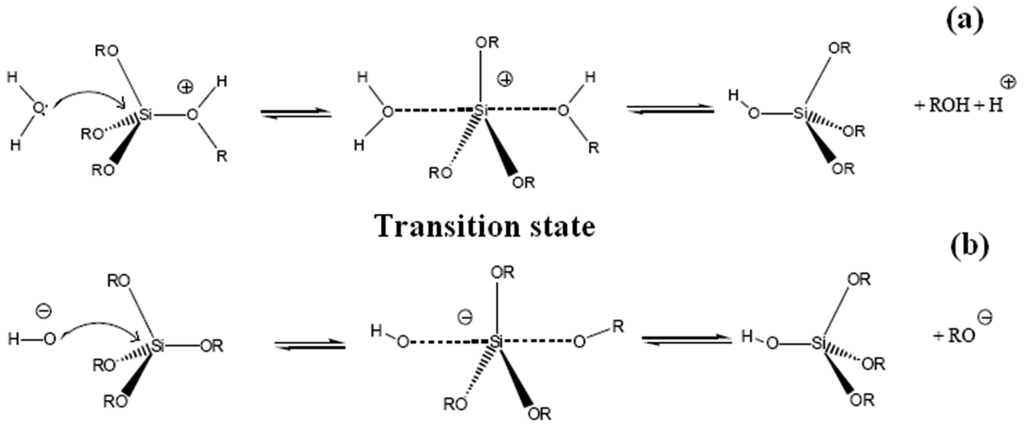

Figure 37. Hydrolysis mechanisms of TEOS for both acidic (a) and basic (b) media.

4.1.2.1. Sol−Gel Method. The sol−gel process is a wet-chemical technique widely used in material research related to science and technology applications, in particular for metal oxide nanoparticle synthesis. This process is a combination of two steps, hydrolysis and polycondensation of suitable molecular precursors (usually metal alkoxides or chlorides), which leads to the gradual formation of the solid-phase network.

The interest in sol−gel processing can be traced back to the mid-1880s. Later on this method was modified by Werner Stöber in 1968.[575] During the 1990s, research activities increased significantly in this area, and as a result, up to 2000 more than 35 000 papers were published worldwide on this process for the synthesis of different nanoparticles.[576−578] Different research groups used modified sol−gel methods for the synthesis of different metal oxides.[347,352,427,536,579−582] Sol−gel processes are mainly classified into three different approaches: (i) gelation of solutions of a colloidal powder; (ii) hydrolysis and polycondensation of metal alkoxides or metal salt precursors followed by hypercritical drying of the gels; (iii) hydrolysis and polycondensation of metal alkoxide precursors followed by aging and drying under ambient atmosphere.[503] The last method is commonly used for the synthesis of metal oxides. These three approaches can be divided into seven steps, as describes below.

Step 1. Mixing. For the first method, the suspension of colloidal powder or sol is formed by the mechanical mixing of colloidal particles in water at a suitable pH without any precipitation. For the other two methods, metal alkoxide or metal salt are used as a precursors, which are hydrolyzed to form hydrated metal hydroxides in the presence of water, which subsequently undergo condensation to form an oxo bridge (−M−O−M−). When sufficient M−O−M bonds are formed in a region, then they cooperatively respond to form colloidal particles or sol. The size of the particles depends on the pH of the medium and the ratio of water to metal alkoxide or metal salt.

$$\text{Hydrolysis}: \mathrm{M(OR)}_n + n\mathrm{H_2O} \rightarrow \mathrm{M(OH)}_n + n\mathrm{ROH} \quad (12)$$

$$\text{Condensation}: \mathrm{M(OH)}_n + \mathrm{M(OH)}_n \rightarrow (\mathrm{OH})_{n-1}\mathrm{M-O-M-(OH)}_{n-1} + \mathrm{H_2O} \quad (13)$$

Step 2. Casting. Since the sol is a low-viscosity liquid, it can be cast into a mold.

Step 3. Gelation. With time, the colloidal particles and condensed species link together to form a three-dimensional network with increased viscosity, which finally becomes solid.

Step 4. Aging. The aging of the gel involves maintaining the cast object for a period of time, completely immersed in liquid for polycondensation, syneresis, coarsening, and phase transformation.

Step 5. Drying. The liquid is removed from the interconnected pore network during the drying process.

Step 6. Dehydration or chemical stabilization. The surface metal−hydroxide bonds are removed in this step, and the material is converted into a stable ultraporous solid with sufficient interconnected porosity, optical transparency, and good mechanical strength.

Step 7. Densification. After dehydration, solid materials are heated at high temperatures to increase density by reducing the internal porosity.

During the last four steps, the shrinkage and densification occurs because of (1) capillary contraction, (2) condensation, (3) structural relaxation, and (4) viscous sintering.[576] In the first step, the rate of hydrolysis of metal or metalloid alkoxide or salt is affected by some physical parameters such as (i) pH, (ii) substituents, (iii) solvent, and (iv) water. The effects of these parameters are discussed as follows.

4.1.2.1.1. Effect of pH. The hydrolysis reaction of the alkoxide is possible in both acidic and alkaline pH with different mechanisms. In acidic media, initially the alkoxide group is protonated and simultaneously a lone pair of the water oxygen becomes attached to the metal from the back side. However, in the basic medium, initially a hydroxyl group is attached to the metal and simultaneously one alkoxide group is released for each substitution. Both these mechanisms for hydrolysis of TEOS are shown in Figure 37.

The rate of hydrolysis is minimal at neutral pH but with increasing or decreasing pH the rate of hydrolysis increases. The rate of condensation of the silicic species also depends on the degree of ionization value. It is minimum at the isoelectric point pH ≈ 2 and becomes faster with increasing pH. Therefore, for the synthesis of silica from TEOS, it is better to use a higher pH

or basic conditions.[583,584] Figure 38 shows the effect of pH on the hydrolysis of TEOS and then condensation.

4.1.2.1.2. Effect of Substituents. Considering the specific case of tetraalkoxy silane, in both acidic and alkaline media, the nucleophilic substitution reaction proceeds on the central Si atom from the back side compared with the leaving group. The steric effects on the Si atom are also another important factor. Normally, with increasing alkyl chain length and branching in the alkyl group, the rate of the reaction decreases because of the steric hindrance introduced by the alkyl groups on the central Si atom; as a result, nucleophile (OH^-) attack on the central Si atom is difficult from the back side. In addition, during the reaction, the transition state (TS) Si attains sp^2 hybridization, that is, except for the leaving group and nucleophile, all other alkyl groups are present in the same plane. During this process, it is also difficult to attain a planar structure with increasing branch chain. The decreasing order of the rate of reaction is given below:

$$Si(OCH_3)_4 > Si(OEt)_4 > Si(O^nPr)_4 > Si(O^iPr)_4 > Si(O^nBu)_4 > Si(Ohex)_4$$

The rate of reaction also depends on the electronic stabilization of the transition state complex and the stability of the leaving group. The electronic density on the Si atom reduces in the following order, R−Si > RO−Si > HO−Si > Si−O−Si.

4.1.2.1.3. Effect of Solvent. Because metal or metalloid alkoxides are soluble in alcohol but insoluble in water, a certain amount of alcohol is always used to improve the miscibility of the alkoxide in water. Generally, the corresponding alcohol common to the alkoxide ligand is preferable. With the change in alkyl group, such as increasing chain length or branching in the alkyl group of the alkoxide, the partial solubility of the related alcohol in water decreases. As a result, the reactivity of the metal alkoxide also decreases because of improper miscibility. Therefore, in general, ethanol is the solvent of choice.

4.1.2.1.4. Effect of Water. Water is also one of the reactants in the hydrolysis reaction. According to the stoichiometry, four moles of water are required for complete hydrolysis of one mole of alkoxide. Subsequently during the condensation additional water is produced. In the hydrolysis step, the reaction rate decreases with decreasing water concentration in the system, whereas in the presence of more water the reaction rate decreases because of dilution of the reactants. As a result, in order to attain the optimum reaction rate, an optimum water to alkoxide ratio (R = [water]/[alkoxide]) is essential.

Aqueous phase sol−gel chemistry is a complex process, mainly because of the high reactivity of the metal oxide precursors and the double role of water as a ligand and solvent. In many cases, three types of reactions (hydrolysis, condensation, and aggregation) occur almost simultaneously, and these are also difficult to control individually, so slight changes in experimental conditions result in altered particle morphologies. Furthermore, the as-synthesized metal oxides are often amorphous, and it is difficult to retain full control over the crystallization process during any additional annealing step. Although all these parameters can be controlled well enough for the preparation of bulk metal oxides, there is a big challenge in the case of nanoparticle synthesis by sol−gel methods. Therefore, to overcome these problems, researchers are trying to change the aqueous to a nonaqueous system. In nonaqueous systems, the exclusion of water as a continuous phase can minimize some of the limitations of the aqueous system. Water not only acts as the oxygen-supplying agent for the metal or metalloid oxide but also strongly influences particle size, shape, and surface and assembly properties. In specific cases, even the composition and crystal structure are affected. In 2007, Niederberger[585] explained the mechanism of the sol−gel process in nonaqueous systems. Different metal oxides, such as TiO_2,[586] SiO_2−GeO_2,[587] CeO_2,[588] and rare earth doped Al_2O_3,[589,590] are synthesized by this technique.

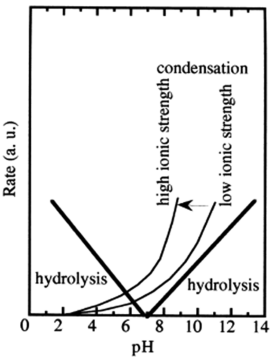

Figure 38. Effect of pH on the rate of hydrolysis of TEOS and the rate of condensation of silicate species at different electrolyte concentrations. Reprinted with permission from ref 584. Copyright 1999 Elsevier B. V.

4.1.2.2. Coprecipitation Technique. Precipitation is a most common type of reaction that can be used to prepare wide varieties of nanoparticles. In a precipitation reaction, two or more water-soluble salts react with each other to form at least one water insoluble salt that precipitates out from the media. The solubility product of the precipitated compound is the most important parameter for such a precipitation reaction. In this technique, first the product will form in the liquid phase immediately after the completion of the reaction. When the concentration of the product crosses the solubility product value of that compound in the reaction media, particle formation will start.

The mechanism of nanoparticle formation via precipitation is a combination of three separate steps one after another: (i) nucleation, (ii) growth, and (iii) agglomeration. However, there may be different types of reactions, such as acid−base precipitation reaction and redox precipitation reaction. In this process, reaction takes place in the liquid phase but the particles formed are in the solid state; for that reason it is also known as reactive crystallization, and it also depends on several energy terms. The first step, the reaction in the liquid phase, is associated with the activation energy of the reaction. The rate of reaction is faster with a lower activation energy than for that of higher activation energy. After the completion of this reaction, embryos (consisting of few atoms) are generated in the bulk liquid phase. When the size of the embryos crosses, a critical radius (called a nucleus), then only the liquid state will be converted to solid. When the solid particles are formed in the bulk phase, a new solid−liquid interfacial area is generated with a specific surface energy proportional to the square of its radius. In considering the bulk energy, because of the formation of a solid then the energy gain is proportional to the cube of the particle radius. These two energy terms are opposite in nature. The change in total energy is mainly the contribution of these two energies, but some other factor, such as motion of the particles in the media, defects in crystal energies, and electrostatic contributions, also contribute a little bit to the overall energy of the system.[591] Normally nucleation is the faster step if the solubility product of the particle material is very low; in that case growth rate will be controlled by

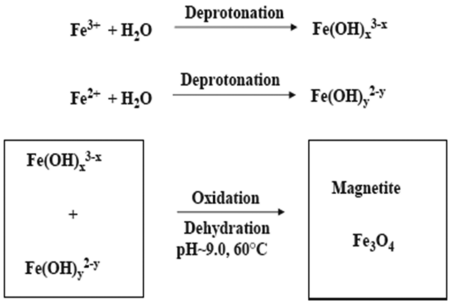

Figure 39. Scheme showing the reaction mechanism of magnetite particle formation by a wet process from an aqueous mixture of ferrous and ferric chloride by the addition of a base. The precipitated magnetite is black in color.
Reprinted with permission from ref 90. Copyright 2005 Elsevier Ltd.

the overall reaction rate. In the growth process, embryos form after the reaction diffuses to the nuclei surface from the bulk phase. Ultimately the growth rate depends on either the reaction rate or the diffusion of the molecules from the bulk phase to the nuclei surface, whichever is slow.[592] The final step is agglomeration. Here small sized particles are converted to a larger size as a result of Oswald ripening with a decreasing specific solid−liquid interface area to reduce the overall energy of the system.

An example of the coprecipitation reaction is where it is used for the preparation of core/shell nanoparticles such as Fe_3O_4/TiO_2.[185] For the synthesis of Fe_3O_4, hydrated ferrous chloride ($FeCl_2 \cdot 4H_2O$) and ferric chloride ($FeCl_3 \cdot 6H_2O$) are used, and for the TiO_2 synthesis, $Ti(SO_4)_2$ is the reactant. As a precipitating agent of iron oxide $NH_3 \cdot H_2O$ is used, and the chemical reaction can be written as

$$Fe^{2+} + 2OH^- \rightarrow Fe(OH)_2 \quad (14)$$

$$Fe^{3+} + 3OH^- \rightarrow Fe(OH)_3 \quad (15)$$

$$Fe(OH)_2 + Fe(OH)_3 \rightarrow Fe_3O_4 + 4H_2O \quad (16)$$

The overall reaction can be written as

$$Fe^{2+} + 2Fe^{3+} + 8OH^- \rightarrow Fe_3O_4 + 4H_2O \quad (17)$$

After complete core (Fe_3O_4) formation, in the same solution, $Ti(SO_4)_2$ and urea are added for TiO_2 formation. Urea does not react with $Ti(SO_4)_2$; however, it decomposes to ammonia and that reacts with $Ti(SO_4)_2$ to form TiO_2. The reaction proceeds through the following mechanism:

$$CO(NH_2)_2 + 3H_2O \rightarrow CO_2 + 2NH_3 \cdot H_2O \quad (18)$$

$$Ti(SO_4)_2 + 4NH_3 \rightarrow H_2O \cdot Ti(OH)_4 + 2(NH_4)_2SO_4 \quad (19)$$

$$Ti(OH)_4 \rightarrow TiO_2 + 2H_2O \quad (20)$$

An alternate route for preparing Fe_3O_4 nanoparticles has been reported by Gupta and Gupta.[90] The schematic diagram of magnetite Fe_3O_4 particle formation by a precipitation reaction is shown in Figure 39.

Similarly, other core/shell nanoparticles, such as $CaCO_3/SiO_2$, can also be prepared by precipitation techniques using CaO and $Na_2SiO_3 \cdot 9H_2O$ as the reactants.[146] Both the core and shells were synthesized in the same media. The schematic

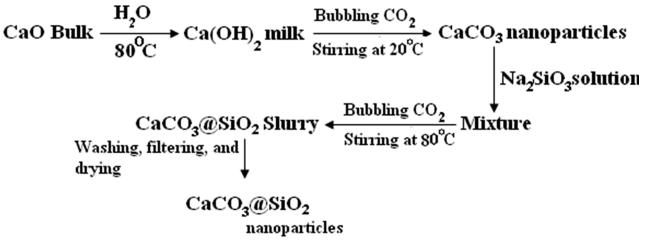

Figure 40. Reaction steps for $CaCO_3/SiO_2$ core/shell nanoparticle formation by precipitation reactions.
Reprinted with permission from ref 146. Copyright 2004 Elsevier B. V.

diagram of the reaction steps of core and shell formation are shown in Figure 40. By similar techniques, different metal or metalloid oxides such as ZnO,[197] SiO_2,[131] Fe_3O_4,[221] and Y_2O_3[220] were synthesized either as a core or as a shell by different research groups.

4.1.2.3. Thermal Decomposition Technique. Thermal decomposition is another technique used for the decomposition of metal complex compounds to form metal oxides; it is also known as thermolysis. This method is used mainly for the synthesis of metal oxide as a core particle in the presence of air or oxygen. The associated reaction is normally endothermic in nature. This method is more common for the synthesis of transition metal oxides, because this is only applicable to stable metal complexes. In general, because of the presence of a vacant d-orbital in the valence orbital, the transition metals can easily form metal complexes through the formation of a secondary bond between the metal and electron-donating ligands.

In this process, initially a surfactant solution is used to stabilize the metal salts and then the surfactant-stabilized metal salt is mixed with a higher molecular weight organic compound to form an organometallic complex. Finally, the resulting organometallic complex is decomposed to form a metal oxide in a hydrophobic solvent in the presence of pure oxygen at high temperatures. After complete decomposition, reaction particles are separated by centrifugation and then washed with a suitable solvent. This method has been used for the synthesis of ZnO from [bis(2-hydroxyacetophenato)zinc(II)][593] or [bis(acetylacetonato)zinc(II)]−oleylamine complex,[316] zirconium oxide (ZrO_2) from zirconyl nitrate pentahydrate ($ZrO(NO_3)_2 \cdot 5H_2O$) using two separate stabilizing agents, oleylamine and PEG,[594] or from bis-aqua,tris-2-hydroxyacetophenato zirconium(IV) nitrate [$Zr(HAP)_3(H_2O)_2](NO_3)$] as a precursor in oleylamine ($C_{18}H_{37}N$) and triphenylphosphine ($C_{18}H_{15}P$),[595] cobalt oxide (Co_3O_4) from Co(oxalate)[596] and [bis(2-hydroxyacetophenato)cobalt(II)],[597] and iron oxide (Fe_3O_4) from $Fe(acac)_3$ with 1,2-hexadecanediol, oleic acid, and oleylamine at elevated temperature.[179] The schematic diagram of zirconium oxide formation by the thermal decomposition method is shown in Figure 41.

4.1.3. Synthesis of Metal Salt and Metal Chalcogenide Nanoparticles. Apart from metal or metal oxides, inorganic nanoparticles, such as a metal salt and chalcogenide, are a separate class of compounds extensively used for different industrial applications. Specially, chalcogenide (sulfide) salts of transition metals such as Zn, Cd, or Hg, are extensively used as semiconductor materials in different electronic industries and rare earth metal salts are also used for bioimaging purposes for their active fluorescence properties. This category of nanoparticles is usually synthesized using precipitation reactions.

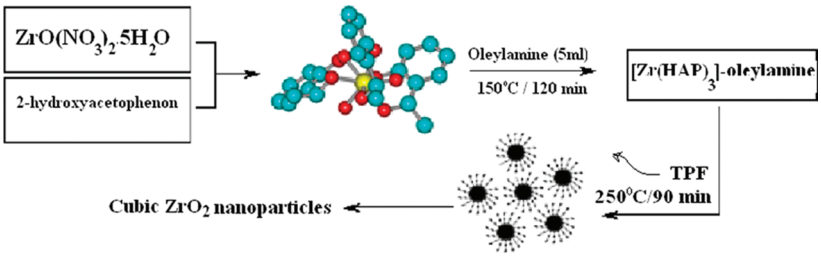

Figure 41. Schematic diagram of synthesis route of ZrO_2 nanoparticles by the thermal decomposition method. Reprinted with permission from ref 594. Copyright 2009 Elsevier B. V.

Different rare earth metal compounds such as $LaPO_4$,[224,228,230] LaF_3[224,230] and β-$NaYF_4$[227,229] are synthesized either as core or as shell nanoparticles. The reaction technique is the same as a normal precipitation process, but in addition, continuous stirring and a high temperature are required. In some cases, the reaction requires an inert gas atmosphere.

Chalcogenide semiconductors are a group of compounds mainly synthesized by the coprecipitation technique. In the semiconductor group, the compounds are mainly sulfides, halides, or oxides of transition metals, and the most common technique for the synthesis of these compounds is the slow precipitation reaction between the metal salt and the corresponding counterions in the presence of a suitable capping agent under good stirring conditions. Some common examples of semiconductor core/shell nanoparticles formation by precipitation reaction are CdS/CdSe,[111,201,275] CdS/ZnS,[82,202] Mn-doped CdS,[598] CdS/PbS,[6,200] ZnS/CdSe,[81] and FePt/CdS.[178]

$CaCO_3$ is another common metal salt that is also synthesized by a precipitation process to use as a core material.[146] The basic mechanisms of this process are the same as the mechanism for metal oxide synthesis by a precipitation reaction.

The "successive ionic layer adsorption and reaction" (SILAR) technique is another common method for the synthesis of metal salts, especially semiconductor materials.[299,599−604] This technique is used for attaining better particle growth control and is based on a comparatively new idea, first proposed by Ristov et al.[605] Later on in 1985, this technique was named the SILAR method by Nicolau.[606] Normally, the core particles are synthesized by a normal precipitation method, but the shell materials are synthesized by SILAR to achieve better photoluminescence properties of the semiconductor materials. The purpose of SILAR shell growth is mainly threefold. First, it prevents independent nucleation of the shell material; as a result the core is coated by the shell material with less formation of separate shell material nanocrystals. Second, the slow addition of the reactants maintains low precursor concentration in the media throughout the period of the reaction time, which favors isotropic and uniform growth. This in turn results in formation of spherical quantum dots and symmetric photoluminescence (PL) spectra. Finally, annealing between the deposition of the alternative shell materials (transition metal salt and other precursors) allows sufficient time for one material to react so that the chemical composition, structural improvement, surface morphology, and optical and electrical properties of the shell are not biased toward the core or other shell materials. Tolstoy has reviewed the mechanism for the synthesis of various classes of substances (inorganic, organic, and hybrid, i.e., inorganic/organic) by successive ionic, ionic−molecular, and ionic−colloidal layer deposition.[607]

4.2. Synthesis of Organic Nanoparticles

The majority of organic nanoparticles fall into the category of polymers. Polymerization is the most widely applicable technique for organic core or shell formation;[418,426,480,482,535,538] usually by either addition or step polymerization. In the polymerization process, monomer molecules are combined successively into three-dimensional networks in the presence of a suitable initiator and under appropriate reaction conditions. Therefore, depending on the phase behavior, polymerization processes can be also classified into different groups, (i) bulk polymerization, (ii) solution polymerization, (iii) suspension polymerization, and (iv) emulsion polymerization.

Normally, the organic polymer cores are synthesized separately using emulsion polymerization[353,419,426,449,463,483] and then directly supplied as a pure template into the reaction media for subsequent core/shell nanoparticle synthesis. The coating of polymer shell onto the organic or inorganic core is normally done *in situ*. In order to enhance the shell coating, the core surface is normally modified either by a polyelectrolyte for an organic core or a surface modifier (surfactants) for inorganic cores. Then the polymerization takes place on the core surface by either bulk or solution polymerization. There are a number of studies available on the use of polymer nanoparticles as cores,[330,353,418,419,426,463,483,608] shells,[330,339,342,348,384,582,609] or both core and shell,[481,482,496] as well as review articles on inorganic core/polymer shells[322] and silica/polymer composite nanoparticles.[348] A summary of different polymers synthesized by different methods is presented in Tables 3, 4, and 5. The basic importance of the different hydrophilic polymer coatings on the inorganic particles is to increase the stability and biocompatibility of those inorganic particles. A suitable hydrophilic initiator is used for the polymerization process; simultaneously the initiator may also act as a surface modifier.[581] For the different polymerization processes, either hydrophilic inorganic compounds[93,105,135,481,483,582,609] or hydrophobic compounds[93] are used as initiator. Pena et al.[581] synthesized TiO_2/polymer composite materials by free radical polymerization. They used poly(methyl methacrylate) (PMMA) in acrylic acid with 0.5% of benzoyl peroxide (PBO_2) for the core surface modification. In addition, they used an initiator. Dresco et al.[93] discussed the different microemulsion methods for the formation of magnetite core (Fe_3O_4) and hydrophilic polymeric shell coating using both inorganic ($K_2S_2O_8$) and organic (2,2′-azobis(isobutyronitrile)) initiators. Apart from the chemical initiators, judicious choice of light wavelength is also used as an initiator for the synthesis of organic polymers.[494,610]

For organic core or shell synthesis in aqueous media, bulk polymerization is a more common technique; in this method both the monomers and polymers are present in the liquid phase. The main disadvantages of this method are the progressive

increase in molecular weight and viscosity and reaction only proceeding in the liquid phase at high temperatures. Solution polymerization is another common technique for polymerization. The disadvantage of this technique is the necessity of removing the solvent in order to isolate pure solid polymer. In suspension polymerization, monomers are soluble in the medium, and the reaction occurs within the droplet. A protective agent is used, under constant vigorous stirring, to maintain the droplets in a suspended state. The next technique to be discussed is emulsion polymerization. Here, the monomer is dispersed in water containing a surfactant (usually 10−12% by weight) to form, as the name implies, an emulsion. This is a widely used technique for industrial purposes. The main advantage of this technique is that because it forms a stable suspension there is no requirement for continuous stirring. Heat transfer efficiency is very high, and the viscosity change is also low compared with either solution or suspension polymerization processes. But the most important task in emulsion polymerization is the formation of stable emulsions of the monomer water mixture in the presence of a suitable emulsifying agent. The disadvantage of this process is the presence of a surfactant, which is difficult to remove completely. However, this technique is the most widely used for either organic core[419,420,422,426,483,611] or shell[336,345,346] synthesis.

Depending on the mechanism, polymerization reactions can be further classified into two different categories: (i) addition and (ii) step polymerization. These mechanisms are briefly described below.

4.2.1. Addition Polymerization. Addition polymerization has the features of a chain reaction. Addition polymerization occurs through the propagation of the active species by the successive addition of large number of monomer molecules in a chain reaction occurring in a matter of, at the most, a second or more usually in a much shorter time. The reaction has its origins in the reaction with an initiator, which can be a free radical, a cation, or an anion. Depending on the initiator, addition polymerization itself can also be subclassified into three different groups: (i) free radical polymerization, (ii) cationic polymerization, and (iii) anionic polymerization.[468]

4.2.2. Step Polymerization. Step polymerization is another well-known technique. Here, polymerization proceeds through the reaction between the functional groups of the monomers. The reaction takes place in a stepwise manner; it is therefore a slow polymerization process requiring more time than addition polymerization processes. Step polymerization reactions are mostly accompanied by the elimination of small molecules. For this polymerization reaction, many known reactions with organic functional groups are used: condensations, additions, ring openings, amidation, and last ester interchange reactions. These types of reactions mainly follow the bulk polymerization technique. The step polymerization reaction between bifunctional monomers with the elimination of water can be written as

$$x\mathrm{HO-R-OH} + x\mathrm{HOCO-R'-}\mathit{COOH} \rightarrow \mathrm{HO[-R-OCO-R'-}\mathit{COO}\mathrm{-]}_x\mathrm{H} + (2x-1)\mathrm{H_2O} \quad (21)$$

Among the different step polymerization reactions, condensation polymerization is the most widely used technique; mostly water molecules are condensed from the mixture. This technique is used for the organic/organic "smart" core/shell nanoparticle synthesis.[463,481,612,613]

5. FACTORS AFFECTING THE SIZE AND DISTRIBUTION OF CORE/SHELL NANOPARTICLES

Both particle size and distribution are important parameters in the synthesis and subsequent applications of nanoparticles. With increase in particle size, the specific surface area and the energy gap between the valence and conductance bands decreases. As a result, the particle properties also change. Therefore, particles across the whole nano range (1−100 nm) do not show the same properties. Up to a certain size range, the particles have better optical and quantum mechanical properties. As a specific example, magnetic nanoparticles are important for *in vivo* applications, such as controlled drug delivery and MRI. However, particles sized above 50 nm cannot be used in *in vivo* applications because they are difficult to transport by the blood and the particles tend to coagulate within the cell. In general, for a particular application, particles with a wide size distribution are also unacceptable. Therefore, smaller sized particles with a narrow size distribution and less tendency to agglomerate are the important factors to be considered.

However, these important factors can be controlled by selectively choosing the reaction media, the physical parameters of the reaction such as temperature, reactant concentration, pH of the media, and nature of the reaction, and also any external applied force.

5.1. Synthesis Media

The synthesis media is an important factor for determining the final particle size and its distribution after reaction. In general, for a "bottom-up" approach, the particles are synthesized using a chemical route either in the bulk phase (aqueous or nonaqueous) or in microemulsion media. Both these media have inherent advantages and disadvantages. Either is acceptable depending on the situation.

5.1.1. Synthesis in the Bulk Phase. The synthesis of nanoparticles in a bulk aqueous phase is an easy method compared with any of the other methods even including microemulsion. This is because of the easy separation of the particles, ease of up-scaling, and fascile post-treatment to obtain a pure product. In addition, it is easy to maintain the required reactant concentration necessary to obtain the desire product. On the other hand, in the case of bulk aqueous phase synthesis, proper control of particle size by changing the external parameters is difficult, especially when the material is hydrophobic. As a result, a bigger sized particle with a wide size distribution is, in general, expected. Apart from the size and distribution of the particles, uniform coating of the core with the shell material to make a complete core/shell particle is also difficult. To facilitate uniform coating either a suitable surface modifier (surfactant or block polymer) or selectively oppositely charged material is directly used. Even then, the incomplete or nonuniform coating of the shell materials and the possibility of forming individual pure particles instead of coating are also there. The hydrophilic particles (mainly magnetic or semiconductor core/shell particles) are synthesized in an aqueous bulk phase. The magnetic nanoparticles thus synthesized generally have good crystallinity and magnetization properties. But the main difficulty is the production of higher sized particles with a wide distribution. Therefore, the ongoing challenge is to synthesize core/shell nanoparticles with proper surface modification in order to reduce agglomeration of the core particles, to induce uniform coating of the shell materials, and to produce overall small sized particles with a narrow distribution.[5,83−85,87,88,91,92,184,197,260,261,326,368−374,614]

The effects of the different reaction parameters on core/shell nanoparticles prepared by this method will be discussed in the following sections.

5.1.2. Microemulsion Method. The synthesis of nanoparticles using a microemulsion as a nanoreactor created huge interest over at least the past two decades because of easy control of the particle size, narrow size distribution, and also uniform coating. Apart from these advantages, the disadvantages are as follows: a microemulsion is a complex system consisting of a huge surfactant, cosurfactant, and oil phases, the separation and purification of the particles are difficult, and also there are difficulties in producing large quantities of particles. In a microemulsion system, surfactants form reverse micelles and cosurfactant molecules help in the micellization process by reducing the electrostatic repulsive forces between the charged headgroups of the surfactant molecules. As a result, the aqueous phase is present as a discrete nanodroplet inside the continuous oil phase, and the particle formation reaction proceeds within the droplets. The reverse micelles act as a center for both nucleation and epitaxial growth of the nanoparticles. In a microemulsion system, the particle size and morphology mainly depend on the droplet size. The size of the droplet in turn also depends on the surfactant hydrophile−lipophile balance (HLB) value, the chain length of the surfactant, and the water to surfactant ratio. This method is mainly used for different types of inorganic nanoparticle synthesis for which the chemical reaction proceeds within the aqueous phase. Different surfactants (either ionic or nonionic) can be used for microemulsion formation with a cosurfactant and oil as the continuous phase.

Different research groups have synthesized different core/shell nanoparticles, characterized them, and applied them in some applications. A wide range of core/shell nanoparticles such as CdS/Ag_2S,[203,204] Fe/Au,[544] Fe_3O_4/SiO_2,[136] PbTe/CdTe,[217] CaO/Fe_2O_3,[615] CaO/Fe_2O_3,[195] MgO/Fe_2O_3,[195] and ZnO/Fe_2O_3[195] have all been synthesized using the microemulsion method. On the other hand, in order to simplify the scope of experiments attention has recently focused on the theoretical importance of the microemulsion system.[616−621] These have mainly focused on the different mechanisms and kinetics of particle formation in microemulsion systems. Some have considered the intermiceller exchange of reactants and newborn particles by both single and double microemulsion systems. In these cases, particle size and polydispersity depend not only on the droplet size or the reactant concentration but also on other physical parameters, such as nature of the reactant, polar volume fraction, mixing pattern of the reactants, and even types of oils used. The effects of these different parameters are briefly explained below.

5.1.2.1. Water to Surfactant Mole Ratio (R). Where microemulsion techniques are concerned, the molar ratio of water to surfactant is the most important parameter for controlling the particle size and morphology. Normally with increasing molar ratio, the water droplet size also increases so that the rigidity of the surfactant film layer decreases. That causes more intermicellar nucleation compared with intramicellar nucleation. In addition, it also increases the aggregation of the particles because of the collision between nanoparticle populated reverse micelles or because of intermicellar exchange among the reverse micelles.[622−629] Finally, a higher water content reduces the interaction between the headgroups of the surfactant molecules and nanoparticles and that in turn increases the aggregation of the particles.

There is also some evidence from the literature available showing that the particle size initially increases with increasing R and ultimately although the size reaches a plateau[630−633] region the polydispersity still continues to increase. Pineli and co-workers[630,632,633] explain this as follows. At low water content, the number of water molecules per surfactant molecule is too few to hydrate the counterions and the surfactant headgroups. This induces strong interactions between the water molecules and the polar headgroups, so that the water molecules present as "bound" water. With a progressive increase in the water content, there is a change from "bound" to "free" water in the water pool; as a result, the particle size also increases. But whenever it reaches a plateau any further increase in R does not effectively increase the particle size because the excess water can no longer contribute to the hydration of new ions. Another trend is also evident from the literature. It shows that initially the particle size increases with increasing R until a certain value is reached, beyond which particle size again starts to decrease.[634] This may be because of the decrease in the rate of effective collision and intermicellar transfer after a certain R value is attained.

5.1.2.2. Polar Volume Fraction. In a reverse microemulsion with increasing polar volume fraction, the population of reverse micelles or nanoreactors increases in the continuous oil phase. Therefore, the collisions between particles in populated reverse micelles also increases, which in turn leads to an increase in the probability of aggregation. Another reason for increasing size with increasing polar fraction may be concomitant increases in reactant concentration so that the nucleation and growth mechanism changes from intramicellar to intermicellar and hence ultimately particle size increases.[625,627,628,635]

5.1.2.3. Effect of Reagents. During the process of a reduction reaction, normally the reducing agents have no effect on controlling the particle size. However, with weak reducing agents, polydispersity increases because of the slow reaction rates.[631,632] In general, when the reaction is fast the nuclei concentration increases because of more intra- and intermicellar exchange; as a result, small sized particles are obtained. For example, in the case of CdS nanoparticle synthesis by single as well as double microemulsion techniques, H_2S gas was used as a sulfide precursor for the single microemulsion method, whereas in the case of the double microemulsion method aqueous Na_2S was used as the sulfide precursor.[636] The results show that in the case of H_2S bubbling, the particle size is larger because of excess sulfide ion concentration. Generally, particle size depends slightly on the nature of the reactant also. In contrast, some literature reports support the view that particle size and its polydispersity do not depend on the nature of the reactant.[627,628,635,637]

5.1.2.4. Effect of the Oil Phase. The organic phase is an important factor in nanoparticle synthesis using microemulsion techniques. Not all organic solvents are suitable for the formation of (w/o) microemulsions. The viscosity is an important parameter for controlling the mechanism of particle formation. Indirectly it controls the intramicellar exchange dynamics. For example, when cyclohexane (viscosity = 0.85 cP) was used as the continuous phase instead of isooctane (0.32 cP), a 10-fold reduction in the rate of intermicellar exchange occurred; therefore, although the size of the water pools remained constant, because of less intermicellar exchange the ultimate particle size was reduce by 2-fold in the case of cyclohexane (as shown in Figure 42).[630] The decrease in particle size when using cyclohexane instead of isooctane (all other parameters kept constant)

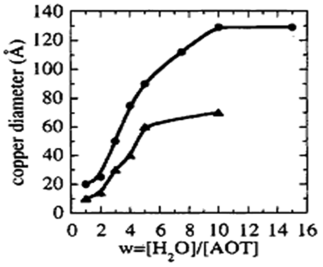

Figure 42. Variation of the diameter of copper particles synthesized in $Cu(AOT)_2$ Na(AOT) water solvent reverse micelles at various water contents: [AOT] = 0.1 M; $[Cu(AOT)_2] = 10^{-2}$ M; $[N_2H_4] = 3 \times 10^{-2}$ M. The solvents are isooctane (●) and cylohexane (▲).
Reprinted with permission from ref 630. Copyright 1995 American Chemical Society.

can be explained in terms of intramicellar nucleation and growth mechanism, and lower aggregation for cyclohexane system. A decrease in the rate of intermicellar collisions because of the higher viscosity of cyclohexane is the result.

5.1.2.5. Effect of Mixing. Mixing is another factor used to control particle size especially for single microemulsion systems with a liquid or solid as one of the reagents. The literature confirms that the addition of a liquid reagent, even without phase separation, increases the particle aggregation,[634,638] whereas ultrasound sonications effectively improve the reactant distribution within the reverse micelles, which ultimately gives more uniformly small sized particles. For double microemulsion systems, effective mixing reduces the particle size with a concomitant narrow size distribution. In contrast, some literature reports also hold the view that the mixing has no effect on the particle size and polydispersity.[626,635]

5.2. Effect of Temperature

Temperature is the most common reaction parameter used to control the reaction kinetics for nanoparticle formation. In general, for exothermic reactions, the reaction rate decreases with increasing temperature, whereas the opposite is the case for endothermic reactions. Normally, temperature is not an important parameter for reductions or sol−gel reactions[639] or wire electrical explosions, but it is in fact a very important parameter for thermal decompositions, polymerizations, or precipitation reactions. Generally, higher temperature is required for thermal decomposition reactions, but for exothermic polymerization reactions, a low temperature is much better for the conversion. In the case of precitipitation reactions, the situation is little bit different. For particle formation through precititation, a reaction can be divided into three different steps: (i) nucleation, (ii) growth, and (iii) agglomeration. As a result, the size of the particles depends on the relative rate of these three different steps. The nucleation process depends on the nature of the chemical reaction, whether it is endothermic or exothermic, whereas the growth process is more complicated. It depends on the nature of the reaction as well as the diffusion of the atoms or embryo from the bulk to the nuclei surface. The diffusion coefficient of the atoms or embryo increases with increasing temperature, but the product concentration depends on the nature of the reaction. If the reaction is endothermic in nature, then the diffusion increases because of an increase in product concentration in the bulk, since the endothermic reaction rate increases with temperature and vice versa for the exothermic reaction. However, if the nucleation rate is very fast because of an overall fast reaction, then the growth rate depends on the diffusion rate only. According to the Lifshitz−Slyozov−Wagner (LSW) model, the critical volume grows linearly with time and the number of particles decreases proportional to t^{-1}. For a diffusion-controlled coarsening process, the kinetics of coarsening can be written as[592,640,641]

$$r_{av}^3 - r_0^3 = k_c t \tag{22}$$

where r_{av} is the average particle size at a time t, r_0 is the particle size at time $t = 0$, and k_c is the coarsening rate constant. The coarsening rate constant (k_c) can be obtained from the slopes of the graph of r_{av}^3 vs t. According to the Arrhenius equation, the rate constant is again related to temperature and the activation energy can be written as

$$k_c = A e^{-E_a/(RT)} \quad \text{or} \quad \ln k_c = -\frac{E_a}{RT} + \ln A \tag{23}$$

where E_a is the activation energy for the growth process, A is a constant, R is the universal gas constant, and T is the temperature (in K). It can be seen that the rate constant for the coarsening, k_c, inversely depends on the temperature. The coarsening or growth rate constant, k_c, can be also written as

$$k_c = \frac{8\gamma D V_m^2 C_\infty}{9RT} \tag{24}$$

where γ is the surface energy of the particles (J/m^2), V_m is molar volume for the particles, C_∞ is the particle bulk concentration, R is the universal gas constant, and T is the working temperature. D is the diffusivity of the particles, which can be calculated by using the Stokes−Einstein equation,

$$D = \frac{k_B T}{6\pi\eta a} \tag{25}$$

Here k_B is the Boltzmann constant (1.38×10^{-23} J/K), η is viscosity of the media (kg/(m·s), and a is the hydrodynamic radius (nm) of the particles.

Finally, the working temperature range depends mainly on the reaction mechanism of core or shell formation. Normally, a low temperature (∼100 °C) is preferred for coprecipitation reactions, a medium temperature is preferable (∼100−500 °C) for hydrothermal and thermal decomposition reactions, and high temperatures (above 500 °C) are only used when calcinations are included in the mechanism. However, in general, a low temperature is favorable for core/shell nanoparticle synthesis. This is mainly because of the need to maintain unsaturated shell material formation within the reaction mixture, which influences appropriate coating on the core surface rather than the formation of separate nuclei. Also a low temperature leads to less intermixing of core and shell atoms at the interface. As mentioned before, for *in situ* core/shell particle synthesis, core surface modification is essential for good coating. The modification is normally done by the adsorption of an appropriate surface active agent onto the core surface so that the oppositely charged shell material is selectively deposited on the core surface. But at high temperatures, the adsorption density of the surface active agent on the core surface is reduced; as a result selective uniform coating presents a difficult task. Therefore, taking into consideration all these factors, if a higher temperature is favorable for the reaction, then an optimum temperature is maintained throughout the reaction so that both the parameters are taken into consideration. In general, a low temperature is preferred for core/shell particle

synthesis in the presence of a surface modifier.[159,183,192,215,278,483,642] However, if the shell material can be coated onto the core surface without any surface modifier then normally the temperature is maintained according to the reaction requirements.[182,185,425] Yin et al.[159] synthesized a Fe_2O_3 shell material using the thermal decomposition of $Fe(CO)_5$ in the presence of the surface modifier dodecanethiol for the synthesis of Au/Fe_2O_3 core/shell nanoparticles at a comparatively low temperature (200 °C), lower than normal thermal decomposition reactions.

5.3. Effect of Reactant Concentration

The reactant concentration is another important parameter for the control of core size or shell thickness. The establishment of the reaction equilibrium and hence the final particle size most probably consists of two steps: (i) reaction between the reactants to form nuclei and (ii) collision between nuclei or diffusion of molecules to the nuclei surface and deposition to create a final particle size. The first step may be considered the reaction step, which is then followed by growth. The first step can be very fast. If the reaction rate is fast, then the result is that the final particle size depends totally on the growth process. There appears to be no particular trend reported in the literature relating to the change in particle size with increasing reactant concentration. On the other hand, increasing trends,[640,643−646] decreasing trends,[647,648] or both[649] on particle size are found to be dependent on the types of particles and the synthesis media. In general, an increasing trend is quite common because of increases in the total amount of the product. When there is more than one reactant present, at low reactant concentration, the number of nuclei formed will be less, probably because of the slow reaction rate. The atoms (embryo) formed at a later period will collide with the nuclei that have already formed instead of forming new nuclei; this in turn leads to larger sized particles. When the reactant concentration is increased because of an increase in reaction rate, a greater number of nuclei will form. This leads to smaller sized particles.

In the case of microemulsion systems, with increasing reactant concentration, the particle size also decreases because of a change in the mechanism of particle formation. Actually, with increasing reactant concentration, the occupancy number of reacting species increases for the individual micelles. The occupancy number is defined as the number of reactant species in a reverse micelle. Therefore, nuclei formation and the growth mechanism change from intermicellar to intramicellar exchange; as a result, the ultimate particle size decreases.[625,627,630,635]

Shell formation in the presence of a core particle normally occurs through a heterogeneous nucleation process. The embryos of shell material are directly deposited onto the core surface and continue the formation of nuclei and growth on the surface itself, instead of forming new nuclei in the bulk phase. As a result, a slow reaction rate favors the formation of a uniform coating. Therefore, a low reactant concentration is more favorable for core/shell nanoparticle synthesis. In general, the overall core/shell particle size or shell thickness increases with increasing reactant concentration.[150,154]

5.4. Effect of Surface Modifier Concentration

Surface modifier concentration also plays an important role in the control of size and morphology of core/shell nanoparticles. Ionic surface modifiers adsorb onto the core surface and generate a uniform charge on the particle surface. It is therefore possible to generate smaller sized core particles by reducing the agglomeration tendency of the particles. Consequently, an oppositely charged shell material will selectively and uniformly deposit onto the core surface. Experimental results show that the monomers that constitute the surface modifiers are responsible for the actual surface modification. They adsorb onto the surface and play a dual role (namely, in size control and through surface modification enhance the driving force for shell formation) in core/shell particle synthesis.[80,182,532,582] The adsorption density of the surface modifier depends on the concentration of the modifier. The density increases with increase in concentration up to a certain limit and then becomes constant. Studies show that CMC or slightly higher CMC concentrations are sufficient for modification of the core surface in order to control the particle size. Similarly, the ultimate size of the core/shell particles can also be controlled by using a surface modifier. But the particle size distribution mainly depends on the surface charge of the particles. In general, a narrow particle size distribution is obtained for ionic surface modifiers.

5.5. Effect of pH

The effect of pH on the particle size depends mainly on the reaction mechanism involved. This is especially true when H^+ or OH ions are directly involved in the reaction. Reduction and precipitation reactions are also strongly affected by changes in the media pH. In a redox reaction, the compound with the highest reduction potential is reduced by oxidizing the compound with the lower reduction potential. The half-cell reduction potential of a redox couple depends on the pH of the media. Hence a favorable pH is highly desirable for controlling the reaction. The extent of surface modification can also be controlled by adjusting the pH of the media. When the core is hydrophilic, the surface charge depends on the pH, especially when polyelectrolyte (PE) modifiers are used for the surface modification of the uniform shell coating. Therefore, the pH of the synthesis media is usually maintained with a view to maximizing the driving force (relative charge difference between core and shell materials) for depositing the uniform shell coating. Lecommandoux et al.[650] developed a pH-responsive hollow magnetic nanoparticle by using micelles and vesicles of an amphiphilic polybutadiene block polymer.

5.6. The Effect of an External Force

Other than the above-mentioned reaction parameters, the application of an external force on the system can also be used to control the particle size. Among the different forces used for particle synthesis, sonication and electrical forces are the most common.

5.6.1. Sonochemical Synthesis. The sound energy process used to induce physical or chemical changes within a medium is termed sonochemistry. This synthesis technique involves promoting chemical reaction for the nanoparticle synthesis by using constant sonication to improve the reaction rate, to breakdown the agglomerates, and to enhance the dispersion of the particles in the solvent media. The range of ultrasound used is from 20 kHz to 10 MHz. This range can be roughly subdivided into three main regions: (i) low-frequency, high-power ultrasound (20−100 kHz); (ii) intermediate-frequency, medium-power ultrasound (100 kHz to 2 MHz); (iii) high-frequency, low-power ultrasound (2−10 MHz). The frequency range from 20 kHz to ~2 MHz is used in sonochemistry. Frequencies above 3 MHz are more commonly used in nondestructive testing and medical imaging. Ultrasonic irradiation speeds up the reaction because of the formation of localized cavities, which only last for a short time. Thus, reaction takes place within these cavities, which act as microreactors. In addition, there is a mechanical effect. In this process, a mixture of reactants is prepared in a suitable solution

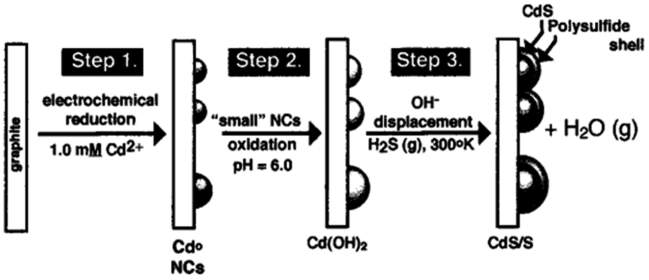

Figure 43. The electrochemical/chemical (E/C) synthesis of CdS/S core/shell nanocrystals.
Reprinted with permission from ref 663. Copyright 1999 American Chemical Society.

with the correct temperature and pH; it is then subjected to ultrasonic waves in order to obtain the nanoparticles; core and shell may be synthesized stepwise. It is generally accepted that there are three main effects of the sonication for the phenomenon of sonocrystallization: (i) the local transient heating of the liquid after the bubble collapses, (ii) the shock waves generated during bubble implosion, which hinder agglomeration, and (iii) the excellent mixing conditions created by acoustic cavitation.[651] All these phenomena lead to a reduction in particle size and an increase in homogeneity owing to control of the local nuclei population.

The core/shell particle size or morphology under ultrasonic vibration depends on the shell material formation if the core is synthesized separately and subsequently added to the reactant mixture.[652−655] Composites such as iron oxide coated with gold[656] or silica[653] shell, bimetallic core/shell composites such as Fe/Co,[657] Au/Ag,[658] Au/Pd alloy,[659] SiO_2/Ag coated silica,[655] and TiO_2/europium oxide coated[654] core/shell nanoparticles have all been synthesized using this method.

5.6.2. Electrodeposition. Electrodeposition is another technique used for the synthesis of core/shell nanoparticles in the presence of an external electrical field. Formation of the shell over the core using charged polymers or inorganic materials can be carried out in the presence of an external electrical potential using this method. When the reaction proceeds in an aqueous phase at room temperature, the thickness of the shell material can be precisely controlled by this method. In electrodeposition, the material is deposited on a supported matrix material, which can be used as either one of the electrodes or the electrolyte medium. Once the matrix material core is attached because of the electrostatic force, the shell is deposited onto the core surface (as shown in the Figure 43). In general, the electric field is varied like a wave with positive and negative cycles. It has been reported that the inorganic material deposits onto the core surface during the negative cycle, whereas the charged polymer (for the polymer shell) is deposited during the positive cycle. Therefore, by controlling the cycle time span, in turn the thickness of the shell material can also be controlled. Banerjee et al.[660] studied the synthesis of iron oxide (either Fe_3O_4 or γ-Fe_2O_3) coated iron-doped silica matrix core/shell nanoparticles using the electrodeposition method. Chipara et al.[661] studied polypyrole (PPy)/iron nanoparticle formation by the same method. In both the cases, the procedure is very similar. However, silica gel was used by Banerjee et al.[660] as a matrix material, whereas in the latter study Fe was just coated onto PPy to get the PPy/Fe core/shell nanoparticles without using any matrix material. Au/CuI and

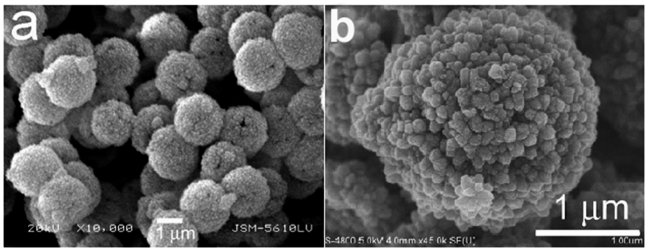

Figure 44. SEM (a) and FESEM (b) of hollow TiO_2 synthesized from SiO_2/TiO_2 core/shell nanoparticles.
Reprinted with permission from ref 664. Copyright 2008 American Chemical Society.

Au/CdS core/shell nanoparticles were also synthesized by using electrochemical atomic layer deposition.[161,178] Similarly, in the synthesis of semiconductor-coated hybrid polymer core/shell nanoparticles, the electrodeposition method was used during the shell coating.[662] Here, a polyelectrolyte−nanoparticle aqueous solution was used as the electrolyte media for electrodeposition; it contained 7 wt % poly(vinyl acetate-*co*-crotonic acid), 8 wt % 2-propanol (used as plasticizer), and 84.65−84.98 wt % water.

6. CHARACTERIZATION OF CORE/SHELL NANOPARTICLES

The characterization of core/shell nanoparticles is critical because of the presence of shell material on the core surface; hence, a suitable characterization technique is always required for both the core and shell. Most characterization techniques used are the same as those used for single particles, but one technique may not be sufficient. The most significant characterization techniques used for core/shell nanoparticles are those for the measurement of size, shell thickness, elemental and surface analysis, optical properties, and thermal stability among others. Therefore, the usual characterization techniques such as dynamic light scattering (DLS), scanning electron microscopy (SEM), transmission electron microscopy (TEM), thermal gravimetric analysis (TGA), X-ray photoelectron spectroscopy (XPS), photoluminescence (PL), and UV−vis spectroscopy are the ones most often used. Depending on the characterization techniques and different instruments, analysis can be classified as described in the following sections.

6.1. Microscopic Analysis

Microscopic analysis is the most common and reliable technique for the direct visualization of the different types of nanoparticles. Scanning electron microscopy (SEM) is the most common microscopic technique used for size and shape analysis of nanoparticles. It can reach a magnification of 10^5−10^6. However, for core/shell nanoparticles, it is difficult to distinguish the difference between core and shell materials, since it can only generate a surface image (as shown in Figure 44a). But when SEM is connected to energy-dispersive X-ray spectroscopy (EDX), it can be used for the elemental analysis of the shell surface. Most recently FESEM (field-emission SEM), which can go to a much higher magnification than normal SEM, has proven useful. High-magnification FESEM images can provide information about whether the shell surface is smooth or rough. Smooth surfaces are possible when the shell material molecules are grown directly onto the core surface because of heterogeneous nucleation. However, the shell surface becomes rough when small sized

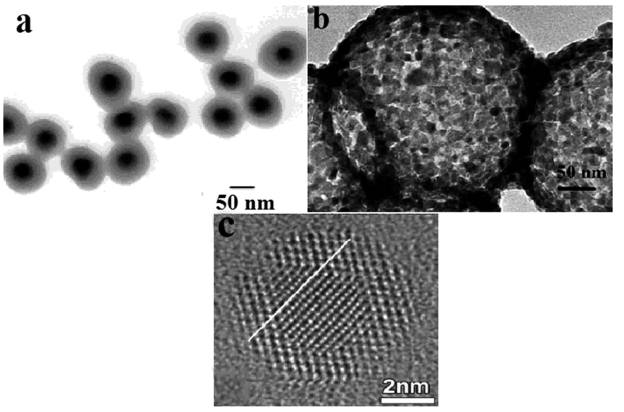

Figure 45. (a) TEM image of gold nanoparticles after coating with 20 nm thick amorphous silica shells, (b) TiO_2 hollow spheres, synthesized from styrene−methyl methacrylate copolymer/TiO_2 core/shell nanoparticles by calcination, and (c) HRTEM image of PbTe/CdTe nanoparticles.
(a) Reprinted with permission from ref 120. Copyright 2002 American Chemical Society. (b) Reprinted with permission from ref 435. Copyright 2009 Elsevier B. V. (c) Reprinted with permission from ref 217. Copyright 2009 American Chemical Society.

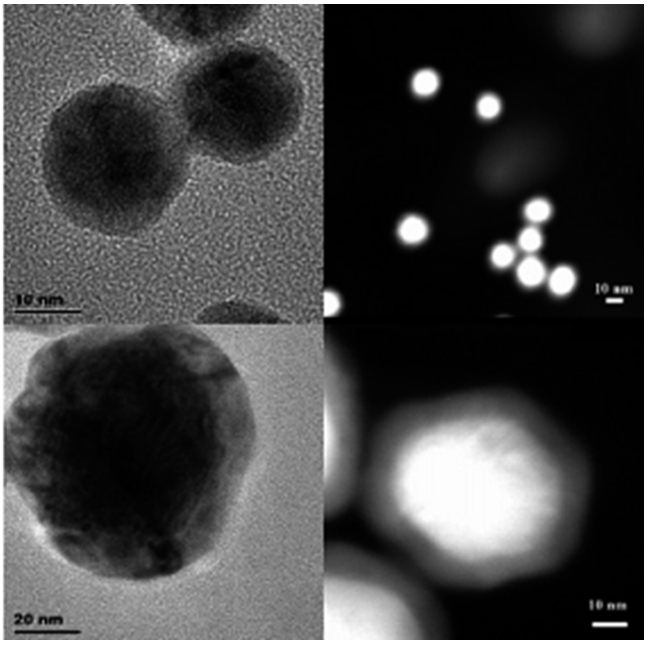

Figure 46. HRTEM (left) and STEM (right) images of the Au/Pd nanoparticles. The top two images are of the nanoparticles with 12 nm core and 2.25 nm shell, and the bottom two images correspond to nanoparticles with 55 nm core and 6.8 nm shell. The STEM images are scanned in a dark-field mode.
Reprinted with permission from ref 154. Copyright 2007 American Chemical Society.

particles are formed in the bulk media and deposited onto the core surface as a result of an appropriate driving force (electrical or van der Waals) as shown in Figure 44b.

Transmission electron microscopy (TEM) provides much more important information: confirmation of core/shell formation through contrast difference, overall particle size, core size,

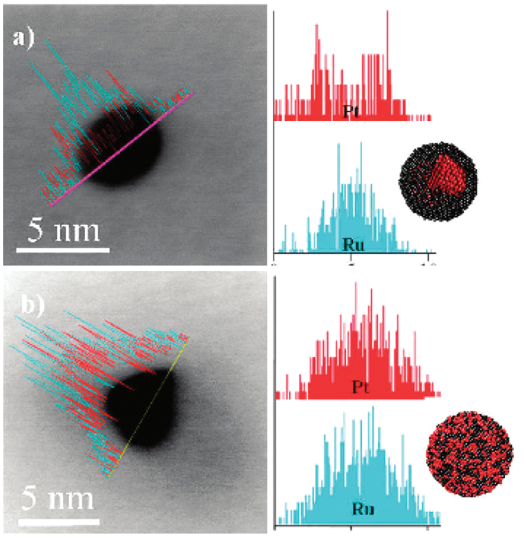

Figure 47. Representative STEM−EDS line spectra of (a) 4.0 nm Ru/Pt NP and (b) 4.4 nm PtRu (1:1) alloy nanoparticles. Relative atomic % composition values (vertical axis) of Pt (red) and Ru (blue) are plotted against the line scan probe position (horizontal axis) and are shown next to the STEM images. A 1.5 nm probe was used to trace 10−15 nm scans across each particle. The particle centers are at ~5 nm in panel a and ~7 nm in panel b.
Reprinted with permission from ref 668. Copyright 2009 American Chemical Society.

shell thickness, uniform or nonuniform shell coating, lattice fringes of the shell material, etc. (shown in Figure 45). From the contrast difference of the core and shell material, the size and morphology of the particles can be easily measured. For much higher magnification, capable of seeing resolution even at the molecular level, HR-TEM (high-resolution TEM) is used. Images yield information on crystallinity, lattice fringes, and even the *d*-spacing of the core/shell materials (as shown in Figure 45c).

Scanning transmission electron microscopy (STEM) coupled with electron energy loss spectroscopy (EELS) or with energy-dispersive X-ray spectroscopy (EDS) is used to give more valuable insight into the core/shell structure (shown in Figure 45). Figure 46 clearly demonstrates that the resulting image clarity is much better for understanding the particle morphology compared with TEM images alone. In particular, STEM−EDS is seen to clearly distinguish the differences between core/shell and alloy or composite material (as shown in Figure 47.). This figure shows that for Ru/Pt nanoparticles, with Ru as the core material, the line spectra are mainly concentrated in the center, whereas the line spectra of Pt are concentrated toward the outside of the core/shell nanoparticle. Interestingly, the line spectra of Ru−Pt alloy particles are totally different from those of the core/shell particle; the line spectra for Ru and Pt are distributed throughout the material. The limitation of these electron microscopy (SEM, TEM) techniques is their inability to generate two-dimensional images of the surface; as a result, it is difficult to understand the roughness of the surface.

Therefore, in order to get additional information, scanning probe microscopy (STM, AFM, etc.) techniques, which have both advantages and disadvantages, are exploited. The diameter and height of the particles can be obtained using such microscopy techniques (see Figure 48). As seen from the phase data shown in

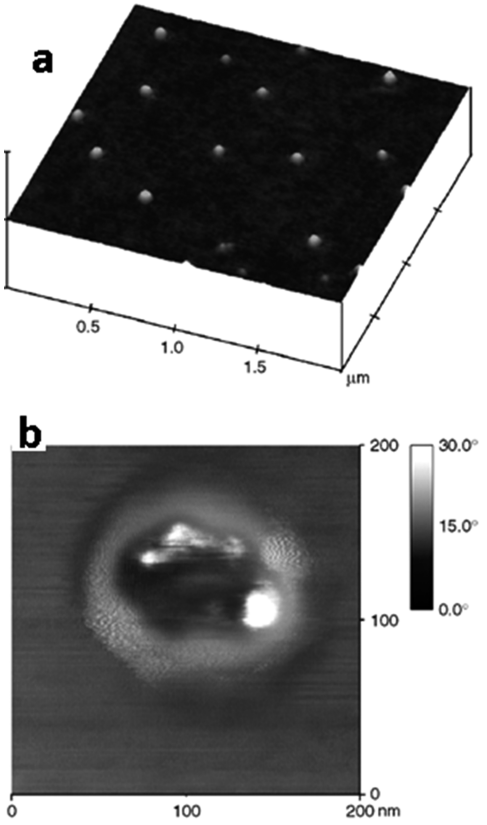

Figure 48. AFM images of the morphology of starch/Ag composite particles .
Reprinted with permission from ref 669. Copyright 2007 Elsevier B. V.

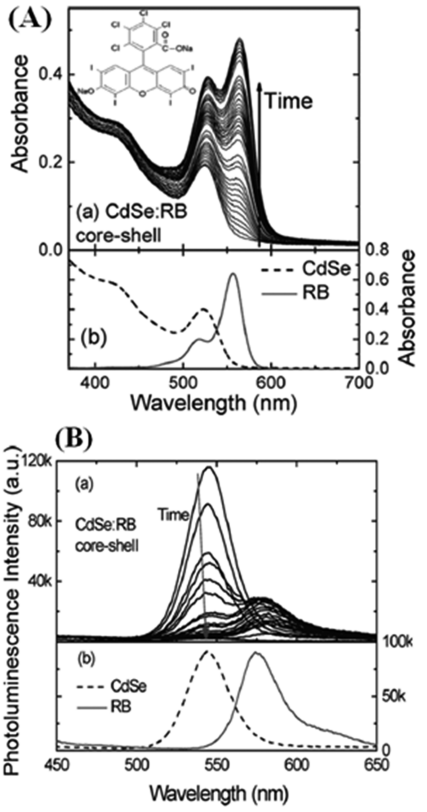

Figure 49. (A) Electronic absorption spectra of (a) CdSe/RB core/shell and (b) CdSe nanoparticles in dispersed chloroform solution and RB solution in methanol. In part a, spectra at different times after addition of RB solution in CdSe dispersed solution from the top are shown. Time range from 0 to 120 min, as marked by an arrow. The structural formula of RB is shown in part a. (B) Photoluminescence spectra of (a) CdSe/RB core/shell and (b) CdSe nanoparticles in dispersed solution in chloroform and RB solution in methanol. In part a, spectra at different times after addition of RB solution in CdSe dispersed solution from the top are shown. The duration of time ranged from 0 to 30 min, as marked by an arrow. The excitation wavelength for all the spectra was 375 nm.
Reprinted with permission from ref 670. Copyright 2009 American Chemical Society.

Figure 48b, AFM also confirms the formation of a two-phase composite structure in the core/shell nanoparticles. Similar to SEM, surface topography data can be obtained using scanning probe microscopy. Unlike electron microscopy, the advantage of scanning probe microscopy is that analysis can be done in either an ambient or a liquid environment.[665−667]

6.2. Spectroscopic Analysis

Optical properties are generally extremely sensitive to any nanocrystal surface modification; consequently they can give some indirect ideas about the coating of the shell materials on the core surface. UV−vis spectroscopy is a common spectroscopic technique used in the analysis of different types of nanoparticles. In particular, those with energy absorption capacity in the UV−vis region that give an absorbance spectrum in this region. In core/shell nanoparticle characterization, UV−vis is used to compare the individual spectra of core, shell, and core/shell material. Fluorescence or photoluminescence spectroscopy is also used as another valuable characterization technique for materials, such as semiconductor materials, which have fluorescence properties. In both the UV and PL spectra, the intensity (absorbed or emitted light) and peak wavelengths change after coating. In addition, with increasing thickness of the shell material, the intensity and peak wavelengths are shifted toward those of the pure shell materials as shown in Figure 49. However, UV or PL spectroscopy largely provides indirect support for the shell material coating on the core surface.

X-ray photoelectron spectroscopy (XPS) is another important spectroscopic technique used to reveal surface information such as (i) elemental composition, (ii) chemical status, (iii) empirical formula, (iv) electronic state or binding modes of surface ligands, and (v) depth analysis or atomic composition with depth. An example of using XPS spectroscopy to examine Au/Pt core/shell nanoparticles is shown in Figure 50. The figure shows the high-intensity peak in the 80−90 eV binding energy region at the 0 min time point due to the pure gold particles. However, after coating and with increasing time, the gold intensity peak decreases. Concomitantly another peak arises at 65−75 eV binding energy because of the Pt surface atoms and after 30 min as the shell thickness is sufficiently thick that the peak for the gold atoms has totally vanished. The measurement of the kinetic energy (KE) and the number of electrons escaping from a 1−10 nm thick layer of the surface is possible using this technique. The main disadvantages of XPS are that it requires an ultrahigh vacuum (UHV) chamber and characterization is only possible to a depth 10 nm from the particle surface.

The same technique with some advanced modifications, namely, "extended X-ray absorption fine structure" (EXAFS) is

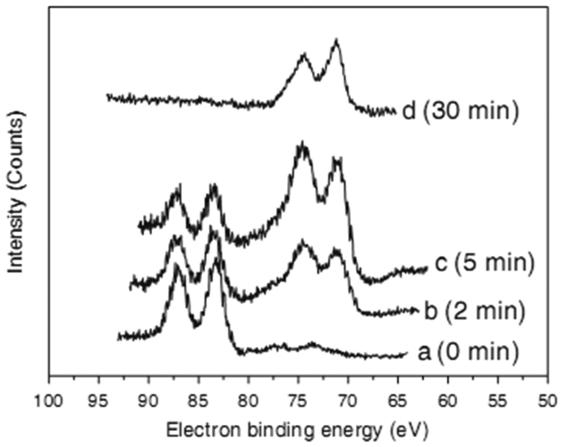

Figure 50. XPS of (a) gold nanoparticles and Au/Pt core/shell nanoparticles after growth for (b) 2, (c) 5, and (d) 30 min on the glass. Reprinted with permission from ref 665. Copyright 2006 Elsevier B. V.

also used for characterizing the nature and binding modes of nanocrystal surface ligands. Raman spectroscopy is another useful analytical tool for investigating the crystallographic orientation and phonon spectra associated with core/shell nanoparticles.

6.3. Scattering Analysis

Light, electron, or neutron scattering from materials is one of the major techniques for nanoparticle characterization either in the colloidal state or in powder form. Dynamic light scattering (DLS), sometimes referred to as photon correlation spectroscopy or quasi-elastic light scattering, is another major technique used for direct particle size measurement in nanoparticle suspensions. By measurement of the size of the particles both before and after coating, the shell thickness can be measured.[667,671−673] Indirect evidence of the extent of core surface modification can also be obtained by measuring the ζ potential of the core particles in the solution.[609,674] This method gives the hydrodynamic diameter of the particles.

Powder X-ray diffraction is also extensively used for the characterization of synthesized crystalline materials. It is used mainly for the identification of unknown materials and to characterize the crystallographic structure, crystalline size (grain size), and preferred orientation in polycrystalline or powder solid samples. The effect of finite crystallite sizes as measured by the broadening and intensity change of the peaks in X-ray diffraction is explained by the Scherrer equation. For core/shell nanoparticles, it is an indirect proof of the presence of a complete uniform coating. Because of the coating on the shell materials, the diffraction peak intensity of the core material decreases,[182,197,542] and after a sufficient thickness is laid down, the peak completely disappears (as shown in Figure 51a). Some studies show that low-intensity diffraction peaks of the core material can appear after the coating, but this may be due to insufficient shell thickness and the amorphous nature of the shell material (as shown in Figure 51b).[129,131,133,136,146,183,675]

Both small-angle X-ray scattering (SAXS) and wide-angle X-ray scattering (WAXS) are used separately for the same analytical purpose. For SAXS the operating angle 2θ is in the range of 0.1°−10° and the main advantages are that the sample can be solid, liquid, or even a mixture of solid and liquid of the same or another material in any combination. For WAXS, the

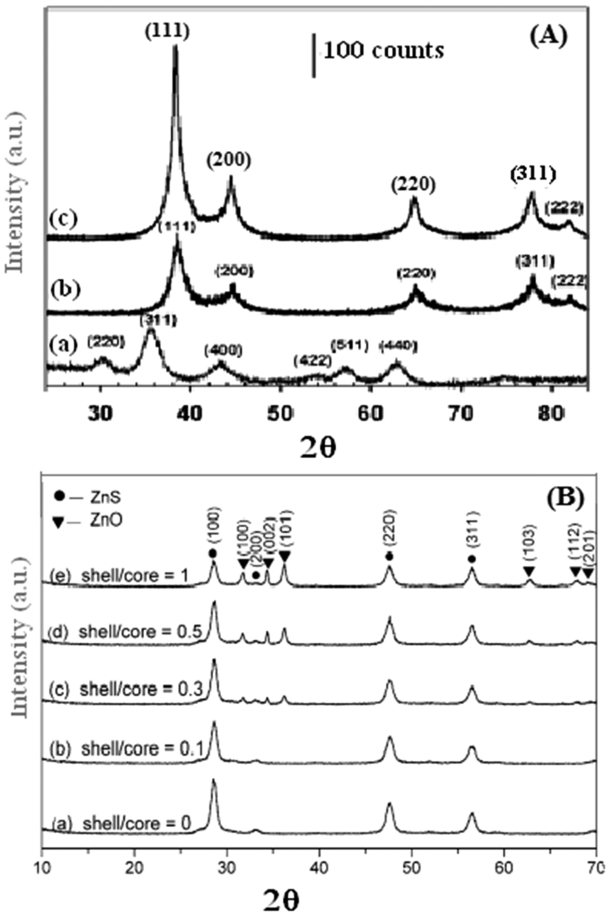

Figure 51. (A) XRD for (a) Fe_3O_4, (b) Au, and (c) Fe_3O_4/Au nanoparticles and (B) XRD patterns of ZnS/Mn nanoparticles (a) without and (b−e) with ZnO coatings of different shell thicknesses. (A) Reprinted with permission from ref 182. Copyright 2005 American Chemical Society. (B) Reprinted with permission from ref 197. Copyright 2009 Springer.

operating angle 2θ is greater than 5°, and it is mainly used to characterize polymer compounds.

Neutron scattering is another important characterization technique, especially in the case of magnetic or organic cores with nonmagnetic shells made of either a polymer or metal oxide nanoparticles.[676−678] This technique provides valuable information regarding the microstructure and composition at the core/shell interfaces. It does this by contrast variation through measuring the angular dependence of the neutron intensity scattered by the sample. In the case of neutron scattering, the microstructure is represented by the scattering length density (SLD), which is analogous to the electron density in the case of XRD. Additionally, this technique is also used to reveal information about the formation of homogeneous organic cores with high cross-linking between the core and shell polymer through the internal networks for organic/organic core/shell nanoparticles.[679−681]

6.4. Thermal Gravimetric Analysis

Thermal gravimetric analysis (TGA−DTA) is another technique used to characterize the thermal stability of compounds. TGA analysis is the measurement of weight loss, and differential thermal analysis (DTA) gives a thermal profile of any material as

the temperature increases. This technique is also used to support the removal of the organic core from the core/shell particles in the process of hollow particle formation.[415−417,435,439]

7. APPLICATIONS

Compared with single particles, core/shell particles have many practical applications, especially in the biomedical and electronics fields. In this section, these applications will be discussed briefly.

7.1. Biomedical Applications

Core/shell nanoparticles have many potential and exciting applications in the biomedical field. Although over more than a decade some applications have already been developed there are major applications still at the innovation stage.[441,682,683] In the biomedical field, core/shell nanoparticles are mainly used for controlled drug delivery,[78,94,109,466,684−689] for bioimaging,[78,79,94,107,683,684,690−693] for cell labeling,[94,107,465,684,688,690,694] as biosensors,[98,107,113,690,691,693] and in tissue engineering applications[128,695−698] etc.

7.1.1. Controlled Drug Delivery and Specific Targeting. Recently, the performance of drug delivery systems has improved enormously because of the development of controlled release of drugs over the more traditional uncontrolled release. Advances in this area have become easier and more precise because of nanotechnology developments. Simultaneously, very specific drug delivery is now possible to a particular location inside the body or to an organ in what is called "targeted delivery". The combination of these two approaches can be exploited for targeted drug delivery at a specific location with controlled release. Therefore, in order to further improve the drug delivery system, some crucial properties of the free drugs such as solubility, *in vivo* stability, pharmacokinetics, and biodistribution must be considered. The overall efficacy can be improved by using suitable nanoparticles with increasing drug selectivity toward the targeted tissue.[98]

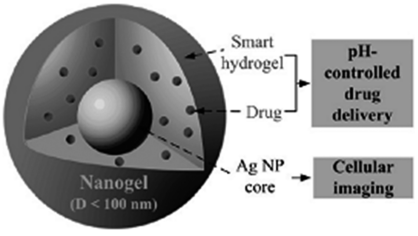

Figure 52. Schematic illustration of drug-loaded core/shell hybrid nanogels with the smart gel shell immobilized on the Ag NP core for integration of tumor-cell imaging and pH-triggered drug delivery.
Reprinted with permission from ref 711. Copyright 2010 American Chemical Society.

In this process, first the drug is encapsulated inside the mesoporous nanoparticles already prepared with a proper surface coating for selective attachment to a specific cell surface. Second, in order to release its cargo after reaching the target cell, the nanocarrier disintegrates or opens up supramolecular gates chemically attached close to the outlet of the particle's mesopores. This release can be stimulated either externally by heat or light or even better by exploiting the local chemical environment of the target, such as pH or concentration of specific ions. If the material is coated with a fluorescent active material, then the particles also serve as a sensor to allow particle tracking, thereby verifying the controlled drug delivery.

There are two approaches used for drug controlled delivery purposes, (i) active and (ii) passive targeting. Active targeting is a more specific targeting with customized ligands attached to the drug-encapsulating nanoparticles, which can be selectively adsorbed by the target cell receptors. For example, folic acid or methotrexate are selectively used for cancer cell therapies because cancer cells have folate receptors[98,381] that are overexpressed on the cell surface. However, in the case of passive targeting, the encapsulated drugs target the body with appropriate surface modification so that they selectively accumulate with the targeted cells due to physicochemical or pharmacological factors.[699−701]

Hence for purposes such as these, magnetic nanoparticles with fluorescence properties are considered more widely acceptable. Therefore, magnetic nanoparticles such as iron oxide, Fe, Ni, Co, and super paramagnetic iron oxide (SPION) core particles with suitable shell coatings for *in vivo* drug release are used.[135,136,167,684] Polymer-coated magnetic core/shell nanoparticles and hollow organic nanoparticles are used for controlled drug delivery, cell labeling and separation,[702−705] enzyme transplantation,[705] contaminated waste removal, and gene therapy. Silica- or polymer-coated magnetic core/shell nanoparticles are more biocompatible compared with free naked magnetic particles and hence are used for controlled drug delivery within a living cell.[135,136,167]

7.1.2. Bioimaging. Different types of molecular imaging techniques, such as optical imaging (OI), magnetic resonance imaging (MRI), ultrasound imaging, positron emission tomography, and others are used for the imaging of both *in vivo* and *in vitro* biological specimens. However, optical and magnetic resonance imaging techniques are the most acceptable because

Figure 53. Delineation of a GFP-expressing 9L glioma tumor by optical imaging in an intraoperative setting. Craniotomy was performed on a Fischer 344 rat bearing a 3-mm diameter 9L glioma tumor. The brain tissue overlying the tumor was removed, and optical imaging was performed. White light image (A), GFP channel (B), and Cy5.5 channel (C).
Reprinted with permission from ref 690. Copyright 2003 American Association for Cancer Research.

they utilize the inherent luminescent and magnetic properties of the nanoparticles. The two principal types of nanoparticles that have been used for imaging *in vivo* systems are luminescent nanoprobes for optical imaging and magnetic nanoparticles for magnetic resonance imaging. In some specific cases, dual-mode nanoparticles are used for simultaneous optical and magnetic resonance imaging.[690,693,706]

Normally, quantum dots (QDs) and dye-doped QDs are used for optical imaging purposes. Quantum dots are photochemically and metabolically stable, are bright, and have a narrow tunable and symmetric emission spectrum. They do, however, have the disadvantage of a tendency to photooxidation, toxicity, and low water solubility. However, these limitations can be minimized by coating them with a suitable material. Subsequently these core/shell nanoparticles can be used directly for *in vivo* optical imaging purposes.[707−709] Pinaud et al.[710] reviewed the different choices of coating for improving the properties of these QDs. The surface plasmon effects of Ag metal can also be used for tumor-cell imaging and adequate local delivery to the tumor site as a result of coating with a smart gel polymer.[711] The morphology of a hydrogel-modified encapsulated Ag and drug is shown in Figure 52. Here, Ag is used for the cellular imaging, but the copolymer hydrogel is used for pH-controlled drug delivery. The detection of tumor cells in a rat species was carried out using Cy5.5−CLIO nanoparticles synthesized from NH_2−CLIO (cross linked iron oxide) and Cy5.5 (Amersham-Pharmacia). After deposition of the particles onto the tumor cells and exposure to light for 500 ms, the fluorescent material emits light that makes it possible to detect the tumor cells (shown in Figure 53). Lanthanide earth metals also have good fluorescence and photoluminescence properties. Hence lanthanide metal salts with suitable biocompatible shell coatings are also used for bioimaging and biodetection purposes in living systems. In such applications, the doping of some lanthanide ions such as, Er, Tm, or Yb onto other lanthanide salts shifted the emission spectrum to a blue, green, or red wavelength, and the spectrum intensity was also found to increase.[205,227−229]

The approach is similar for magnetic resonance imaging (MRI). Here magnetic nanoparticles such as iron oxide, Fe, Ni, Co, or super paramagnetic iron oxide (SPION) core particles are used with incorporation of the correct shell coating in order to increase the contrast for *in vivo* applications. Since these particles have better spin−lattice relaxation times, after entering into the cell, the particles give better contrast images.[94,378,379,689−691,712,713] Kircher et al.[690] reported an MRI study for brain tumor cells of rats using Cy5.5−CLIO, which contains Fe nanoparticles. The Prussian blue color demonstrated the accumulation of the particles on the tumor cell because staining was negative in uninjected animals (shown in Figure 54). These core/shell nanoparticles also have selective drug releasing and magnetic data storage capabilities.[94,378,379,712]

7.1.3. Sensors, Replacement, Support, and Tissues. Sensors are devices that measure a physical quantity and convert it into an analog or digital signal that can be read by an observer or an instrument. In *in vivo* applications, nanoparticles are used as a sensor for the detection of damaged cells, DNA, RNA, glucose, cholesterol, etc. A magnetic material coated with a fluorescence material can be used as sensor. Here the fluorescent dye tracks the particle location, whereas the magnetic shell serves to transfer heat at that position via magnetic excitation.[113] Magnetic-based

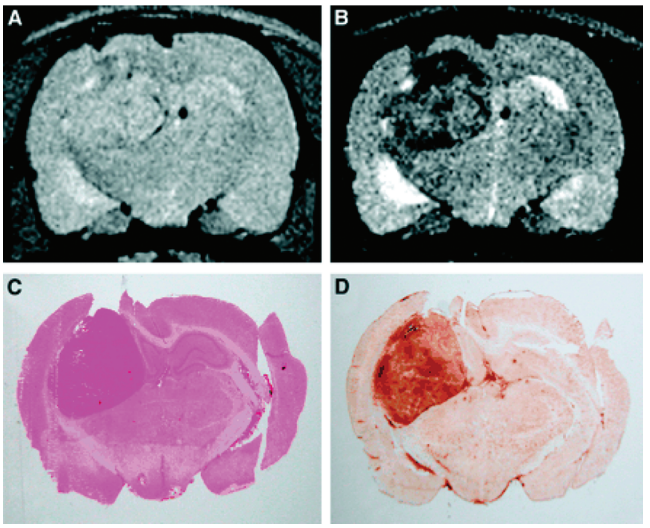

Figure 54. Cy5.5−CLIO nanoparticles as a preoperative MRI contrast agent. Proton density and T_2-weighted images are shown in panels A and B, respectively. Tumor uptake of iron is evident on T_2-weighted images as regions of low signal intensity, whereas the tumor is isointense to surrounding tissue using proton density images. Panel C shows H&E staining of histological sections corresponding to MRI slices in A and B. Panel D shows DAB-amplified Prussian Blue staining of histological sections corresponding to MRI slices in panels A and B.
Reprinted with permission from ref 690. Copyright 2003 American Association for Cancer Research.

nanocomposites coated with any other material, such as a fluorescent one, a metal, silica, or a polymer, are used as bioanalytical sensors.[698,714,715] Silica-coated ZnS/Mn nanoparticles are used for sensing Cu^{2+} ions.[144] Bimetallic core/shell nanoparticles are useful as a sensor in *in vivo* systems. One such example is where Au/Ag core/shell nanocomposite particles are used for sensing cancer and tumor cells in the body.[132] However, the main limitation of such particles is that they require functionalization with an antibody for selective binding with the analyte molecules. Fe/Fe_2O_3 core/shell nanoparticles are selectively used for the detection of damaged DNA.[534] These particles are attached with bioactive proteins such as cytochrome P450, myoglobin (Mb), and hemoglobin (Hb), which are used to mimic the *in vivo* toxicity.[716]

Polymeric core/shell nanoparticles are commonly used as transplant materials. These can be either polymer/polymer or polymer/metallic material forming core/shell structures. They are used in dental braces and in joint replacements.[696,717] Ultrahigh molecular weight polyethylene (UHMWPE)/silver, is one such material used in joint replacement.[697] Hollow TiO_2 coated with high-density PAA polymers is used for the secretion of neurotransmitters from cells present in the brain.[539] The salient features of the particles used in joint repair are abrasion resistance, high impact strength, and resistance to corrosion. Core/shell nanoparticles consisting of polymers, bioceramics, and other inorganic materials appear to be better materials for joint replacement[129,718−720] and bone regeneration because of superior mechanical properties, improved durability, and surface bioactivity compared with conventional polymers or composites.

7.2. Catalytic, Electronic and Other Applications

Magnetic particles coated with a functional material such as a noble metal, semiconductor, or appropriate oxide increase the

physical properties (optical, catalytic activity, electrical, magnetic, and thermal) of the combined particles compared with the pure core particles.[129,159,183,194,721] Nanosized metal oxides (MgO, CaO) have destructive adsorption capacity of halogenated hydrocarbons and organophosphorous compounds but a coating of a transition metal oxide [Fe_2O_3,[195,247,615] V_2O_5[272]] onto the original metal oxide increases the destructive adsorption capacity several fold. Similarly, the catalytic conversion of CO to CO_2 by Fe_2O_3-coated Au nanoparticles supported on SiO_2 was studied by Yin et al.[159] Their results showed that the conversion efficiency is more than that for Au alone supported on SiO_2. They also found that the efficiency increases with preheating of the catalyst but that excess heating can decrease the efficiency mainly because of the increase in percentage of Au metal and crystalline nature of the Fe_2O_3. The conversion efficiency of the Au/Fe_2O_3 particles is improved because of the presence of the support material. In adition, results show that the percent improvement is almost independent of the nature of the support material (SiO_2, C, Fe_2O_3) except for TiO_2. Similarly, a porous stable silica coating on metal cores (Fe, Co, Ni, Ru) increases the core stability and also improves the catalytic activity for the production of CO_x-free H_2 in the decomposition of NH_3.[721] Normally, because of the synergetic effect, bimetallic core/shell nanoparticles show better catalytic activity compared with the single pure metallic nanoparticles. Bimetallic core/shell nanoparticles,[722] especially Au/Pd,[157,723,724] Au/Ag,[725] Au/Pt,[726] Pt/Pd,[727] and Co/Pt[563,564] are used as catalysts in a range of reactions.

Core/shell nanoparticles with either core or shell made of a semiconductor or a metal are equally important in the electronics field.[352,406,407,409,614,728−731] Polymeric materials are easy to process, but these materials have low dielectric constant. On the other hand, ceramic materials have high dielectric constants but are more difficult to process. Interestingly, a combination of these two materials in the form of core/shell with ceramic core and a thin polymer shell increases the dielectric constant compared with the pure polymer. At the same time, it renders them more easily processable. Because of their high capacitance these materials are used in electronics.[352,731] Similar to other applications, here the basic advantage of the core/shell particles is the shell material coating the core surface, which increases the colloidal stability and prevents photodegradation of the core particle. Among the different inorganic materials used, silica is the most common one. Silica is an inert material and hence does not affect the redox reaction of the core material. Instead it just blocks the core particle so that the colloidal stability of the particle increases. In addition, the silica shell is optically transparent so that chemical reaction of the core particle can be easily studied spectroscopically.[118,124,732] In addition, it reduces the bulk conductivity of the metal core particle thus preventing the photocatalytic degradation of the polymeric materials. Silica shells are also used to modulate the position and intensity of the colloidal metal surface plasmon adsorption band.[124]

Carbon coatings on TiO_2 increase the stability of the anatase phase as well as improving the adsorption capacity and photocatalytic activity.[733,734] For example, carbon-coated $Li_3V_2(PO_4)_3$ core/shell particles[17] are used to increase the efficiency of lithium ion batteries. Carbon-coated Fe_3O_4 is used for the solid phase extraction of polycyclic aromatic hydrocarbons from environmental water samples.[186] The main application of the carbon

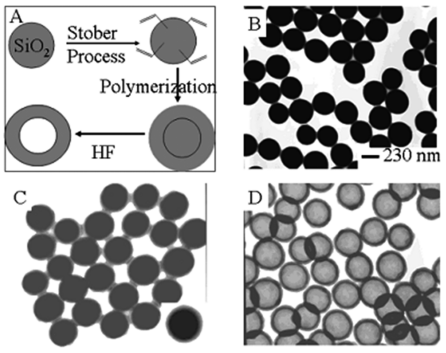

Figure 55. (A) Synthesis scheme for monodispersed hollow polymeric particles; (B) 300 nm silica particles; (C) silica particles coated with 48 nm polystyrene shells; (D) hollow polymeric particles produced by etching out the silica cores with HF.
Reprinted with permission from ref 745. Copyright 2004 American Chemical Society.

coating on the metal or metal oxide nanoparticles is to increase the core particle stability with a subsequent increase in catalytic properties, biocompatibility, and nontoxicity.[187,735,736] Organic/silica core/shell nanoparticles combine the properties of both the polymeric (e.g., flexibility, ductility, dielectric) and silica (e.g., high thermal stability, strength, hardness, UV−vis absorbance) components while including some additional special or novel properties, which are a result of their special microstructures. These have potential use in many fields: plastics, rubbers, coatings, inks, etc.[454,737,738]

7.3. Synthesis of Hollow Nanoparticles

Hollow nanoparticle synthesis using a sacrificial core technique is an important application of core/shell nanoparticles. For the synthesis of different hollow particles both inorganic and organic cores are used and even in some cases composite materials are also used as the sacrificial core. In this technique, the core can be easily removed from the core/shell particle by either dissolution using a suitable solvent, acid, or alkali solution, or by calcination at higher temperatures to create the hollow particle. The organic or polymer cores, especially polystyrene[413,414,420−422,438,458,739] or different polystyrene-based copolymers[434,435,455,740] are more commonly used. However, some other polymers[80,426,454] and organic aggregates[669,741,742] are also used for the synthesis of different inorganic hollow particles. Similarly, inorganic cores are also equally important for using as sacrificial cores for the synthesis of hollow nanoparticles. The main difference between an organic and inorganic core is its removal technique; normally organic cores are removed by calcination or dissolution by suitable solvents, whereas dissolution by acid or alkali solutions is more common for inorganic cores. Silica,[425,461,514,664,743−745] Au,[122] Ag,[611] Pt,[746] $CaCO_3$,[146,743] and CdSe−ZnS[747] are the most common materials used as sacrificial inorganic cores. Silica, Au, and Ag cores can be removed by the dissolution method because they have high solubilities in hydrofluoric acid (HF),[446,454,745] KCN/$K_3[Fe(CN)_6]$,[541,748] and NH_3[526,749,750] solutions, respectively. Even silica cores can be used for hollow polymeric particle synthesis.[745] Figure 55 shows the schematic route of the polymeric hollow particle synthesis using a silica core with the image of core, core/shell, and hollow polystyrene spheres. So where the shell material is concerned using

Table 9. Different Classes of Hollow Particles Synthesized from Core/Shell Nanoparticles by Sacrificial Core Techniques[a]

				core removal technique		
core type	shell type	core material	shell material	dissolution	calcination	ref
organic	metal	sulfonated PS	Ag	0.4 M SDS solution	500 °C, 3 h	422
		modified starch	Ag	aqueous 1 α-amylase solution		669
		bees wax	Ag	ethanol, 70 °C		754
		PS	Cu		500 °C, N_2 atmosphere	415
	semiconductor	PVP	TiO_2		550 °C, 2 h	427
		PS			450 °C, 6 h	421
		MF copolymer	CdS		1000 °C, 1 h	439
		SMMA copolymer			500 °C, 4 h	434
		CTAB	Ag_2S	water and CS_2		431,432
		PSAA	ZnS	toluene		441
		PS			450 °C, 6 h	458
	oxide compounds	PAA	SiO_2			741
		poly(L-lysine)			540 °C	742
		CTAB		water		430,442
		PS			450 °C, 6 h	421
					600 °C, 4 h	420
					Spray pyrolysis	739
		PS−PVP−PEO micelle			500 °C, 4 h	740
		PEG			600 °C, 6 h	444
		PS	Fe_2O_3−SiO_2 composite		500 °C	438
		PSAA	Ag−TiO_2 composite		550 °C, 2 h	542
		PEG	Si/Al composite oxide		650 °C, 8 h	460
		PS	Y compound		high temperature, 3 h	414
			Zr compound		high temperature	459
	organic	PNIPAM	HEMA	dialysis against deionized water, 5 °C for 1 month		753
inorganic	inorganic−organic composite	SiO_2	PMMA−Ag	HF		454
	metal	Ag	Pt	NH_4OH		749,755
		SiO_2	Ag	alkaline solution		611
	oxide compounds	CTAB-$CaCO_3$	SiO_2	acidic solution, 8 h	550 °C, 5 h	146,743
		CdSe-ZnS		acid or ammonia solution, 5 days		747
		Au		NaCN solution		122
		Ag	SiO_2	NH_4OH		750
		carbon	Al_2O_3		300 °C, 3 h and then 600 °C	682
	semiconductor	S	Ag_2S	CS_2		751
	organic	Au	polypyrrole	KCN/$K_3[Fe(CN)_6]$		541,748
		SiO_2	PMMA	HF		461
		SiO_2	polypyrrole	10 wt % HF, 8 h		744
		SiO_2−PS composite	polypyrrole	THF, 12 h		752
		SiO_2	PS	HF		745

[a] Abbreviations: HEMA, 2-hydroxyethyl methacrylate; PNIPAM, poly(*N*-isopropylacrylamide); SMMA, styrene−methyl methacrylate; CTAB, cetyltrimethylammonium bromide; PSAA, poly(styrene−methyl acrylic acid); PAA, poly(acrylic acid); PEG, poly(ethylene glycol); PVP, poly(vinyl pyrrolidone); PS−PVP−PEO, polystyrene−poly(vinyl pyrrolidone)−poly(ethylene oxide); MF, melamine formaldehyde; PS, polystyrene; PMMA, poly(methyl methacrylate).

an inorganic or organic core, different types of hollow nanoparticles, such as semiconductors,[421,427,434,435,439,751] ceramics,[414,421,430,442,459,741,742] metals,[415,416,422,611,669] organics,[456,461,752,753] and even inorganic−organic composite hollow particles,[454] can be synthesized. Depending on the nature of the core and shell material properties, some examples of core removal techniques are given in Table 9.

8. CONCLUSIONS

This review seeks to emphasize how the research area of core/shell nanoparticles has been diversifying into a new dimension over the past two decades. Eventually this field will continue to produce breakthrough discoveries for the synthesis, properties, modification, and applications of this new class of nanomaterials. The future generations of core/shell

dx.doi.org/10.1021/cr100449n |*Chem. Rev.* 2012, 112, 2373–2433

nanoparticles will exhibit many new properties that will surely result in new applications with improved performance. Generally core/shell nanoparticles are well-known for better stability, for being able to protect the core material from the surrounding environment, for improved physical and chemical properties, for improved semiconductor properties, for easy biofunctionalization, etc. Most of the recent exciting discoveries show that there is tremendous scope in biomedical applications such as controlled drug delivery and release, targeted drug delivery, bioimaging, cell leveling, biosensors, diagnostics, immunoassays, and many more. In the near future, the development of new materials has the potential for improving the treatment of cancer and many other life-threatening diseases.

The literature cited in this review confirm that the different types of core/shell nanoparticles, inorganic/inorganic nanoparticles, more specifically magnetic and fluorescence core materials coated with other inorganic materials, are extensively studied because of their wide applications in the biomedical and electronics fields. For *in vivo* biological applications such as bioimaging or controlled drug delivery purposes, magnetic or semiconductor cores are generally coated with a polymer or other inert inorganic material (silica, gold etc.) in order to enhance their biocompatibility.

The efficiency of a core/shell semiconductor particle can be enhanced in terms of increased quantum yield and reduced response time by selective coating of the core material with higher band gap shell materials. In early research, core/shell nanoparticles of type I and reverse type I semiconductor materials were highlighted, whereas presently type II semiconductors attract more interest because of the positive change in the effective band gap than either the pure core or shell materials. In addition, more great advances have been made in this area as a result of the invention of core/multishell (CSS) devices to supplant the normal core/shell materials. This is especially true for the QDQW combination (CdS/HgS/CdS, CdS/CdSe/CdS, etc.), where electrons and holes are confined within a low band gap first shell layer; as a result, these materials have excellent photoluminescence properties.

Compared with semiconductor materials, the other core/shells are not highlighted to the same extent. Although some organic/organic and organic/inorganic core/shell nanoparticles are important because of the changes in some of their physical properties (glass transition temperature, mechanical strength, abrasion capability) and chemical properties (oxidation stability), this in turn increases the scope of applications of such particles in different industrial fields. Among the most studied polymeric compounds, polystyrene can be either core or shell because of its easy availability and its inert nature. In addition, other biocompatible polymers such as poly(ethylene glycol) are used extensively as a shell material with a view to increasing the biocompatibity of the core for biosensing and drug delivery applications. Among the common inorganic shell materials, metals (Au, Ag) and oxides (SiO_2, TiO_2) are the more important ones because of the increase in biocompatible properties, mechanical strength, and oxidation, thermal, and colloidal stability of the core particles that they introduce.

The results of studies related to magnetic core/shell (inorganic/organic) nanoparticles show that the magnetic core of metal or metal oxide (Fe, Ni, Fe_2O_3) are usually coated with a biocompatible organic shell for *in vivo* biomedical applications. Superparamagnetic iron oxide nanoparticles are preferably used for bioimaging, and control drug delivery applications because of their excellent properties such as high biocompatibility, less undesirable residues, and finally the magnetic properties of the particles vanish after removal of the external magnetic field. In the 1990s, interest was mainly concentrated on the synthesis and characterization of different core/shell nanoparticles, whereas during the past decade along with the synthesis of more advanced particles, attention has focused more on the application of these particles in different fields such as biomedicine, catalysis, and electronics. As a result, a huge database is available on the synthesis and applications of the core/shell nanoparticles.

Semiconducting fluorescence nanoparticles are generally toxic to the human body and emit light in the UV region; as a result, their direct *in vivo* application is restricted. To improve their light emission properties as well as their biocompatibility, either the core or shell can be made of a lanthanide material that has light emitting properties in the visible wavelength range, or they can be doped with a very low amount of biocompatible core or shell materials. A further improvement in core/shell particle development is the synthesis of particles with dual properties (magnetic and light emitting). These have the potential of direct use in both imaging and selective drug release.

In more recent developments, research has not been limited to spherical particles but has also explored different shaped core/shell nanoparticles. They are generally synthesized either using a similarly shaped core particle as the template or by controlling the shell growth on a core material. Unlike the symmetrical growth of shell material on the core surface of a spherical core/shell nanoparticle, the shell coating is nonuniform for other shapes of core/shell nanoparticles. These not only are of academic interest but also possess new properties that may prove useful for suitable applications.

In the synthesis domain, developments are not limited by synthesizing rigid core/shell particles; researchers have shown that they are able to synthesize more complicated structures such as movable cores within hollow shells and hollow movable cores within hollow shells. Again already one step ahead of the common spherical shape, ellipsoidal shaped movable core with hollow shell particles have also been reported. Apart from the pure academic interest, these particles also seem promising in many applications, such as magnetically separable photocatalysts, self-assembled photonic crystals with controlled bandgaps, and magnetic inks and toners; they have good encapsulation ability, and hence the targeted release of biomolecules is an option. Application of a specific type of nanoparticle is also known such as for a Sn movable core within a carbon hollow shell, which has shown promise as an anode material in secondary lithium batteries.

Where mechanisms are concerned, over the past few years, some new mechanisms such as ion exchange and reduction transmetalation have been proposed by different research groups to support the formation of different core/shell nanoparticles.

From the application point of view also, it can be seen that there is a wide range of applications that can be broadly described as biomedical applications, electronics, catalysis, and chemical and biomedical sensors.

Where the future is concerned, along with the development of new core/shell materials, insight into new mechanisms will be needed in order to facilitate the synthesis process. This in turn should lead to new application areas, in particular biological applications are expected to be fast-tracked from laboratory to clinical trials. The importance of process scalability from laboratory to a commercial scale should not be underestimated. Finally,

with such advances in the experimental work, it is also expected that more theoretical studies will lead to a better understanding and facilitate experimental trials. It is hoped that this review will play some small part in helping future developments in this important field.

AUTHOR INFORMATION

Corresponding Author

*E-mail: santanuparia@yahoo.com or sparia@nitrkl.ac.in. Fax: +91 661 246 2999.

BIOGRAPHIES

Rajib Ghosh Chaudhuri was born in 1982 in India. He received degrees from University of Calcutta, B.S. in Chemistry (2004) and B. Tech. in Chemical Engineering (2007). In 2009, he received M. Tech. in Chemical Engineering from National Institute of Technology, Rourkela, with Dr. Santanu Paria. His M. Tech. thesis was nominated for IIChE (Indian Institute of Chemical Engineers) Ambuja's Young Researcher's award for the year 2009. Currently he is working on his Ph.D. thesis at the Department of Chemical Engineering, National Institute of Technology, Rourkela, under the supervision of Dr. Santanu Paria. His research interests are mainly synthesis and characterization of inorganic core/shell and hollow nanoparticles for different applications.

Dr. Santanu Paria was born in the state of West Bengal, India, in 1970. He received degrees from University of Calcutta (Ramakrishna Mission Vidyamandira, Belurmath; B.S. in Chemistry, 1991), University of Calcutta (B. Tech., 1994; M. Tech., 1996 in Chemical Technology), Indian Institute of Technology, Bombay (Ph.D. in Chemical Engineering, 2003 under the supervision of late Prof. K. C. Khilar). He worked as a postdoctoral fellow with Prof. Pak K. Yuet at Department of Chemical Engineering, Dalhousie University, Halifax, Canada, from 2003 to 2005. After a short time working in National Metallurgical Laboratory, Jamshedpur, India (2006), as a scientist, he moved to National Institute of Technology, Rourkela (July 2006), as an Assistant Professor and currently works as Associate Professor. During his Ph.D. and postdoctoral research, he worked on surfactant adsorption onto solid−liquid interfaces. His research interests include synthesis and application of nanoparticles, colloids and interfaces, and surfactant adsorption.

ACKNOWLEDGMENT

The financial support from the Department of Science and Technology (DST) under Nanomission, New Delhi, India, Grant No. SR/S5/NM-04/2007, is gratefully acknowledged.

REFERENCES

(1) Henglein, A. *Chem. Rev.* **1989**, *89*, 1861.
(2) Spanhel, L.; Weller, H.; Henglein, A. *J. Am. Chem. Soc.* **1987**, *109*, 6632.
(3) Youn, H.-C.; Baral, S.; Fendler, J. H. *J. Phys. Chem.* **1988**, *92*, 6320.
(4) Hoener, C. F.; Allan, K. A.; Bard, A. J.; Campion, A.; Fox, M. A.; Malluok, T. E.; Webber, S. E.; White, J. M. *J. Phys. Chem.* **1992**, *96*, 3812.
(5) Honma, I.; Sano, T.; Komiyama, H. *J. Phys. Chem.* **1993**, *97*, 6692.
(6) Zhou, H. S.; Sasahara, H.; Honma, I.; Komiyama, H.; Haus, J. W. *Chem. Mater.* **1994**, *6*, 1534.
(7) Ahmed, J.; Sharma, S.; Ramanujachary, K. V.; Lofland, S. E.; Ganguli, A. K. *J. Colloid Interface Sci.* **2009**, *336*, 814.
(8) El-Safty, S. A. *J. Colloid Interface Sci.* **2008**, *319*, 477.
(9) Song, Q.; Zhang, Z. J. *J. Am. Chem. Soc.* **2004**, *126*, 6164.
(10) Salazar-Alvarez, G.; Qin, J.; Sepelak, V.; Bergmann, I.; Vasilakaki, M.; Trohidou, K. N.; Ardisson, J. D.; Macedo, W. A. A.; Mikhaylova, M.; Muhammed, M.; Baro, M. D.; Nogues, J. *J. Am. Chem. Soc.* **2008**, *130*, 13234.
(11) Schmidt, E.; Vargas, A.; Mallat, T.; Baiker, A. *J. Am. Chem. Soc.* **2009**, *131*, 12358.
(12) Wang, Z. L.; Ahmad, T. S.; El-Sayed, M. A. *Surf. Sci.* **1997**, *380*, 302.
(13) Wei, X. W.; Zhu, G. X.; Liu, Y. J.; Ni, Y. H.; Song, Y.; Xu, Z. *Chem. Mater.* **2008**, *20*, 6248.
(14) Yamada, M.; Kon, S.; Miyake, M. *Chem. Lett.* **2005**, *34*, 1050.
(15) Hu, J. S.; Guo, Y. G.; Liang, H. P.; Wan, L. J.; Jiang, L. *J. Am. Chem. Soc.* **2005**, *127*, 17090.
(16) Jitianu, M.; Goia, D. V. *J. Colloid Interface Sci.* **2007**, *309*, 78.
(17) Ren, T. Z.; Yuan, Z. Y.; Hu, W.; Zou, X. *Microporous Mesoporous Mater.* **2008**, *112*, 467.
(18) Ren, X.; Han, D.; Chen, D.; Tang, F. *Mater. Res. Bull.* **2007**, *42*, 807.
(19) Suematsu, N. J.; Ogawa, Y.; Yamamoto, Y.; Yamaguchi, T. *J. Colloid Interface Sci.* **2007**, *310*, 648.
(20) Wu, L.; Yu, J. C.; Zhang, L.; Wang, X.; Li, S. *J. Solid State Chem.* **2004**, *177*, 3666.
(21) Qu, X.; Omar, L.; Le, T. B.; Tetley, L.; Bolton, K.; Cjooi, K. W.; Wang, W.; Uchegbu, I. F. *Langmuir* **2008**, *24*, 9997.
(22) Cao, G.; Liu, D. *Adv. Colloid Interface Sci.* **2008**, *136*, 45.
(23) Kline, T. R.; Tian, M.; Wang, J.; Sen, A.; Chan, M. W. H.; Mallouk, T. E. *Inorg. Chem.* **2006**, *45*, 7555.
(24) Li, M.; Mayer, T. S.; Sioss, J. A.; Keating, C. D.; Bhiladvala, R. B. *Nano Lett.* **2007**, *7*, 3281.
(25) Liu, Z.; Elbert, D.; Chien, C. L.; Searson, P. C. *Nano Lett.* **2008**, *8*, 2166.

(26) Pena, D. J.; Mbindyo, J. K. N.; Carado, A. J.; Mallouk, T. E.; Keating, C. D.; Razavi, B.; Mayer, T. S. *J. Phys. Chem. B* **2002**, *106*, 7458.
(27) Routkevitch, D.; Bigioni, T.; Moskovits, M.; Xu, J. M. *J. Phys. Chem.* **1996**, *100*, 14037.
(28) Sioss, J. A.; Keating, C. D. *Nano Lett.* **2005**, *5*, 1779.
(29) Wu, Y.; Livneh, T.; Zhang, Y. X.; Cheng, G.; Wang, J.; Tang, J.; Moskovits, M.; Stucky, G. D. *Nano Lett.* **2004**, *4*, 2337.
(30) Bok, H. M.; Kim, S.; Yoo, S. H.; Kim, S. K.; Park, S. *Langmuir* **2008**, *24*, 4168.
(31) Bok, H. M.; Shuford, K. L.; Kim, S.; Kim, S. K.; Park, S. *Nano Lett.* **2008**, *8*, 2265.
(32) Nicewarner-Pena, S. R.; Freeman, R. G.; Reiss, B. D.; He, L.; Pena, D. J.; Walton, I. D.; Cromer, R.; Keating, C. D.; Natan, M. J. *Science* **2001**, *294*, 137.
(33) Park, S.; Chung, S. W.; Mirkin, C. A. *J. Am. Chem. Soc.* **2004**, *126*, 11772.
(34) Park, S.; Lim, J. H.; Chung, S. W.; Mirkin, C. A. *Science* **2004**, *303*, 348.
(35) Paxton, W. F.; Kistler, K. C.; Olmeda, C. C.; Sen, A.; Angelo, S. K. S.; Mallouk, T. E.; Lammert, P. E.; Crespi, V. H. *J. Am. Chem. Soc.* **2004**, *126*, 13424.
(36) Peng, X.; Manna, L.; Yang, W.; Wickham, J.; Scher, E.; Kadavanich, A.; Alivisatos, A. P. *Nature* **2000**, *404*, 59.
(37) Yoo, S. H.; Park, S. *Adv. Mater.* **2007**, *19*, 1612.
(38) Michailowski, A.; Almawlawi, D.; Cheng, G.; Moskovits, M. *Chem. Phys. Lett.* **2001**, *349*, 1.
(39) Shelimov, K. B.; Moskovits, M. *Chem. Mater.* **2000**, *12*, 250.
(40) Shin, T. Y.; Yoo, S. H.; Park, S. *Chem. Mater.* **2008**, *20*, 5682.
(41) Xiao, R.; Cho, S. I.; Liu, R.; Lee, S. B. *J. Am. Chem. Soc.* **2007**, *129*, 4483.
(42) Han, W.; Yi, L.; Zhao, N.; Tang, A.; Gao, M.; Tang, Z. *J. Am. Chem. Soc.* **2008**, *130*, 13152.
(43) Libor, Z.; Zhang, Q. *Mater. Chem. Phys.* **2009**, *114*, 902.
(44) Min, M.; Kim, C.; Lee, H. *J. Mol. Catal. A* **2010**, *333*, 6.
(45) Radi, A.; Pradhan, D.; Sohn, Y.; Leung, K. T. *ACS Nano* **2010**, *4*, 1553.
(46) Wu, Y.; Jiang, P.; Jiang, M.; Wang, T.-W.; Guo, C.-F.; Xie, S.-S.; Wang, Z.-L. *Nanotechnology* **2009**, *20*, No. 305602.
(47) Chen, J.; Herricks, T.; Xia, Y. *Angew. Chem., Int. Ed.* **2005**, *44*, 2589.
(48) Zheng, Y.; Cheng, Y.; Wang, Y.; Bao, F.; Zhou, L.; Wei, X.; Zhang, Y.; Zheng, Q. *J. Phys. Chem. B* **2006**, *110*, 3093.
(49) Narayanan, R.; El-Sayed, M. A. *J. Am. Chem. Soc.* **2004**, *126*, 7294.
(50) Lee, H.; Habas, S. E.; Kweskin, S.; Butcher, D.; Somorjai, A.; Yang, P. *Angew. Chem., Int. Ed.* **2006**, *45*, 7824.
(51) Lieber, C. M. *Solid State Commun.* **1998**, *107*, 607.
(52) Smalley, R. E.; Yakobson, B. I. *Solid State Commun.* **1998**, *107*, 597.
(53) Stuart, D. A.; Haes, A. J.; Yonzon, C. R.; Hicks, E. M.; Duyne, R. P. van *IEEE Proc. Nanobiotechnol.* **2005**, *152*, 13.
(54) Millstone, J. E.; Hurst, S. J.; Métraux, G. S.; Cutler, J. I.; Mirkin, C. A. *Small* **2009**, *5*, 646.
(55) Gupta, S. K.; Talati, M.; Jha, P. K. *Mater. Sci. Forum* **2008**, *570*, 132.
(56) Sun, Y.; Xia, Y. *Adv. Mater.* **2003**, *15*, 695.
(57) Bardhan, R.; Mukherjee, S.; Mirin, N. A.; Levit, S. D.; Nordlander, P.; Halas, N. J. *J. Phys. Chem. C* **2010**, *114*, 7378.
(58) Radloff, C.; Halas, N. J. *Nano Lett.* **2004**, *4*, 1323.
(59) Wang, S.; Jarrett, B. R.; Kauzlarich, S. M.; Louie, A. Y. *J. Am. Chem. Soc.* **2007**, *129*, 3848.
(60) Wang, H.; Brandl, D. W.; Nordlander, P.; Halas, N. J. *Acc. Chem. Res.* **2007**, *40*, 53.
(61) Subramanian, R.; Denney, P. E.; Singh, J.; Otooni, M. *J. Mater. Sci.* **1998**, *33*, 3471.
(62) Kumar, P.; Kumar, R.; Kanjilal, D.; Knobel, M.; Thakur, P.; Chae, K. H. *J. Vac. Sci. Technol. B: Microelectron. Nanometer Struct.—Process., Meas., Phenom.* **2008**, *26*, L36.
(63) Jang, D.; Oh, B.; Kim, D. *Proc. SPIE* **2002**, 1024.
(64) Hong, L. I.; Vilar, R. M.; Youming, W. *J. Mater. Sci.* **1997**, *32*, 5545.
(65) Dodd, A. C. *Powder Technol.* **2009**, *196*, 30.
(66) Deng, W. J.; Xia, W.; Li, C.; Tang, Y. *J. Mater. Process. Technol.* **2009**, *209*, 4521.
(67) Salari, M.; Mousavi Khoie, S. M.; Marashi, P.; Rezaee, M. *J. Alloys Compd.* **2009**, *469*, 386.
(68) Sasikumar, R.; Arunachalam, R. M. *Mater. Lett.* **2009**, *63*, 2426.
(69) Sneh, O.; Clark-Phelps, R. B.; Londergan, A. R.; Winkler, J.; Seidel, T. E. *Thin Solid Films* **2002**, *402*, 248.
(70) Wang, Y. Y.; Cai, K. F.; Yao, X. *J. Solid State Chem.* **2009**, *182*, 3383.
(71) Yoo, S. H.; Liu, L.; Park, S. *J. Colloid Interface Sci.* **2009**, *339*, 183.
(72) Oldenberg, S. J.; Averitt, R. D.; Westcott, S. L.; Halas, N. J. *Chem. Phys. Lett.* **1998**, *288*, 243.
(73) Daniel, M. C.; Astruc, D. *Chem. Rev.* **2004**, *104*, 293.
(74) Caruso, F. *Adv. Mater.* **2001**, *13*, 11and references therein.
(75) Karele, S.; Gosavi, S. W.; Urban, J.; Kularni, S. K. *Curr. Sci.* **2006**, *91*, 1038.
(76) Balakrishnan, S.; Bonder, M. J.; Hadjipanayis, G. C. *J. Magn. Magn. Mater.* **2009**, *321*, 117.
(77) Kim, M. J.; Chao, Y. H.; Kim, D. H.; Kim, K. H. *Magn., IEEE Trans.* **2009**, *45*, 2446.
(78) Laurent, S.; Forge, D.; Port, M.; Roch, A.; Robic, C.; Elst, L. V.; Muller, R. N. *Chem. Rev.* **2008**, *108*, 2064.
(79) Salgueiriño-Maceira, V.; Correa-Duarte, M. A. *Adv. Mater.* **2007**, *19*, 4131.
(80) Phadtare, S.; Kumar, A.; Vinod, V. P.; Dash, C.; Palaskar, D. V.; Rao, M.; Shukla, P. G.; Sivaram, S.; Sastry, M. *Chem. Mater.* **2003**, *15*, 1944.
(81) Kortan, A. R.; Hull, R.; Opila, R. L.; Bawendi, M. G.; Steigerwald, M. L.; Carroll, P. J.; Brus, L. E. *J. Am. Chem. Soc.* **1990**, *112*, 1327.
(82) Qi, L.; Ma, J.; Cheng, H.; Zhao, Z. *Colloids Surf. A.* **1996**, *111*, 195.
(83) Mews, A.; Eychmüller, A.; Giersig, M.; Schooss, D.; Weller, H. *J. Phys. Chem.* **1994**, *98*, 934.
(84) Ma, G. H.; He, J.; Rajiv, K.; Tang, S. H.; Yang, Y.; Nogami, M. *Appl. Phys. Lett.* **2004**, *84*, 4684.
(85) Kamat, P. V.; Shanghavi, B. *J. Phys. Chem. B* **1997**, *101*, 7675.
(86) Scodeller, P.; Flexer, V.; Szamocki, R.; Calvo, E. J.; Tognalli, N.; Trooani, H.; Fainstein, A. *J. Am. Chem. Soc.* **2008**, *130*, 12690.
(87) Babes, L.; Denizot, B.; Tanguy, G.; Le Jeune, J. J.; Ballet, P. *J. Colloid Interface Sci.* **1999**, *212*, 474.
(88) De Farias, P. M. A.; Santos, B. S.; Menezes, F. D.; Brasil, A. G., Jr.; Ferreira, R.; Motta, M. A.; Castro-Neto, A. G.; Vieira, A. A. S.; Silva, D. C. N.; Fontes, A.; Cesar, C. L. *Appl. Phys. A: Mater. Sci. Process.* **2007**, *89*, 957.
(89) Menezes, F. D. de; Brasil, A. G., Jr.; Moreira, W. L.; Barbosa, L. C.; Cesar, C. L.; Ferreira, R. D. C.; Farias, P. M. A. de; Santos, B. S. *Microelectron. J.* **2005**, *36*, 989.
(90) Gupta, A. K.; Gupta, M. *Biomaterials* **2005**, *26*, 3995.
(91) Schreder, B.; Schmidt, T.; Ptatschek, V.; Spanhel, L.; Materny, A.; Kiefer, W. *J. Cryst. Growth* **2000**, *214*, 782.
(92) Zimmer, J. P.; Kim, S. W.; Ohnishi, S.; Tanaka, E.; Frangioni, J. V.; Bawendi, M. G. *J. Am. Chem. Soc.* **2006**, *128*, 2526.
(93) Dresco, P. A.; Zaitsev, V. S.; Gambino, R. J.; Chu, B. *Langmuir* **1999**, *15*, 1945.
(94) Sounderya, N.; Zhang, Y. *Recent Pat. Biomed. Eng.* **2008**, *1*, 34.
(95) Yan, E.; Ding, Y.; Chen, C.; Li, R.; Hu, Y.; Jiang, X. *Chem. Commun.* **2009**, 2718.
(96) Jaiswal, J. K.; Mattoussi, H.; Mauro, J. M.; Simon, S. M. *Nat. Biotechnol.* **2003**, *21*, 47.
(97) Michalet, X.; Pinaud, F. F.; Bentolila, L. A.; Tasy, J. M.; Doose, S.; Li, J. J.; Sundaresan, G.; Wu, A. M.; Gambhir, S. S.; Weiss, S. *Science* **2005**, *307*, 538.
(98) De, M.; Ghosh, P. S.; Rotello, V. M. *Adv. Mater.* **2008**, *20*, 4225.

(99) Sakanishi, K.; Hasuo, H. U.; Kishino, M.; Mochida, I.; Okuma, O. *Energy Fuels* **1996**, *10*, 216.
(100) Zhao, D.; Feng, J.; Huo, Q.; Melosh, N.; Fredrickson, G. H.; Chmelka, B. F.; Stucky, G. D. *Science* **1998**, *279*, 548.
(101) Sugama, T.; Lipford, B. *J. Mater. Sci.* **1997**, *32*, 3523.
(102) Wijnhoven, J. E. G. J.; Vos, W. L. *Science* **1998**, *281*, 802.
(103) Ansermet, J. P. H; Baeriswyl, E. *J. Mater. Sci.* **1994**, *29*, 2841.
(104) Kickelbick, G.; Liz-Marzán, L. M. *Encycl. Nanosci. Nanotechnol.* **2004**, 199.
(105) Li, D.; He, Q.; Li, J. *Adv. Colloid Interface Sci.* **2009**, *149*, 28.
(106) Zou, H.; Wu, S.; Shen, J. *Chem. Rev.* **2008**, *108*, 3393.
(107) Knopp, D.; Tang, D.; Niessner, R. *Anal. Chim. Acta* **2009**, *647*, 14.
(108) Sanchez, C.; Julian, B.; Belleville, P.; Popall, M. *J. Mater. Chem.* **2005**, *15*, 3559.
(109) Schärtl, W. *Adv. Mater.* **2000**, *12*, 1899.
(110) Hao, R.; Xing, R.; Xu, Z.; Hou, Y.; Gao, S.; Sun, S. *Adv. Mater.* **2010**, *22*, 2729.
(111) Dorfs, D.; Eychmuller, A. *Z. Phys. Chem.* **2006**, *220*, 1539.
(112) Reiss, P.; Protiere, M.; Li, L. *Small* **2009**, *5*, 154.
(113) Schärtl, W. *Nanoscale* **2010**, *2*, 829.
(114) Ye, J.; De Broek, B.; van; Palma, R. D.; Libaers, W.; Clays, K.; Roy, W. V.; Borghs, G.; Maes, G. *Colloids Surf. A.* **2008**, *322*, 225.
(115) Liu, T.; Li, D.; Zou, Y.; Yang, D.; Li, H.; Wu, Y.; Jiang, M. *J. Colloid Interface Sci.* **2010**, *350*, 58.
(116) Qi, Y.; Chen, M.; Liang, S.; Yang, W.; Zhao, J. *Appl. Surf. Sci.* **2008**, *254*, 1684.
(117) Qi, Y.; Chen, M.; Liang, S.; Zhao, J.; Yang, W. *Colloids Surf. A.* **2007**, *302*, 383.
(118) Liz-Marzán, L. M.; Giersig, M.; Mulvaney, P. *Langmuir* **1996**, *12*, 4329.
(119) Poovarodom, S.; Bass, J. D.; Hwang, S. J.; Katz, A. *Langmuir* **2005**, *21*, 12348.
(120) Lu, Y.; Yin, Y.; Li, Z. Y.; Xia, Y. *Nano Lett.* **2002**, *2*, 785.
(121) Alejandro-Arellano, M.; Ung, T.; Blanco, A.; Mulvaney, P.; Liz-Marzán, L. M. *Pure Appl. Chem.* **2000**, *72*, 257.
(122) Masayuki, K.; Yuka, W.; Toshiharu, T. *J. Nanosci. Nanotechnol.* **2009**, *9*, 673.
(123) Li, T.; Moon, J.; Morrone, A. A.; Mecholsky, J. J.; Talham, D. R.; Adair, J. H. *Langmuir* **1999**, *15*, 4328.
(124) Ung, T.; Liz-Marzan, L. M.; Mulvaney, P. *Langmuir* **1998**, *14*, 3740.
(125) Cha, H. J.; Kim, Y.; H. Kang, Y. C.; Kang, Y. S. *IEEE Nanotechnol. Mater. Devices Conf* **2006**No. 4.
(126) Fu, W.; Yang, H.; Chang, L.; Li, M.; Bala, H.; Yu, Q.; Zou, G. *Colloids Surf. A* **2005**, *262*, 71.
(127) NuJiang, T.; LiYa, L.; Wei, Z.; ChakTong, A.; YouWei, D. *Sci. China, Ser. G: Phys., Mecha. Astron.* **2009**, *52*, 31.
(128) Wang, G.; Harrison, A. *J. Colloid Interface Sci.* **1999**, *217*, 203.
(129) Zhang, X. F.; Dong, X. L.; Huang, H.; Lv, B.; Zhu, X. G.; Lei, J. P.; Ma, S.; Liu, W.; Zhang, Z. D. *Mater. Sci. Eng. A.* **2007**, *454*−*455*, 211.
(130) Mazaleyrat, F.; Ammar, M.; LoBue, M.; Bonnet, J. P.; Audebert, P.; Wang, G. Y.; Champion, Y.; Hytch, M.; Snoeck, E. *J. Alloys Compd.* **2009**, *483*, 473.
(131) Lu, X.; Liang, G.; Sun, Z.; Zhang, W. *Mater. Sci. Eng. B.* **2005**, *117*, 147.
(132) Lee, J.; Lee, Y.; Youn, J. K.; Na, H. B.; Yu, T.; Kim, H.; Lee, S. M.; Koo, Y. M.; Kwak, J. H.; Park, H.; Chang, H. N.; Hwang, M.; Park, J. G.; Kim, J.; Hyeon, T. *Small* **2008**, *4*, 143.
(133) Chen, J.; Wang, Y. G.; Li, Z. Q.; Wang, C.; Li, J. F.; Gu, Y. J. *J. Phys.: Conf. Ser.* **2009**, *152*, No. 012041.
(134) Aliev, F. G.; Correa-Duarte, M. A.; Mamedov, A.; Ostrander, J. W.; Giersig, M.; Liz-Marzan, L. M.; Kotov, N. A. *Adv. Mater.* **1999**, *11*, 1006.
(135) Lien, Y. H.; Wu, T. M. *J. Colloid Interface Sci.* **2008**, *326*, 517.
(136) Santra, S.; Tapec, R.; Theodoropoulou, N.; Dobson, J.; Hebard, A.; Tan, W. *Langmuir* **2001**, *17*, 2900.
(137) Zhai, J.; Tao, X.; Pu, Y.; Zeng, X.-F.; Chen, J.-F. *Appl. Surf. Sci.* **2010**, *257*, 393.
(138) Chang, S.-Y.; Liu, L.; Asher, S. A. *J. Am. Chem. Soc.* **1994**, *116*, 6739.
(139) Correa-Duarte, M. A.; Giersig, M.; Liz-Marzán, L. M. *Chem. Phys. Lett.* **1998**, *286*, 497.
(140) Kobayashi, Y.; Shimizu, N.; Misawa, K.; Takeda, M.; Ohuchi, N.; Kasuya, A.; Konno, M. *Surf. Eng.* **2008**, *24*, 248.
(141) Rogach, A. L.; Nagesha, D.; Ostrander, J. W.; Giersig, M.; Kotov, N. A. *Chem. Mater.* **2000**, *12*, 2676.
(142) Zhu, M. Q.; Han, J. J.; Li, A. D. Q. *J. Nanosci. Nanotechnol.* **2007**, *7*, 2343.
(143) Gerion, D.; Pinaud, F.; Williams, S. C.; Parak, W. J.; Zanchet, D.; Weiss, S.; Alivisatos, A. P. *J. Phys. Chem. B* **2001**, *105*, 8861.
(144) Dong, B.; Cao, L.; Su, G.; Liu, W.; Qu, H.; Jiang, D. *J. Colloid Interface Sci.* **2009**, *339*, 78.
(145) Sun, J.; Zhuang, J.; Guan, S.; Yang, W. *J. Nanopart. Res.* **2008**, *10*, 653.
(146) Zhang, S.; Li, X. *Powder Technol.* **2004**, *141*, 75.
(147) Sun, Q.; Zhao, H.; Chen, X.; Wang, F.; Cai, W.; Jiang, Z. *Mater. Chem. Phys.* **2010**, *123*, 806.
(148) Wu, Y.; Wang, Y.; He, D.; Fu, M.; Chen, Z.; Li, Y. *J. Lumin.* **2010**, *130*, 1768.
(149) Güzel, R.; Ustündağ, Z.; Ekşi, H.; Keskin, S.; Taner, B.; Durgun, Z. G.; Turan, A. A. İ.; Solak, A. O. *J. Colloid Interface Sci.* **2010**, *351*, 35.
(150) Bao, F.; Li, J. F.; Ren, B.; Yao, J. L.; Gu, R. A.; Tian, Z. Q. *J. Phys. Chem. C* **2008**, *112*, 345.
(151) Kumar, S.; Zou, S. *Langmuir* **2007**, *23*, 7365.
(152) Li, J. F.; Yang, Z. L.; Ren, B.; Liu, G. K.; Fang, P. P.; Jiang, Y. X.; Wu, D. Y.; Tian, Z. Q. *Langmuir* **2006**, *22*, 10372.
(153) Zhang, P.; Chen, Y. X.; Cai, J.; Liang, S. Z.; Li, J. F.; Wang, A.; Ren, B.; Tian, Z. Q. *J. Phys. Chem. C* **2009**, *113*, 17518.
(154) Hu, J.-W.; Li, J.-F.; Ren, B.; Wu, D.-Y.; Sun, S.-G.; Tian, Z.-Q. *J. Phys. Chem. C* **2007**, *111*, 1105.
(155) Lee, Y. W.; Kim, M.; Kim, Z. H.; Han, S. W. *J. Am. Chem. Soc.* **2009**, *131*, 17036.
(156) Yang, Z.; Li, Y.; Li, Z.; Wu, D.; Kang, J.; Xu, H.; Sun, M. *J. Chem. Phys.* **2009**, *130*, No. 234705.
(157) Xiong, D.; Li, Z.; An, Y.; Ma, R.; Shi, L. *J. Colloid Interface Sci.* **2010**, *350*, 260.
(158) Chen, Y.; Zhu, B.; Yao, M.; Wang, S.; Zhang, S. *Catal. Commun.* **2010**, *11*, 1003.
(159) Yin, H.; Ma, Z.; Chi, M.; Dai, S. *Catal. Today* **2011**, *160*, 87.
(160) Lu, W.; Wang, B.; Zeng, J.; Wang, X.; Zhang, S.; Hou, J. G. *Langmuir* **2005**, *21*, 3684.
(161) Gu, C.; Xu, H.; Park, M.; Shannon, C. *Langmuir* **2009**, *25*, 410.
(162) Gao, Y.-H.; Zhang, N.-C.; Zhong, Y.-W.; Cai, H.-H.; Liu, Y.-L. *Appl. Surf. Sci.* **2010**, *256*, 6580.
(163) Xia, L.; Hu, X.; Kang, X.; Zhao, H.; Sun, M.; Cihen, X. *Colloids Surf. A* **2010**, *367*, 96.
(164) Lu, L.; Zhang, W.; Wang, D.; Xu, X.; Miao, J.; Jiang, Y. *Mater. Lett.* **2010**, *64*, 1732.
(165) Wang, G.; Wu, H.; Wexler, D.; Liu, H.; Savadogo, O. *J. Alloys Comp.* **2010**, *503*, L1.
(166) Nadagouda, M. N.; Varma, R. S. *Cryst. Growth Des.* **2007**, *7*, 2582.
(167) Lee, W. R.; Kim, M. G.; Choi, J. R.; Park, J.-I.; Ko, S. J.; Oh, S. J.; Cheon, J. *J. Am. Chem. Soc.* **2005**, *127*, 16090.
(168) Zhang, X. B.; Yan, J. M.; Han, S.; Shioyama, H.; Xu, Q. *J. Am. Chem. Soc.* **2009**, *131*, 2778.
(169) Sun, X.; Li, Y. *Langmuir* **2005**, *21*, 6019.
(170) Cao, H.; Huang, G.; Xuan, S.; Wu, Q.; Gu, F.; Li, C. *J. Alloys Comp.* **2008**, *448*, 272.
(171) Liang, Y.-C.; Hwang, K. C.; Lo, S.-C. *Small* **2008**, *4*, 405.
(172) Ma, C.; Luo, B.; Song, H.-H.; Zhi, L.-J. *New Carbon Mater.* **2010**, *25*, 199.
(173) Mu, Q.; Yang, L.; Davis, J. C.; Vankayala, R.; Hwang, K. C.; Zhao, J.; Yan, B. *Biomaterials* **2010**, *31*, 5083.

(174) Tan, H.; Li, S.; Fan, W. Y. *J. Phys. Chem. B* **2006**, *110*, 15812.
(175) Jose, D.; Jagirdar, B. R. *J. Solid State Chem.* **2010**, *183*, 2059.
(176) Kim, H.; Achermann, M.; Balet, L. P.; Hollingsworth, J. A.; Klimov, V. I. *J. Am. Chem. Soc.* **2005**, *127*, 544.
(177) Korshunov, A.; Heyrovský, M. *J. Electroanal. Chem.* **2009**, *629*, 23.
(178) Gu, H.; Zheng, R.; Zhang, X.; Xu, B. *J. Am. Chem. Soc.* **2004**, *126*, 5664.
(179) Zeng, H.; Li, J.; Wang, Z. L.; Liu, J. P.; Sun, S. *Nano Lett.* **2004**, *4*, 187.
(180) Khan, W. S.; Cao, C.; Nabi, G.; Yao, R.; Bhatti, S. H. *J. Alloys Comp.* **2010**, *506*, 666.
(181) Zhang, X.; Zhu, H.; Guo, Z.; Wei, Y.; Wang, F. *Int. J. Hydrogen Energy* **2010**, *35*, 8841.
(182) Wang, L.; Luo, J.; Fan, Q.; Suzuki, M.; Suzuki, I. S.; Engelhard, M. H.; Lin, Y.; Kim, N.; Wang, J. Q.; Zhong, C. J. *J. Phys. Chem. B* **2005**, *109*, 21593.
(183) Xuan, S.; Wang, Y. X. J.; Yu, J. C.; Leung, K. C. F. *Langmuir* **2009**, *25*, 11835.
(184) Mikhaylova, M.; Kim, D. K.; Bobrysheva, N.; Osmolowsky, M.; Semenov, V.; Tsakalakos, T.; Muhammed, M. *Langmuir* **2004**, *20*, 2472.
(185) He, Q.; Zhang, Z.; Xiong, J.; Xiong, Y.; Xiao, H. *Opt. Mater.* **2008**, *31*, 380.
(186) Zhang, S.; Niu, H.; Hu, Z.; Cai, Y.; Shi, Y. *J. Chromatogr. A* **2010**, *1227*, 4745.
(187) Yu, G.; Sun, B.; Pei, Y.; Xie, S.; Yan, S.; Qiao, M.; Fan, K.; Zhang, X.; Zong, B. *J. Am. Chem. Soc.* **2010**, *132*, 935.
(188) Xie, W.; Li, Y.; Sun, W.; Huang, J.; Xie, H.; Zhao, X. *J. Photochem. Photobiol. A* **2010**, *216*, 149.
(189) Li, F.; Yuan, Y.; Luo, J.; Qin, Q.; Wu, J.; Li, Z.; Huang, X. *Appl. Surf. Sci.* **2010**, *256*, 6076.
(190) Bahadur, N. M.; Furusawa, T.; Sato, M.; Kurayama, F.; Suzuki, N. *Mater. Res. Bull.* **2010**, *45*, 1383.
(191) Xu, S.; Sun, S.; Chen, G.; Song, X. *J. Cryst. Growth* **2009**, *311*, 2742.
(192) Zanella, R.; Sandoval, A.; Santiago, P.; Basiuk, V. A.; Saniger, J. M. *J. Phys. Chem. B* **2006**, *110*, 8559.
(193) Dembski, S.; Rupp, S.; Milde, M.; Gellermann, C.; Dyrba, M.; Schweizer, S.; Batentschuk, M.; Osvet, A.; Winnacker, A. *Opt. Mater.* **2010**, *10*, 3.
(194) Shen, H.; Yao, J.; Gu, R. *Trans. Nonferrous Met. Soc. China* **2009**, *19*, 652.
(195) Carnes, C. L.; Klabunde, K. J. *Chem. Mater.* **2002**, *14*, 1806.
(196) Pana, O.; Turcu, R.; Soran, M. L.; Leostean, C.; Gautron, E.; Payen, C.; Chauvet, O. *Synth. Met.* **2010**, *160*, 1692.
(197) Jiang, D.; Cao, L.; Liu, W.; Su, G.; Qu, H.; Sun, Y.; Dong, B. *Nanoscale Res. Lett.* **2009**, *4*, 78.
(198) Vaidya, S.; Patra, A.; Ganguli, A. K. *Colloids Surf. A* **2010**, *363*, 130.
(199) Kobayashi, Y.; Nozawa, T.; Nakagawa, T. *Quantum* **2010**, *55*, 79.
(200) Zhou, H. S.; Honma, I.; Komiyama, H.; Haus, J. W. *J. Phys. Chem.* **1993**, *97*, 895.
(201) Tian, Y.; Newton, T.; Kotov, N. A.; Guldi, D. M.; Fendler, J. H. *J. Phys. Chem.* **1996**, *100*, 8927.
(202) Korgel, B. A.; Monbouquette, H. G. *Langmuir* **2000**, *16*, 3588.
(203) Hota, G.; Idage, S. B.; Khilar, K. C. *Colloids Surf. A* **2007**, *293*, 5.
(204) Hota, G.; Jain, S.; Khilar, K. C. *Colloids Surf. A* **2004**, *232*, 119.
(205) Wang, Y.; Tang, Z.; Correa-Duarte, M. A.; Pastoriza-Santos, I.; Giersig, M.; Kotov, N. A.; Liz-Marzán, L. M. *J. Phys. Chem. B* **2004**, *108*, 15461.
(206) Yordanov, G. G.; Yoshimura, H.; Dushkin, C. D. *Colloid Polym. Sci.* **2008**, *286*, 1097.
(207) Peng, X.; Schlamp, M. C.; Kadavanich, A. V.; Alivisatos, A. P. *J. Am. Chem. Soc.* **1997**, *119*, 7019.
(208) Hines, M. A.; Guyot-Sionnest, P. *J. Phys. Chem.* **1996**, *100*, 468.
(209) Dabbousi, B. O.; Rodriguez-Viejo, J.; Mikulec, F. V.; Heine, J. R.; Mattoussi, H.; Ober, R.; Jensen, K. F.; Bawendi, M. G. *J. Phys. Chem. B* **1997**, *101*, 9463.
(210) Hao, E.; Sun, H.; Zhou, Z.; Liu, J.; Yang, B.; Shen, J. *Chem. Mater.* **1999**, *11*, 3096.
(211) Talapin, D. V.; Mekis, I.; Gotzinger, S.; Kornowski, A.; Benson, O.; Weller, H. *J. Phys. Chem. B* **2004**, *108*, 18826.
(212) Danek, M.; Jensen, K. F.; Murray, C. B.; Bawendi, M. G. *Chem. Mater.* **1996**, *8*, 173.
(213) Kim, S.; Fisher, B.; Eisler, H. J.; Bawendi, M. *J. Am. Chem. Soc.* **2003**, *125*, 11466.
(214) Liftshitz, E.; Eychmüller, A. *J. Cluster Sci.* **2007**, *18*, 5.
(215) Liu, Y. F.; Yu, J. S. *J. Colloid Interface Sci.* **2009**, *333*, 690.
(216) Wang, J.; Han, H. *J. Colloid Interface Sci.* **2010**, *351*, 83.
(217) Lambert, K.; Geyter, B. D.; Moreels, I.; Hens, Z. *Chem. Mater.* **2009**, *21*, 778.
(218) Han, M. Y.; Huang, W.; Chew, C. H.; Gan, L. M.; Zhang, X. J.; Ji, W. *J. Phys. Chem. B* **1998**, *102*, 1884.
(219) Cao, J.; Xue, B.; Li, H.; Deng, D.; Gu, Y. *J. Colloid Interface Sci.* **2010**, *348*, 369.
(220) Min, Y. L.; Wan, Y.; Yu, S. H. *Solid State Sci.* **2009**, *11*, 96.
(221) Lu, H.; Yi, G.; Zhao, S.; Chen, D.; Guo, L. H.; Cheng, J. *J. Mater. Chem.* **2004**, *14*, 1336.
(222) Kusakari, Y.; Ishizaki, S.; Kobayashi, M. *Mater. Res. Soc. Symp. Proc.* **2005**, *829*, 485.
(223) Kömpe, K.; Borchert, H.; Storz, J.; Lobo, A.; Adam, S.; Möller, T.; Haase, M. *Angew. Chem., Int. Ed.* **2003**, *42*, 5513.
(224) Stouwdam, J. W.; van Veggel, F. C. J. M. *Langmuir* **2004**, *20*, 11763.
(225) DiMaio, J. R.; Sabatier, C.; Kokuoz, B.; Ballato, J. *Proc. Natl. Acad. Sci. U.S.A.* **2008**, *105*, 1809.
(226) DiMaio, J.; Kokuoz, B.; James, T. L.; Harkey, T.; Monofsky, D.; Ballato, J. *Opt. Express* **2008**, *16*, 11769.
(227) Wang, Y.; Tu, L.; Zhao, J.; Sun, Y.; Kong, X.; Zhang, H. *J. Phys. Chem. C* **2009**, *113*, 7164.
(228) Ghosh, P.; Oliva, J.; la Rosa, E. D.; Halder, K. K.; Solis, D.; Patra, A. *J. Phys. Chem. C* **2008**, *112*, 9650.
(229) Qian, H. S.; Zhang, Y. *Langmuir* **2008**, *24*, 12123.
(230) DiMaio, J. R.; Kokuoz, B.; James, T. L.; Ballato, J. *Adv. Mater.* **2007**, *19*, 3266.
(231) Lehmann, O.; Kömpe, K.; Haase, M. *J. Am. Chem. Soc.* **2004**, *126*, 14935.
(232) Cha, H. J.; Kim, Y. H.; Cha, H. G.; Kang, Y. S. *Surf. Rev. Lett.* **2007**, *14*, 693.
(233) Kanehara, M.; Watanabe, Y.; Teranishi, T. *J. Nanosci. Nanotechnol.* **2009**, *9*, 673.
(234) Ma, Z.; Dosev, D.; Nichkova, M.; Dumas, R. K.; Gee, S. J.; Hammock, B. D.; Liu, K.; Kennedy, I. M. *J. Magn. Magn. Mater.* **2009**, *321*, 1368.
(235) Ammar, M.; Mazaleyrat, F.; Bonnet, J. P.; Audebert, P.; Brosseau, A.; Wang, G.; Champion, Y. *Nanotechnology* **2007**No. 285606.
(236) He, R.; You, X.; Shao, J.; Gao, F.; Pan, B.; Cui, D. *Nanotechnology* **2007**, *18*, No. 315601.
(237) Fu, Y.; Shearwood, C. *Scr. Mater.* **2004**, *50*, 319.
(238) Chen, J. P.; Sorensen, C. M.; Klabunde, K. J.; Hadjipanayis, G. C. *Phys. Rev. B* **1995**, *51*, 11527.
(239) Easom, K. A.; Klabunde, K. J.; Sorensen, C. M.; Hadjipanayis, G. C. *Polyhedron* **1994**, *13*, 1197.
(240) Znang, S.; Li, X. *Powder Technol.* **2004**, *141*, 75.
(241) Sun, L.; Wang, J.; Wang, Z. *Nanoscale* **2010**, *2*, 269.
(242) Pham, T. A.; Kumar, N. A.; Jeong, Y. T. *Colloids Surf. A* **2010**, *370*, 95.
(243) Feng, L.; Wu, X.; Ren, L.; Xiang, Y.; He, W.; Zhang, K.; Zhou, W.; Xie, S. *Chem.—Eur. J.* **2008**, *14*, 9764.
(244) Zhang, N.; Gao, Y.; Zhang, H.; Feng, X.; Cai, H.; Liu, Y. *Colloid Surf. B* **2010**, *81*, 537.
(245) Loo, C.; Lin, A.; Hirsch, L.; Lee, M.; Barton, J.; Halas, N.; West, J.; Drezek, R. *Technol. Cancer Res. Treat.* **2004**, *3*, 33.

(246) Zeng, H.; Li, J.; Liu, J. P.; Wang, Z. L.; Sun, S. *Nature* **2002**, *420*, 395.
(247) Decker, S.; Klabunde, K. J. *J. Am. Chem. Soc.* **1996**, *118*, 12465.
(248) Streetman, B. G.; Banerjee, S. *Solid state electronic devices*; Prentice Hall: NJ, 2000; p 534.
(249) Shen, G.; Chen, D.; Chen, P. C.; Zhou, C. *ACS Nano* **2009**, *3*, 1115.
(250) MacChesney, J. B.; Bridenbaugh, P. M.; O'Connor, P. B. *Mater. Res. Bull.* **1970**, *5*, 783.
(251) Tan, S. T.; Chen, B. J.; Sun, X. W.; Fan, W. J.; Kwok, H. S.; Zhang, X. H.; Chua, S. J. *J. Appl. Phys.* **2005**, *98*, No. 013505.
(252) Madelung, O., Ed. *Semiconductors—Basic Data*, 2nd ed.; Springer-Verlag: Berlin, 1996.
(253) Pietryga, J. M.; Schaller, R. D.; Werder, D.; Stewart, M. H.; Klimov, V. I.; Hollingsworth, J. A. *J. Am. Chem. Soc.* **2004**, *126*, 11752.
(254) Murphy, J. E.; Beard, M. C.; Norman, A. G.; Ahrenkiel, S. P.; Johnson, J. C.; Yu, P.; Mićić, O. I.; Ellingson, R. J.; Nozik, A. J. *J. Am. Chem. Soc.* **2006**, *128*, 3241.
(255) Elliott, R. J. *Phys. Rev.* **1961**, *124*, 340.
(256) Taft, E. A.; Philipp, H. R.; Apker, L. *Phys. Rev.* **1958**, *110*, 876.
(257) Jin, Y.; Li, G.; Zhang, Y.; Zhang, L. *J. Phys.: Condens. Matter* **2001**, *13*, L913.
(258) Lin, H. Y.; Chen, Y. F.; Wu, J. G.; Wang, D. I.; Chen, C. C. *Appl. Phys. Lett.* **2006**, *88*, No. 161911.
(259) Sharma, A. K.; Gupta, B. D. *J. Opt. A.: Pure Appl. Opt.* **2007**, *9*, 180.
(260) Yang, Y.; Shi, J.; Chen, H.; Dai, S.; Liu, Y. *Chem. Phys. Lett.* **2003**, *370*, 1.
(261) Yang, Y.; Nogami, M.; Shi, J.; Chen, H.; Liu, Y.; Qian, S. *J. Appl. Phys.* **2005**, *98*, 1.
(262) Colvin, V. L.; Schlamp, M. C.; Alivisatos, A. P. *Nature* **1994**, *370*, 354.
(263) Klimov, V. I.; Mikhailovsky, A. A.; Xu, S.; Malko, A.; Hollingsworth, J. A.; Leatherdale, C. A.; Eisler, H.-J.; Bawendi, M. G. *Science* **2000**, *290*, 314.
(264) Sundar, V. C.; Eisler, H.-J.; Bawendi, M. G. *Adv. Mater.* **2002**, *14*, 739.
(265) Bruchez, M., Jr.; Moronne, M.; Gin, P.; Weiss, S.; Alivisatos, A. P. *Science* **1998**, *281*, 2013.
(266) O'Regan, B.; Gratzel, M. *Nature* **1991**, *353*, 737.
(267) Huynh, W. U.; Dittmer, J. J.; Alivisatos, A. P. *Science* **2002**, *295*, 2425.
(268) Micheletto, R.; Fukuda, H.; Ohtsu, M. *Langmuir* **1996**, *11*, 3333.
(269) Klein, D. L.; Roth, R.; Lim, A. K. L.; Alivisatos, A. P.; McEuen, P. L. *Nature* **1997**, *389*, 699.
(270) Weller, H. *Angew. Chem., Int. Ed.* **1998**, *37*, 1658.
(271) Spanhel, L.; Haase, M.; Weller, H.; Henglein, A. *J. Am. Chem. Soc.* **1987**, *109*, 5649.
(272) Schneider, J. J. *Adv. Mater.* **2001**, *3*, 529.
(273) Resch-Genger, U.; Grabolle, M.; Cavaliere-Jaricot, S.; Nitschke, R.; Nann, T. *Nat. Methods* **2008**, *5*, 763.
(274) Dorfs, D.; Franzl, T.; Osovsky, R.; Brumer, M.; Lifshitz, E.; Klar, T. A.; Eychmuller, A. *Small* **2008**, *4*, 1148.
(275) Xie, W.; Wang, D.; Wu, L.; Yao, A.; Huang, W.; Yu, M. *J. Chin. Ceram. Soc.* **2009**, *37*, 219.
(276) Ivanov, S. A.; Piryatinski, A.; Nanda, J.; Tretiak, S.; Zavadil, K. R.; Wallace, W. O.; Werder, D.; Klimov, V. I. *J. Am. Chem. Soc.* **2007**, *129*, 11708.
(277) Chen, X.; Lou, Y.; Samia, A. C.; Burda, C. *Nano Lett.* **2003**, *3*, 799.
(278) Park, J. J.; Lacerda, S. H. D. P.; Stanley, S. K.; Vogel, B. M.; Kim, S.; Douglas, J. F.; Rahgavan, D.; Karim, A. *Langmuir* **2009**, *25*, 443.
(279) Battaglia, D.; Blackman, B.; Peng, X. *J. Am. Chem. Soc.* **2005**, *127*, 10889.
(280) Bang, J.; Park, J.; Lee, J. H.; Won, N.; Nam, J.; Lim, J.; Chang, B. Y.; Lee, H. J.; Chon, B.; Shin, J.; Park, J. B.; Choi, J. H.; Cho, K.; Park, S. M.; Joo, T.; Kim, S. *Chem. Mater.* **2010**, *22*, 233.
(281) Oron, D.; Kazes, M.; Banin, U. *Phys. Rev. B* **2007**, *75*, No. 035330.
(282) Yu, K.; Zaman, B.; Romanova, S.; Wang, D.-shan; Ripmeester, J. A. *Small* **2005**, *1*, 332.
(283) Bang, J.; Chon, B.; Won, N.; Nam, J.; Joo, T.; Kim, S. *J. Phys. Chem. C* **2009**, *113*, 6320.
(284) Schöps, O.; Le Thomas, N.; Woggon, U.; Artemyev, M. V. *J. Phys. Chem. B* **2006**, *110*, 2074.
(285) Xie, R.; Zhong, X.; Basché, T. *Adv. Mater.* **2005**, *17*, 2741.
(286) Zhong, X.; Feng, Y.; Zhang, Y.; Gu, Z.; Zou, L. *Nanotechnology* **2007**, *18*, No. 385606.
(287) Pietryga, J. M.; Werder, D. J.; Williams, D. J.; Casson, J. L.; Schaller, R. D.; Klimov, V. I.; Hollingsworth, J. A. *J. Am. Chem. Soc.* **2008**, *130*, 4879.
(288) Ivanov, S. A.; Nanda, J.; Piryatinski, A.; Achermann, M.; Balet, L. P.; Bezel, I. V.; Anikeeva, P. O.; Tretiak, S.; Klimov, V. I. *J. Phys. Chem. B* **2004**, *108*, 10625.
(289) Balet, L. P.; Ivanov, S. A.; Piryatinski, A.; Achermann, M.; Klimov, V. I. *Nano Lett.* **2004**, *4*, 1485.
(290) Steckel, J. S.; Zimmer, J. P.; Coe-Sullivan, S.; Stott, N. E.; Bulović, V.; Bawendi, M. G. *Angew. Chem., Int. Ed.* **2004**, *43*, 2154.
(291) Eychmüller, A.; Mews, A.; Weller, H. *Chem. Phys. Lett.* **1993**, *208*, 59.
(292) Mews, A.; Kadavanich, A. V.; Banin, U.; Alivisatos, A. P. *Phys. Rev. B: Condens. Matter Mater. Phys.* **1996**, *53*, 13242.
(293) Mews, A.; Eychmuller, A. *Phys. Chem. Chem. Phys.* **1998**, *102*, 1343.
(294) Porteanu, H. E.; Lifshitz, E.; Pflughoefft, M.; Eychmuller, A.; Weller, H. *Phys. Status Solidi B* **2001**, *226*, 219.
(295) Dorfs, D.; Eychmuller, A. *Nano Lett.* **2001**, *1*, 663.
(296) Kamalov, V. F.; Little, R.; Logunov, S. L.; El-Sayed, M. A. *J. Phys. Chem.* **1996**, *100*, 6381.
(297) Blackman, B.; Battaglia, D.; Peng, X. *Chem. Mater.* **2008**, *20*, 4847.
(298) Kim, S. W.; Zimmer, J. P.; Ohnishi, S.; Tracy, J. B.; Frangioni, J. V.; Bawendi, M. G. *J. Am. Chem. Soc.* **2005**, *127*, 10526.
(299) Xie, R.; Kolb, U.; Li, J.; Basche, T.; Mews, A. *J. Am. Chem. Soc.* **2005**, *127*, 7480.
(300) Aharoni, A.; Mokari, T.; Popov, I.; Banin, U. *J. Am. Chem. Soc.* **2006**, *128*, 257.
(301) Kim, D. W.; Cho, K.; Kim, H.; Park, B.; Sung, M. Y.; Kim, S. *Solid State Commun.* **2006**, *140*, 215.
(302) Battaglia, D.; Li, J. J.; Wang, Y.; Peng, X. *Angew. Chem., Int. Ed.* **2003**, *42*, 5035.
(303) Lifshitz, E.; Porteanu, H.; Glozman, A.; Weller, H.; Pflughoefft, M.; Echymüller, A. *J. Phys. Chem. B* **1999**, *103*, 6870.
(304) Schooss, D.; Mews, A.; Eychmüller, A.; Weller, H. *Phys. Rev. B* **1994**, *49*, 17072.
(305) Little, R. B.; EI-Sayed, M. A.; Bryant, G. W.; Burke, S. *J. Chem. Phys.* **2001**, *114*, 1813.
(306) Li, J. J.; Wang, A.; Guo, W.; Keay, J. C.; Mishima, T. D.; Johnson, M. B.; Peng, X. *J. Am. Chem. Soc.* **2003**, *125*, 12567.
(307) Feng, Z.; Gu, Z.; Zhu, W.; Zhong, X. *J. Nanosci. Nanotechnol.* **2009**, *9*, 5880.
(308) Nizamoglu, S.; Mutlugun, E.; Ozel, T.; Demir, H. V.; Sapra, S.; Gaponik, N.; Eychmuller, A. *LEOS 2008 - 21st Annu. Meet. IEEE Lasers Electro-Opt. Soc.* **2008**, 757.
(309) Sapra, S.; Mayilo, S.; Klar, T. A.; Rogach, A. L.; Feldmann, J. *Adv. Mater.* **2007**, *19*, 569.
(310) Pan, D.; Wang, Q.; Pang, J.; Jiang, S.; Ji, X.; An, L. *Chem. Mater.* **2006**, *18*, 4253.
(311) Faure, A. C.; Barbillon, G.; Ou, M.; Ledoux, G.; Tillement, O.; Roux, S.; Fabregue, D.; Descamps, A.; Bijeon, J. L.; Marquette, C. A.; Billotey, C.; Jamois, C.; Benyatou, T.; Perriat, P. *Nanotechnology* **2008**, *19*, No. 485103.
(312) Xie, M.-Y.; Yu, L.; He, H.; Yu, X.-F. *J. Solid State Chem.* **2009**, *182*, 597.

(313) Yi, S. S.; Bae, J. S.; Moon, B. K.; Jeong, J. H.; Kim, J. H. *Opt. Mater.* **2006**, *28*, 610.
(314) You, J. P.; Choi, J. H.; Kim, S.; Li, X.; Williams, R. S. S.; Ragan, R. *Nano Lett.* **2006**, *6*, 1858.
(315) Ballato, J.; Riman, R. E.; Snitzer, E. *Opt. Lett.* **1997**, *22*, 691.
(316) Salavati-Niasari, M.; Davar, F.; Mazaheri, M. *Mater. Lett.* **2008**, *62*, 1890.
(317) Salavati-Niasari, M.; Davar, F.; Mir, N. *Polyhedron* **2008**, *27*, 3514.
(318) Bharali, D. J.; Klejbor, I.; Stachowiak, E. K.; Dutta, P.; Roy, I.; Kaur, N.; Bergey, E. J.; Prasad, P. N.; Stachowiak, M. K. *Proc. Natl. Acad. Sci. U.S.A.* **2005**, 11539.
(319) Kneuer, C.; Sameti, M.; Bakowsky, U.; Schiestel, T.; Schirra, H.; Schmidt, H.; Lehr, C. M. *Bioconjugate Chem.* **2000**, *11*, 926.
(320) Li, Z.; Zhu, S.; Gan, K.; Zhang, Q.; Zeng, Z.; Zhou, Y.; Liu, H.; Xiong, W.; Li, X.; Li, G. *J. Nanosci. Nanotechnol.* **2005**, *5*, 1199.
(321) Zhu, S. G.; Xiang, J. J.; Li, X. L.; Shen, S. R.; Lu, H. B.; Zhou, J.; Xiong, W.; Zhang, B. C.; Nie, X. M.; Zhou, M.; Tang, K.; Li, G. Y. *Biotechnol. Appl. Biochem.* **2004**, *39*, 179.
(322) Hofman-Caris, C. H. M. *New J. Chem.* **1994**, *18*, 1087.
(323) Cornell, R. M.; Schertmann, U. *Iron Oxides in the Laboratory: Preparation and Characterization*; VCH Publishers: Weinheim: Germany, 1991.
(324) Advincula, R. C. *J. Dispersion Sci. Technol.* **2003**, *24*, 343.
(325) Burke, N. A. D.; Stover, H. D. H.; Dawson, F. P. *Chem. Mater.* **2002**, *14*, 4752.
(326) Molday, R. S.; Mackenzie, D. *J. Immunol. Methods* **1982**, *52*, 353.
(327) Molday, R. S.; Molday, L. L. *FEBS Lett.* **1984**, *170*, 232.
(328) Qin, S.; Wang, L.; Zhang, X.; Su, G. *Appl. Surf. Sci.* **2010**, *257*, 731.
(329) Chen, F.; Gao, Q.; Hong, G.; Ni, J. *J. Magn. Magn. Mater.* **2008**, *320*, 1921.
(330) Omer-Mizrahi, M.; Margel, S. *J. Colloid Interface Sci.* **2009**, *329*, 228.
(331) Chen, S.; Li, Y.; Guo, C.; Wang, J.; Ma, J.; Liang, X.; Yang, L. R.; Liu, H. Z. *Langmuir* **2007**, *23*, 12669.
(332) Yuan, W.; Yuan, J.; Zhou, L.; Wu, S.; Hong, X. *Polymer* **2010**, *51*, 2540.
(333) Zhao, D.-L.; Teng, P.; Xu, Y.; Xia, Q.-S.; Tang, J.-T. *J. Alloys Comp.* **2010**, *502*, 392.
(334) Utech, S.; Scherer, C.; Krohne, K.; Carrella, L.; Rentschler, E.; Gasi, T.; Ksenofontov, V.; Felser, C.; Maskos, M. *J. Magn. Magn. Mater.* **2010**, *322*, 3519.
(335) Thünemann, A. F.; Schütt, D.; Kaufner, L.; Pison, U.; Möhwald, H. *Langmuir* **2006**, *22*, 2351.
(336) Galperin, A.; Margel, S. *J. Biomed. Mater. Res. B* **2007**, *83B*, 490.
(337) Nagao, D.; Yokoyama, M.; Yamauchi, N.; Matsumoto, H.; Kobayashi, Y.; Konno, M. *Langmuir* **2008**, *24*, 9804.
(338) Qin, R.; Li, F.; Jiang, W.; Chen, M. *Mater. Chem. Phys.* **2010**, *122*, 498.
(339) Gopidas, K. R.; Whitesell, J. K.; Fox, M. A. *J. Am. Chem. Soc.* **2003**, *125*, 14168.
(340) Gittins, D. I.; Caruso, F. *J. Phys. Chem. B* **2001**, *105*, 6846.
(341) Hall, S. R.; Davis, S. A.; Mann, S. *Langmuir* **2000**, *16*, 1454.
(342) Clark, H. A.; Campaglora, P. J.; Wuskell, J. P.; Lewis, A.; Loew, L. M. *J. Am. Chem. Soc.* **2000**, *122*, 10234.
(343) Lebedev, V. S.; Vitukhnovsky, A. G.; Yoshida, A.; Kometani, N.; Yonezawa, Y. *Colloids Surf. A* **2008**, *326*, 204.
(344) Wu, W.; Shen, J.; Banerjee, P.; Zhou, S. *Biomaterials* **2010**, *31*, 7555.
(345) Holzinger, D.; Kickelbick, G. *J. Mater. Chem.* **2004**, *14*, 2017.
(346) Palkovits, R.; Althues, H.; Rumplecker, A.; Tesche, B.; Dreier, A.; Holle, U.; Fink, G.; Cheng, C. H.; Shantz, D. F.; Kaskel, S. *Langmuir* **2005**, *21*, 6048.
(347) Sertchook, H.; Avnir, D. *Chem. Mater.* **2003**, *15*, 1690.
(348) Zhang, Y. P.; Lee, S. H.; Reddy, K. R.; Gopalan, A. I.; Lee, K. P. *J. Appl. Polym. Sci.* **2007**, *104*, 2743.
(349) Shin, K.; Kim, J.-J.; Suh, K.-D. *J. Colloid Interface Sci.* **2010**, *350*, 581.
(350) Haldorai, Y.; Lyoo, W. S.; Noh, S. K.; Shim, J.-J. *React. Funct. Polym.* **2010**, *70*, 393.
(351) Liu, Y.-L.; Wu, Y.-H.; Tsai, W.-B.; Tsai, C.-C.; Chen, W.-S.; Wu, C.-S. *Carbohydr. Polym.* **2010**, *84*, 770.
(352) Maliakal, A.; Katz, H.; Cotts, P. M.; Subramoney, S.; Mirau, P. *J. Am. Chem. Soc.* **2005**, *127*, 14655.
(353) Xie, X. L.; Li, R. K. Y.; Liu, Q. X.; Mai, Y. W. *Polymer* **2004**, *45*, 2793.
(354) Xu, P.; Wang, H.; Lv, R.; Du, Q.; Zhong, W.; Yang, Y. *J. Polym. Sci., Part A: Polym. Chem.* **2006**, *44*, 3911.
(355) Du, Z.; Yin, X.; Zhang, M.; Hao, Q.; Wang, Y.; Wang, T. *Mater. Lett.* **2010**, *64*, 2076.
(356) Yu, J.; Guo, Z. X.; Gao, Y. F. *Macromol. Rapid Commun.* **2001**, *22*, 1261.
(357) Hayes, D.; Meisel, D.; Mićić, O. I. *Colloids Surf.* **1991**, *55*, 121.
(358) Jang, J.; Kim, S.; Lee, K. J. *Chem. Commun.* **2007**, 2689.
(359) Oluwafemi, O. S.; Revaprasadu, N.; Adeyemi, O. O. *Mater. Lett.* **2010**, *64*, 1513.
(360) Oluwafemi, O. S.; Revaprasadu, N.; Adeyemi, O. O. *Colloids Surf. B* **2010**, *79*, 126.
(361) Litvinov, D.; Kryder, M. H.; Khizroev, S. *J. Magn. Magn. Mater.* **2001**, *232*, 84.
(362) Ripika, P. *J. Magn. Magn. Mater.* **2000**, *215−216*, 735.
(363) Margel, S.; Lublin-Tennenbaum, T.; Gura, S.; Tsubery, M.; Akiva, U.; Shpaisman, N.; Galperin, A.; Perlstein, B.; Lapido, P.; Boguslavsky, Y.; Goldshtein, J.; Ziv, O. *Lab. Tech. Biochem. Mol. Biol.* **2007**, *32*, 119.
(364) Pouliquen, D.; Perroud, H.; Calza, F.; Jallet, P.; Jeune, J. J. L. *Magn. Res. Med.* **1992**, *24*, 75.
(365) Dobson, J. *Drug Dev. Res.* **2006**, *67*, 55.
(366) Kreuter, J. *Adv. Drug Delivery Res.* **1991**, *7*, 71.
(367) Liu, X.; Kaminski, M. D.; Chen, H.; Torno, M.; Taylor, L.; Rosengart, A. J. *J. Controlled Release* **2007**, *119*, 52.
(368) Cuyper, M.; De; Joniau, M. *Eur. Biophys. J.* **1988**, *15*, 311.
(369) Domingo, C.; Rodriguez-Clemente, R.; Blesa, M. A. *Colloids Surf. A* **1993**, *79*, 177.
(370) Jolivet, J. P.; Belleville, P.; Tronc, E.; Livage, J. *Clays Clay Miner.* **1992**, *40*, 531.
(371) Massart, R. *IEEE Trans. Magn.* **1981**, *17*, 1247.
(372) Berry, C. C.; Wells, S.; Charles, S.; Curtis, A. S. G. *Biomolecules* **2003**, *24*, 4551.
(373) Gamarra, L. F.; Brito, G. E. S.; Pontuschka, W. M.; Amaro, E.; Parma, A. H. C.; Goya, G. F. *J. Magn. Magn. Mater.* **2005**, *289*, 439.
(374) Ziv, O.; Avtalion, R. R.; Morgel, S. *J. Biomed. Mater. Res. A* **2008**, *85*, 1011.
(375) Laurent, S.; Nicotra, C.; Gossuin, Y.; Roch, A.; Ouakssim, A.; Vander Elst, L.; Cornant, M.; Soleil, P.; Muller, R. N. *Phys. Status Solidi C* **2004**, *1*, 3644.
(376) Lee, K. M.; Kim, S.-G.; Kim, W.-S.; Kim, S. S. *Korean J. Chem. Eng.* **2002**, *19*, 480.
(377) Kim, D. K.; Zhang, Y.; Kehr, J.; Klason, T.; Bjelke, B.; Muhammed, M. *J. Magn. Magn. Mater.* **2001**, *225*, 256.
(378) Kim, D. K.; Mikhaylova, M.; Wang, F. H.; Kehr, J.; Bjelke, B.; Zhang, Y.; Tsakalakos, T.; Muhammed, M. *Chem. Mater.* **2003**, *15*, 4343.
(379) Kim, D. K.; Mikhaylova, M.; Zhang, Y.; Muhammed, M. *Chem. Mater.* **2003**, *15*, 1617.
(380) Kim, D. K.; Zhang, Y.; Voit, W.; Rao, K. V.; Muhammed, M. *J. Magn. Magn. Mater.* **2001**, *225*, 30.
(381) Landmark, K. J.; DiMaggio, S.; Ward, J.; Kelly, C.; Vogt, S.; Hong, S.; Kotlyar, A.; Myc, A.; Thomas, T. P.; Penner-Hahn, J. E.; Baker, J. R., Jr.; Holl, M. M. B.; Orr, B. G. *ACS Nano* **2008**, *2*, 773.
(382) Mahmoudi, M.; Simchi, A.; Imani, M.; Milani, A. S.; Stroeve, P. *Nanotechnology* **2009**, *22*, No. 225104.
(383) Artemov, D. *J. Cell. Biochem.* **2003**, *90*, 518.
(384) Watson, K. J.; Zhu, J.; Nguyen, S. T.; Mirkin, C. A. *J. Am. Chem. Soc.* **1999**, *121*, 462.

(385) Kerker, M. *The Scattering of Light and Other Electromagnetic Radiation*; Academic Press: New York, 1969.
(386) Xian, Y.; Hu, Y.; Liu, F.; Wang, H.; Jin, L. *Biosens. Bioelectron.* **2006**, *21*, 1996.
(387) Dang, Z. M.; Peng, B.; Xie, D.; Yao, S. H.; Jiang, M. J.; Bai, J. *Appl. Phys. Lett.* **2008**, *92*, No. 112910.
(388) Lu, J.; Moon, K. S.; Wong, C. P. *J. Mater. Chem.* **2008**, *18*, 4821.
(389) Nair, A. S.; Pradeep, T.; MacLaren, I. *J. Mater. Chem.* **2004**, *14*, 857.
(390) Antonietti, M.; Berton, B.; Goltner, C.; Hentze, H. P. *Adv. Mater.* **1998**, *10*, 154.
(391) Amalvy, J. I.; Percy, M. J.; Armes, S. P. *Langmuir* **2001**, *17*, 4770.
(392) Lal, M.; Levy, L.; Kim, K. S.; He, G. S.; Wang, X.; Min, Y. H.; Pakatchi, S.; Prasad, P. N. *Chem. Mater.* **2000**, *12*, 2632.
(393) Xu, X.; Friedman, G.; Humfeld, K. D.; Majetich, S. A.; Asher, S. *Chem. Mater.* **2002**, *14*, 1249.
(394) Velev, O. D.; Furusawa, K.; Nagayama, K. *Langmuir* **1996**, *12*, 2374.
(395) Bokobza, L.; Garanaud, G.; Mark, J.; Jethmalani, J. M.; Seabolt, E. E.; Ford, W. T. *Chem. Mater.* **2002**, *14*, 162.
(396) Bréchet, Y. J.-Y.; Cavaillé, J.-Y.; Chabert, E.; Chazeau, L.; Dendievel, R.; Flandin, L.; Gauthier, C. *Adv. Eng. Mater.* **2001**, *3*, 571.
(397) Mousa, W. F.; Kobayashi, M.; Kitamura, Y.; Zeineldin, I. A.; Nakamura, T. *J. Biomed. Mater. Res.* **1999**, *47*, 336.
(398) Petrovicova, E.; Knight, R.; Schadler, L. S.; Twardowski, T. E. *J. Appl. Polym. Sci.* **2000**, *77*, 1684.
(399) Ohno, K.; Morinaga, T.; Koh, K.; Tsujii, Y.; Fukuda, T. *Macromolecules* **2005**, *38*, 2137.
(400) McNally, L.; O'Sullivan, D. J.; Jagger, D. C. *Biomed. Mater. Eng.* **2006**, *16*, 93.
(401) Olea, N.; Pulgar, R.; Perez, P.; Olea-Serrano, F.; Rivas, A.; Novillo-Fertrell, A.; Pedraza, V.; Soto, A. M.; Sonnenschein, C. *Environ. Health Perspect.* **1996**, *104*, 298.
(402) Debrujin, J. D.; Brink, I. V. D.; Mendes, S.; Dekker, R.; Bovell, Y. P.; Blitterswijk, C. A. V. *Adv. Dent. Res.* **1999**, *13*, 74.
(403) Guo, Z. S.; Zhao, L.; Pei, J.; Zhou, Z. L.; Gibson, G.; Brug, J.; Lam, S.; Mao, S. S. *Macromolecules* **2010**, *43*, 1860.
(404) Coe-Sullivan, S.; Woo, W.-K.; Steckel, J. S.; Bawendi, M.; Bulovi, V. *Org. Electron.* **2003**, *4*, 123.
(405) Smirnova, T. N.; Sakhno, O. V.; Yezhov, P. V.; Kokhtych, L. M.; Goldenberg, L. M.; Stumpe, J. *Nanotechnology* **2009**, *20*, No. 245707.
(406) Das, B. C.; Pal, A. J. *ACS Nano* **2008**, *2*, 1930.
(407) Guchhait, A.; Rath, A. K.; Pal, A. J. *Chem. Mater.* **2009**, *21*, 5292.
(408) Yan, W.; Feng, X.; Chen, X.; Li, X.; Zhu, J. J. *Bioelectrochemistry* **2008**, *72*, 21.
(409) Sangermano, M.; Marchi, S.; Valentini, L.; Bon, S. B.; Fabbri, P. *Macromol. Mater. Eng.* **2011**, *296*, 401.
(410) Khan, A.; Aldwayyan, A. S.; Alhoshan, M.; Alsalhi, M. *Polym. Int.* **2010**, *59*, 1690.
(411) Yang, Y.; Kong, X. Z.; Kan, C. Y.; Sun, C. G. *Polym. Adv. Technol.* **1999**, *10*, 54.
(412) Deshmukh, G. S.; Pathak, S. U.; Peshwe, D. R.; Ekhe, J. D. *Bull. Mater. Sci.* **2010**, *33*, 277.
(413) Caruso, R. A.; Susha, A.; Caruso, F. *Chem. Mater.* **2001**, *13*, 400.
(414) Kawahashi, N.; Matijevic, E. *J. Colloid Interface Sci.* **1991**, *143*, 103.
(415) Kawahashi, N.; Shiho, H. *J. Mater. Chem.* **2000**, *10*, 2294.
(416) Kawahashi, N.; Shiho, H. *Colloid Polym. Sci.* **2000**, *278*, 270.
(417) Kawahashi, N.; Shiho, H. *J. Colloid Interface Sci.* **2000**, *226*, 91.
(418) Mahdavian, A. R.; Ashjari, M.; Makoo, A. B. *Eur. Polym. J.* **2007**, *43*, 336.
(419) Moore, L. R.; Zborowski, M.; Nakamura, M.; McCloskey, K.; Gura, S.; Zuberi, M.; Margel, S.; Chalmers, J. J. *J. Biochem. Biophys. Methods* **2000**, *44*, 115.
(420) Tissot, I.; Reymond, J. P.; Lefebvre, F.; Bourgreat-Lami, E. *Chem. Mater.* **2002**, *14*, 1325.
(421) Yang, J.; Lind, J. U.; Trogler, W. C. *Chem. Mater.* **2008**, *20*, 2875.
(422) Yang, Z.; Yang, L.; Zhang, Z.; Wu, N.; Xie, J.; Cao, W. *Colloids Surf. A* **2008**, *312*, 113.
(423) Li, H.; Zhou, S. X.; You, B.; Wu, L. M. *Chin. J. Polym. Sci.* **2006**, *24*, 323.
(424) Sung, Y. M.; Lee, J. K. *Cryst. Growth Des.* **2004**, *4*, 737.
(425) Chen, Y. C.; Zhou, S. X.; Yang, H. H.; Wu, L. M. *J. Sol-Gel Sci. Technol.* **2006**, *37*, 39.
(426) Cheng, Z.; Zhang, L.; Zhu, X.; Kang, E. T.; Neoh, K. G. *J. Polym. Sci., Part A: Polym. Chem.* **2008**, *46*, 2119.
(427) Wang, D.; Song, C.; Lin, Y.; Hu, Z. *Mater. Lett.* **2006**, *60*, 77.
(428) Nadagouda, M. N.; Varma, R. S. *Smart Mater. Struct.* **2006**, *15*, 1260.
(429) Fan, W.; Gao, L. *J. Am. Chem. Soc.* **2006**, *297*, 157.
(430) Fowler, C. E.; Khushalani, D.; Mann, S. *J. Mater. Sci.* **2001**, *11*, 1968.
(431) Sun, Y.; Zhou, B. *Mater. Lett.* **2010**, *64*, 1347.
(432) Sun, Y.; Zhou, B.; Gao, P.; Mu, H.; Chu, L. *J. Alloys Compd.* **2010**, *490*, L48.
(433) Kim, I. J.; Kwon, O. S.; Park, J. B.; Joo, H. *Curr. Appl. Phys.* **2006**, *6*, 43.
(434) Song, C.; Gu, G.; Lin, Y.; Wang, H.; Guo, Y.; Fu, X.; Hu, Z. *Mater. Res. Bull.* **2003**, *38*, 917.
(435) Song, C.; Yu, W.; Zhao, B.; Zhang, H.; Tang, C.; Sun, K.; Wu, X.; Dong, L.; Chen, Y. *Catal. Commun.* **2009**, *10*, 650.
(436) Caruso, F.; Caruso, R. A.; Mohwald, H. *Science* **1998**, *282*, 1111.
(437) Chu, B.; Lin, M.; Neese, B.; Zhang, Q. *J. Appl. Phys.* **2009**, *105*, No. 014103.
(438) Dai, Z.; Meiser, F.; Mohwald, H. *J. Colloid Interface Sci.* **2005**, *288*, 298.
(439) Sgraja, M.; Bertling, J.; Kummel, R.; Jansens, P. J. *J. Mater. Sci.* **2006**, *41*, 5490.
(440) Yong, K. K.; Jae, K. H.; Ju, H. O.; Tae, H. K. *Polym. Prepr., Jpn.* **2006**, *55*, 5095.
(441) Song, C.; Yang, M.; Wang, D.; Hu, Z. *Mater. Res. Bull.* **2010**, *45*, 1021.
(442) Fowler, C. E.; Khushalani, D.; Mann, S. *Chem. Commun.* **2001**, 2028.
(443) Fuller, J. E.; Zugates, G. T.; Ferreira, L. S.; Ow, H. S.; Nguyen, N. N.; Wiesner, U. B.; Langer, R. S. *Biomaterials* **2008**, *29*, 1526.
(444) Park, J. H.; Oh, C.; Shin, S.-I.; Moon, S. K.; Oh, S. G. *J. Colloid Interface Sci.* **2003**, *266*, 107.
(445) Tsai, M. S.; Li, M. J. *J. Non-Cryst. Solids* **2006**, *352*, 2829.
(446) Zhang, K.; Zhang, X.; Chen, H.; Chen, X.; Zheng, L.; Zhang, J.; Yang, B. *Langmuir* **2004**, *20*, 11312.
(447) Zhang, F.; Wang, Y.; Chai, C. *Polym. Int.* **2004**, *53*, 1353.
(448) Zhou, S.; Wu, L.; Sun, J.; Shen, W. *Prog. Org. Coat.* **2002**, *45*, 33.
(449) Mahdavian, A. R.; Sarrafi, Y.; Shabankareh, M. *Polym. Bull.* **2009**, *63*, 329.
(450) Feng, L.; Wang, Y.; Wang, N.; Ma, Y. *Polym. Bull.* **2009**, *63*, 313.
(451) Zhou, S.-X.; Wu, L.-M.; Sun, J.; Shen, W.-D. *J. Appl. Polym. Sci.* **2003**, *88*, 189.
(452) Ow, H.; Larson, D. R.; Srivastava, M.; Baird, B. A.; Webb, W. W.; Wiesner, U. *Nano Lett.* **2005**, *5*, 113.
(453) Burns, A.; Ow, H.; Wiesner, U. *Chem. Soc. Rev.* **2006**, *35*, 1028.
(454) Chen, Z.; Gang, T.; Zhang, K.; Zhang, J.; Chen, X.; Sun, Z.; Yang, B. *Colloids Surf. A* **2006**, *272*, 151.
(455) Zhang, G.; Yu, Y.; Chen, X.; Han, Y.; Di, Y.; Yang, B.; Xiao, F.; Shen, J. *J. Colloid Interface Sci.* **2003**, *263*, 467.
(456) Liu, J.; Yang, Q.; Zhang, L.; Yang, H.; Gao, J.; Li, C. *Chem. Mater.* **2008**, *20*, 4268.
(457) Ge, C.; Zhang, D.; Wang, A.; Yin, H.; Ren, M.; Liu, Y.; Jiang, T.; Yu, L. *J. Phys. Chem. Solids* **2009**, *70*, 1432.

(458) Bi, C.; Pan, L.; Guo, Z.; Zhao, Y.; Huang, M.; Ju, X.; Xiao, J. Q. *Mater. Lett.* **2010**, *64*, 1681.
(459) Kawahashi, N.; Persson, C.; Matijevic, E. *J. Mater. Chem.* **1991**, *1*, 577.
(460) Jiang, Y.; Zhao, J.; Bala, H.; Xu, H.; Tao, N.; Ding, X.; Wang, Z. *Mater. Lett.* **2004**, *58*, 2401.
(461) Zhang, K.; Zheng, L.; Zhang, X.; Chen, X.; Yang, B. *Colloids Surf. A* **2006**, *277*, 145.
(462) Yao, L.-F.; Shi, Y.; Jin, S.-R.; Li, M.-J.; Zhang, L.-M. *Mater. Res. Bull.* **2010**, *45*, 1351.
(463) Ballauff, M.; Lu, Y. *Polymer* **2007**, *48*, 1815.
(464) Das, M.; Mardyani, S.; Chan, W. C. E.; Kumacheva, E. *Adv. Mater.* **2006**, *18*, 80.
(465) Nayak, S.; Lee, H.; Chmielewski, J.; Lyon, L. A. *J. Am. Chem. Soc.* **2004**, *126*, 10258.
(466) Soppimath, K. S.; Tan, D. C.-W.; Yang, Y.-Y. *Adv. Mater.* **2005**, *17*, 323.
(467) Hu, Z.; Chen, Y.; Wang, C.; Zheng, Y.; Li, Y. *Nature* **1998**, *393*, 149.
(468) Atansov, V. M. Ph.D. Thesis, Johannes Gutenberg-Universität, Mainz, Germany, 2004.
(469) Bouillot, P.; Vincent, B. *Colloid Polym. Sci.* **2000**, *278*, 74.
(470) Sahiner, N.; Godbey, W. T.; McPherson, G. L.; John, V. T. *Colloid Polym. Sci.* **2006**, *284*, 1121.
(471) Bergbreiter, D. E.; Liu, Y. S.; Osburn, P. L. *Polym. Prepr. (Am. Chem. Soc., Div. Polym. Chem.)* **1998**, *39*, 298.
(472) Biffis, A.; Minati, L. *J. Catal.* **2005**, *236*, 405.
(473) Biffis, A.; Orlandi, N.; Corain, B. *Adv. Mater.* **2003**, *15*, 1551.
(474) Lu, Y.; Mei, Y.; Ballauff, M.; Dreschler, M. *J. Phys. Chem. B* **2006**, *110*, 3930.
(475) Lu, Y.; Mei, Y.; Drechsler, M.; Ballauff, M. *Angew. Chem., Int. Ed.* **2006**, *45*, 813.
(476) Wu, G.; Zhao, J.; Shi, H.; Zhang, H. *Eur. Polym. J.* **2004**, *40*, 2451.
(477) Jang, J.; Oh, J. H. *Adv Funct. Mater.* **2005**, *15*, 494.
(478) Chunyan, L.; Zhaoguo, J.; Wengong, Z. *Front. Chem. China* **2007**, *2*, 21.
(479) Devon, M. J.; Gardon, J. L.; Roberts, G.; Rudin, A. *J. Appl. Polym. Sci.* **1990**, *39*, 2119.
(480) Eliseeva, V. I. *Prog. Org. Coat.* **1985**, *13*, 195.
(481) Kirsch, S.; Doerk, A.; Bartsch, E.; Sillescu, H.; Landfester, K.; Spiess, H. W.; Maechtle, W. *Macromolecules* **1999**, *32*, 4508.
(482) Chan, J. M.; Zhang, L.; Yuet, K. P.; Liao, G.; Rhee, J. W.; Langer, R.; Farokhzad, O. C. *Biomaterials* **2009**, *30*, 1627.
(483) Ni, K. F.; Shan, G. R.; Weng, Z. X.; Sheibat-Othman, N.; Fevotte, G.; Lefebvre, F.; Bourgeat-Lami, E. *Macromolecules* **2005**, *38*, 7321.
(484) Ni, K. F.; Sheibat-Othman, N.; Shan, G. R.; Fevotte, G.; Bourgeat-Lami, E. *Macromolecules* **2005**, *38*, 9100.
(485) Garito, F. A.; Hsiao, Y. L.; Gao, R. U.S. Patent, S20030174994 A1, 2003.
(486) Thomas, M.; Klibanov, A. M. *Proc. Natl. Acad. Sci. U.S.A.* **2003**, *100*, 9138.
(487) Wooley, K. L. *J. Polym. Sci., Part A: Polym. Chem.* **2000**, *38*, 1397.
(488) Huang, H.; Kowalewski, T.; Remsen, E. E.; Gertzmann, R.; Wooley, K. L. *J. Am. Chem. Soc.* **1997**, *119*, 11653.
(489) Tao, J.; Liu, G.; Ding, J.; Yang, M. *Macromolecules* **1997**, *30*, 4084.
(490) Thurmond, K. B.; Kowalewski, T.; Wooley, K. L. *J. Am. Chem. Soc.* **1996**, *118*, 7239.
(491) Zhang, Z.; Liu, G.; Bell, S.; Tn, C. *Macromolecules* **2000**, *33*, 7877.
(492) Bütün, V.; Billingham, N. C.; Armes, S. P. *J. Am. Chem. Soc.* **1998**, *120*, 12135.
(493) Bütün, V.; Lowe, A. B.; Billingham, N. C.; Armes, S. P. *J. Am. Chem. Soc.* **1999**, *121*, 4288.
(494) Lu, Y.; Wittemann, A.; Ballauff, M.; Drechsler, M. *Macromol. Rapid Commun.* **2006**, *27*, 1137.
(495) Atanasov, V.; Sinigersky, V.; Klapper, M.; Müllen, K. *Macromolecules* **2005**, *38*, 1672.
(496) Nah, J. W.; Jeong, Y. I.; Cho, C. S. *J. Polym. Sci., Polym. Phys.* **1998**, *36*, 415.
(497) Chen, S.-B.; Zhong, H.; Zhang, L. L.; Wang, Y.-F.; Cheng, Z.-P.; Zhu, Y.-L.; Yao, C. *Carbohydr. Polym.* **2010**, *82*, 747.
(498) Rodríguez-González, B.; Burrows, A.; Watanabe, M.; Kiely, C. J.; Liz-Marzán, L. M. *J. Mater. Chem.* **2005**, *15*, 1755.
(499) Zhu, Z. H.; Sha, M. J.; Lei, M. K. *Thin Solid Films* **2008**, *516*, 5075.
(500) Zhou, J.; Meng, L.; Lu, Q.; Fu, J.; Huang, X. *Chem. Commun.* **2009**, 6370.
(501) Cheng, D.; Zhou, X.; Xia, H.; Chan, H. S. O. *Chem. Mater.* **2005**, *17*, 3578.
(502) Liu, W. J.; Zhang, Z. C.; He, W. D.; Zheng, C.; Ge, X. W.; Li, J.; Liu, H. R.; Jiang, H. *J. Solid State Chem.* **2006**, *179*, 1253.
(503) Lee, K. T.; Jung, Y. S.; Oh, S. M. *J. Am. Chem. Soc.* **2003**, *125*, 5652.
(504) Kim, M.; Sohn, K.; Na, H. B.; Hyeon, T. *Nano Lett.* **2002**, *2*, 1383.
(505) Min, Y. L.; Wan, Y.; Liu, R.; Yu, S. H. *Mater. Chem. Phys.* **2008**, *111*, 364.
(506) Kamata, K.; Lu, Y.; Xia, Y. *J. Am. Chem. Soc.* **2003**, *125*, 2384.
(507) Ji, H.-F.; Wang, X.-X.; Zhang, X.; Yang, X.-L. *Chin. J. Polym. Sci.* **2010**, *28*, 807.
(508) Lou, X. W.; Yuan, C.; Archer, L. A. *Adv. Mater.* **2007**, *19*, 3328.
(509) Liu, B.; Yang, X.; Ji, H. *Polym. Int.* **2010**, *59*, 961.
(510) Zhang, H.; Yang, X. *Polym. Chem.* **2010**, *1*, 670.
(511) Ji, H.; Wang, S.; Yang, X. *Polymer* **2009**, *500*, 133.
(512) Zhang, H.; Zhang, X.; Yang, X. *J. Colloid Interface Sci.* **2010**, *348*, 431.
(513) Liu, W. *J. Appl. Polym. Sci.* **2008**, *109*, 3204.
(514) Lou, X. W.; Yuan, C.; Archer, L. A. *Small* **2007**, *3*, 261.
(515) Gou, L.; Murphy, C. J. *Nano Lett.* **2003**, *3*, 231.
(516) Huang, C.-C.; Yang, Z.; Chang, H.-T. *Langmuir* **2004**, *20*, 6089.
(517) Zhao, L. Y.; Eldridge, K. R.; Sukhija, K.; Jalili, H.; Heinig, N. F.; Leung, K. T. *Appl. Phys. Lett.* **2006**, *88*, No. 033111.
(518) Nelson, K.; Deng, Y. *Nanotechnology* **2006**, *17*, 3219.
(519) Nayak, B. B.; Vitta, S.; Nigam, A. K.; Bahadur, D. *Thin Solid Films* **2006**, *505*, 109.
(520) Fu, Y. Z.; Xiang, X. D.; Liao, J. H.; Wang, J. M. *J. Dispersion Sci. Technol.* **2008**, *29*, 1291.
(521) Chen, X.; Pan, H.; Liu, H.; Du, M. *Electrochim. Acta* **2010**, *56*, 636.
(522) Wang, X.; Hall, J. E.; Warren, S.; Krom, J.; Magistrelli, J. M.; Rackaitis, M.; Bohm, G. G. A. *Macromolecules* **2007**, *40*, 499.
(523) Aherne, D.; Gara, M.; Kelly, J. M.; Gun'ko, Y. K. *Adv. Funct. Mater.* **2010**, *20*, 1329.
(524) Xue, C.; Chen, X.; Hurst, S. J.; Mirkin, C. A. *Adv. Mater.* **2007**, *19*, 4071.
(525) Kuo, C.-H.; Hua, T. E.; Huang, M. H. *J. Am. Chem. Soc.* **2009**, *131*, 17871.
(526) Yang, J.; Lee, J. Y.; Too, H.-P. *J. Phys. Chem. B* **2005**, *109*, 19208.
(527) Sau, T. K.; Rogach, A. L.; Jäckel, F.; Klar, T. A.; Feldmann, J. *Adv. Mater.* **2010**, *22*, 1805and references therein.
(528) Tréguer-Delapierre, M.; Majimel, J.; Mornet, S.; Duguet, E.; Ravaine, S. *Gold Bull.* **2008**, *41*, 195and references therein.
(529) Narayanan, R.; El-Sayed, M. A. *Nano Lett.* **2004**, *4*, 1343.
(530) Noguez, C. *J. Phys. Chem. C* **2007**, *111*, 3806.
(531) Oyama, H. T.; Sprycha, R.; Xie, Y.; Partch, R. E.; Matijevic, E. *J. Colloid Interface Sci.* **1993**, *160*, 298.
(532) Kobayashi, Y.; Horie, M.; Konno, M.; Rodríguez-Gonzá Lez, B.; Liz-Marzán, L. M. *J. Phys. Chem. B* **2003**, *107*, 7420.
(533) Salgueiriño-Maceira, V.; Correa-Duarte, M. A. *J. Mater. Chem.* **2006**, *16*, 3593.
(534) Wang, X.; Yang, T.; Jiao, K. *Biosens. Bioelectron.* **2009**, *25*, 668.

(535) Imhof, A. *Langmuir* **2001**, *17*, 3579.
(536) Ocana, M.; Hsu, W, P.; Matijevic, E. *Langmuir* **1991**, *7*, 2911.
(537) Okaniwa, M. *J. Appl. Polym. Sci.* **1998**, *68*, 185.
(538) Shenoy, D. B.; Antipov, A. A.; Sukhorukov, G. B.; Mhwald, H. *Biomacromolecules* **2003**, *4*, 265.
(539) Srivastava, S.; Kotov, N. A. *Acc. Chem. Res.* **2008**, *41*, 1831.
(540) Wu, T. M.; Chu, M. S. *J. Appl. Polym. Sci.* **2005**, *98*, 2058.
(541) Marinakos, S. M.; Novak, J. P.; Brousseau, L. C., III; House, A. B.; Edeki, E. M.; Feldhaus, J. C.; Feldheim, D. L. *J. Am. Chem. Soc.* **1999**, *121*, 8518.
(542) Song, C.; Wang, D.; Gu, G.; Lin, Y.; Yang, J.; Chen, L.; Fu, X.; Hu, Z. *J. Colloid Interface Sci.* **2004**, *272*, 340.
(543) Salgueiriño-Maceira, V.; Correa-Duarte, M. A.; Farle, M.; López-Quintela, M. A.; Sieradzki, K.; Diaz, R. *Langmuir* **2006**, *22*, 1455.
(544) Carpenter, E. E.; Sangregorio, C.; O'Connor, C. J. *IEEE Trans. Magn.* **1999**, *35*, 3496.
(545) Li, X.; Zhang, W. *Langmuir* **2006**, *22*, 4638.
(546) Bala, T.; Swami, A.; Prasad, B. L. V.; Sastry, M. *J. Colloid Interface Sci.* **2005**, *283*, 422.
(547) Chen, D. H.; Wang, S. R. *Mater. Chem. Phys.* **2006**, *100*, 468.
(548) Chen, D.; Li, J.; Shi, C.; Du, X.; Zhao, N.; Sheng, J.; Liu, S. *Chem. Mater.* **2007**, *19*, 3399.
(549) Chen, Y.; Yang, F.; Dai, Y.; Wang, W.; Chen, S. *J. Phys. Chem. C* **2008**, *112*, 1645.
(550) Lee, C. C.; Chen, D. H. *Nanotechnology* **2006**, *17*, 3094.
(551) Schlesinger, H. I.; Brown, H. C.; Abraham, B.; Bond, A. C.; Davidson, N.; Finholt, A. E.; Gilbreath, J. R.; Hoekstra, H.; Horvitz, L.; Hyde, E. K.; Katz, J. J.; Knight, J.; Lad, R. A.; Mayfield, D. L.; Rapp, L.; Ritter, D. M.; Schwartz, A. M.; Sheft, I.; Tuck, L. D.; Walker, A. O. *J. Am. Chem. Soc.* **1953**, *75*, 186.
(552) *CRC Handbook of Chemistry and Physics*; Lide, D. R., Ed.l CRC Press: Boca Raton, FL, 2005.
(553) Chen, J. P.; Lim, L. *Chemosphere* **2002**, *49*, 363.
(554) Abdel-Aal, E. A.; Malekzadeh, S. M.; Rashad, M. M.; El-Midany, A. A.; El-Shall, H. *Powder Technol.* **2007**, *171*, 63.
(555) Huang, G. Y.; Xu, S. M.; Xu, G.; Li, L. Y.; Zhang, L. F. *Trans. Nonferrous Met. Soc. China* **2009**, *19*, 389.
(556) Park, J. W.; Chae, E. H.; Kim, S. H.; Lee, J. H.; Kim, J. W.; Yoon, S. M.; Choi, J. Y. *Mater. Chem. Phys.* **2006**, *97*, 371.
(557) Nersisyan, H. H.; Lee, J. H.; Son, H. T.; Won, C. W.; Maeng, D. Y. *Mater. Res. Bull.* **2003**, *38*, 949.
(558) Kobayashi, Y.; Ishida, S.; Ihara, K.; Yasuda, Y. T. M.; Yamada, S. *Colloid Polym. Sci.* **2009**, *287*, 877.
(559) Yadav, O. P.; Palmqvist, A.; Cruise, N.; Holmberg, K. *Colloids Surf. A* **2003**, *221*, 131.
(560) Wu, M. L.; Chen, D. H.; Huang, T. C. *J. Colloid Interface Sci.* **2001**, *243*, 102.
(561) Zhang, X.; Chan, K. Y. *Chem. Mater.* **2003**, *15*, 451.
(562) Chen, D.; Liu, S.; Li, J.; Zhao, N.; Shi, C.; Du, X.; Sheng, J. *J. Alloys Comp.* **2009**, *475*, 494.
(563) Park, J.-I.; Cheon, J. *J. Am. Chem. Soc.* **2001**, *123*, 5743.
(564) Park, J.-I.; Kim, M. G.; Jun, Y. W.; Lee, J. S.; Lee, W. R.; Cheon, J. *J. Am. Chem. Soc.* **2004**, *126*, 9072.
(565) Ji, Y.; Yang, S.; Guo, S.; Song, X.; Ding, B.; Yang, Z. *Colloids Surf. A* **2010**, *372*, 204.
(566) Dinega, D. P.; Bawendi, M. G. *Angew. Chem., Int. Ed.* **1999**, *38*, 1788.
(567) Osuna, J.; de Caro, D.; Amiens, C.; Chaudret, B.; Snoeck, E.; Respand, M.; Broto, J. M.; Fert, A. *J. Phys. Chem.* **1996**, *100*, 14571.
(568) Salavati-Niasari, M.; Davar, F.; Mazaheri, M.; Shaterian, M. *J. Magn. Magn. Mater.* **2008**, *320*, 575.
(569) Salavati-Niasari, M.; Davar, F. *Mater. Lett.* **2009**, *63*, 441.
(570) Dong, S.; Hou, P.; Yang, H.; Zou, G. *Intermetallics* **2002**, *10*, 217.
(571) Gromov, A. A.; Forter-Barth, U.; Teipel, U. *Powder Technol.* **2006**, *164*, 111.
(572) Wang, Q.; Yang, H.; Shi, J.; Zou, G. *Mater. Sci. Eng. A.* **2001**, *307*, 190.
(573) Fu, W.; Yang, H.; Bala, H.; Liu, S.; Li, M.; Zou, G. *Mater. Lett.* **2006**, *60*, 1728.
(574) *Synthesis, Properties, and Application of Oxide Nanomaterials*; Rodríguez, J. A., Fernandez-Garcia, M., Eds.; Wiley-Interscience: Hoboken, NJ, 2007; pp 79−134.
(575) Stober, W.; Fink, A.; Bohn, E. *J. Colloid Interface Sci.* **1968**, *26*, 62.
(576) Brinker, C. J.; Scherer, G. W. *Sol-gel Science: The Physics and Chemistry of Sol-Gel Processing*; Academic Press Ltd: London, 1990.
(577) Hench, L. L.; West, J. K. *Chem. Rev.* **1990**, *90*, 33.
(578) Klein, L. C., Ed. *Sol-Gel Optics: Processing and Applications*; Kluwer Academic Publishers Group: Boston, MA, 1994.
(579) Chen, Z.; Gao, L. *Cryst. Growth Des.* **2008**, *8*, 460.
(580) Koper, O. B.; Lagadic, I.; Volodin, A.; Klabunde, K. J. *Chem. Mater.* **1997**, *9*, 2468.
(581) Pena, J.; Vallet-Regf, M.; San Roman, J. *J. Biomed. Mater. Res.* **1997**, *35*, 129.
(582) Wang, J.; Shi, T. J.; Jiang, X. C. *Nanoscale Res. Lett.* **2009**, *4*, 240.
(583) Cihlar, J. *Colloids Surf. A* **1992**, *70*, 239–251.
(584) Di Renzo, F.; Testa, F.; Chen, J. D.; Cambon, H.; Galarneau, A.; Plee, D.; Fajula, F. *Microporous Mesoporous Mater.* **1999**, *28*, 437.
(585) Niederberger, M. *Acc. Chem. Res.* **2007**, *40*, 793and references therein.
(586) Avci, N.; Smet, P. F.; Poelman, H.; de Velde, N. V.; Buysser, K. D.; Driessche, I. V.; Poelman, D. *J. Sol-Gel Sci. Technol.* **2009**, *52*, 424.
(587) Sigoli, F. A.; Messaddeq, Y.; Ribeiro, S. J. L. *J. Sol-Gel Sci. Technol.* **2008**, *45*, 179.
(588) Xiao, H.; Ai, Z.; Zhang, L. *J. Phys. Chem. C* **2009**, *113*, 16625.
(589) Yang, T.; Wang, H.; Lei, M. K. *Mater. Chem. Phys.* **2006**, *95*, 211.
(590) Dong, B.; Li, C. R.; Wang, X. J. *J. Sol-Gel Sci. Technol.* **2007**, *44*, 161.
(591) Tiller, W. A. *The Science of Crystallization*; Cambridge University Press: Cambridge, 1991; p 338.
(592) Rao, C. N. R.; Muller, A.; Cheetham, A. K. In Rao, C. N. R. Muller, A.; Cheetham, A. K., Eds.; *Nanomaterials chemistry: Recent developments and new directions*; Wiley-VCH Verlag GmbH & Co.: Berlin, 2007.
(593) Salavati-Niasari, M.; Davar, F.; Fereshteh, Z. *Chem. Eng. J.* **2009**, *146*, 498.
(594) Salavati-Niasari, M.; Dadkhah, M.; Davar, F. *Inorg. Chim. Acta* **2009**, *362*, 3969.
(595) Salavati-Niasari, M.; Dadkhah, M.; Davar, F. *Polyhedron* **2009**, *28*, 3005.
(596) Salavati-Niasari, M.; Mir, N.; Davar, F. *J. Phys. Chem. Solids.* **2009**, *70*, 847.
(597) Salavati-Niasari, M.; Fereshteh, Z.; Davar, F. *Polyhedron* **2009**, *28*, 1065.
(598) Nag, A.; Sapra, S.; Sengupta, S.; Prakash, A.; Ghangrekar, A.; Periasamy, N.; Sharma, D. D. *Bull. Mater. Sci.* **2008**, *31*, 561.
(599) Sun, H.; Mu, J. *J. Dispersion Sci. Technol.* **2005**, *26*, 719.
(600) Sankapal, B. R.; Mane, R. S.; Lohande, C. D. *Mater. Res. Bull.* **2000**, *35*, 2027.
(601) Sankapal, B. R.; Mane, R. S.; Lokhande, C. D. *Mater. Chem. Phys.* **2000**, *63*, 230.
(602) Sankapal, B. R.; Mane, R. S.; Lokhande, C. D. *J. Mater. Sci. Lett.* **1999**, *18*, 1453.
(603) Patra, S.; Mondal, S.; Mitra, P. *J. Phys. Sci.* **2009**, *13*, 229.
(604) Lindroos, S.; Puiso, J.; Tamulevicius, S.; Leskela, M. *Solid State Phenom.* **2004**, *99−100*, 243.
(605) Ristov, M.; Sinadinovski, G. J.; Grozdanov, I. *Thin Solids Films* **1985**, *123*, 63.
(606) Nicolau, Y. F. *Appl. Surf. Sci.* **1985**, *22/23*, 1061.
(607) Tolstoy, V. P. *Russ. Chem. Rev.* **2006**, *75*, 161.
(608) Fonseca, T.; Relogio, P.; Martinho, J. M. G.; Farinha, J. P. S *Langmuir* **2007**, *23*, 5227.
(609) Ditsch, A.; Laibinis, P. E.; Wang, D. I. C.; Hatton, T. A. *Langmuir* **2005**, *21*, 6006.

(610) Kuckling, D.; Vo, C. D.; Adler, H.-J. P.; Völkel, A.; Cölfen, H. *Macromolecules* **2006**, *39*, 1585.
(611) Zhang, J.; Zhan, P.; Liu, H.; Wang, Z.; Ming, N. *Mater. Lett.* **2006**, *60*, 280.
(612) Kalinina, O.; Kumacheva, E. *Chem. Mater.* **2001**, *13*, 35.
(613) Qu, T.; Wang, A.; Yuan, J.; Gao, Q. *J. Colloid Interface Sci.* **2009**, *336*, 865.
(614) Yang, Y.; Nogami, M.; Shi, J.; Ruan, M. *J. Nanosci. Nanotechnol.* **2005**, *5*, 179.
(615) Decker, S.; Lagadic, I.; Klabunde, K. J.; Moscovici, J.; Michalowicz, A. *Chem. Mater.* **1998**, *10*, 674.
(616) Ethayaraja, M.; Bandyopadhyaya, R. *Ind. Eng. Chem. Res.* **2008**, *47*, 5982.
(617) Shukla, D.; Mehra, A. *Langmuir* **2006**, *22*, 9500.
(618) Tojo, C.; Barroso, F.; de Dios, M. *J. Colloid Interface Sci.* **2006**, *296*, 591.
(619) Tojo, C.; Blanco, M. C.; Lopez-Quintela, M. A. *Langmuir* **1998**, *14*, 6835.
(620) Tojo, C.; Blanco, M. C.; Rivadulla, F.; López-Quintela, M. A. *Langmuir* **1997**, *13*, 1970.
(621) Viswanadh, B.; Tikku, S.; Khilar, K. C. *Colloids Surf. A* **2007**, *298*, 149.
(622) Bagwe, R. P.; Khilar, K. C. *Langmuir* **1997**, *13*, 6432.
(623) Bagwe, R. P.; Khilar, K. C. *Langmuir* **2000**, *16*, 905.
(624) Hirai, T.; Sato, H.; Komasawa, I. *Ind. Eng. Chem. Res.* **1994**, *33*, 3262.
(625) Husein, M. M.; Rodil, E.; Vera, J. H. *J. Colloid Interface Sci.* **2004**, *273*, 426.
(626) Husein, M. M.; Rodil, E.; Vera, J. H. *Langmuir* **2006**, *22*, 2264.
(627) Husein, M. M.; Rodil, E.; Vera, J. H. *J. Nanopart. Res.* **2007**, *9*, 787.
(628) Husein, M. M.; Rodil, E.; Vera, J. H. *J. Colloid Interface Sci.* **2005**, *288*, 457.
(629) Kurihara, K.; Kizling, J.; Stenius, P.; Frendler, J. H. *J. Am. Chem. Soc.* **1983**, *105*, 2574.
(630) Lisiecki, I.; Pileni, M. P. *J. Phys. Chem.* **1995**, *99*, 5077.
(631) Petit, C.; Lixon, P.; Pileni, M. P. *J. Phys. Chem.* **1990**, *94*, 1598.
(632) Pileni, M. P. *J. Phys. Chem.* **1993**, *97*, 6961.
(633) Pileni, M. P. *Langmuir* **1997**, *13*, 3266.
(634) Sugih, A. K.; Shukla, D.; Heeres, H. J.; Mehra, A. *Nanotechnology* **2007**, *18*, No. 035607.
(635) Husein, M. M.; Rodil, E.; Vera, J. H. *J. Nanopart. Res.* **2006**, *9*, 787.
(636) Pileni, M. P.; Motte, L.; Petit, C. *Chem. Mater.* **1992**, *4*, 338.
(637) Husein, M. M.; Nassar, N. N. *Curr. Nanosci.* **2008**, *4*, 370.
(638) Barnickel, P.; Wokaun, A. *Mol. Phys.* **1990**, *69*, 1.
(639) Luther, W. Future Technologies Division of VDI Technologiezentrum. In *Industrial application of nanomaterials—Chances and risks: Technological analysis*; GmbH: Düsseldorf, Germany, 2004.
(640) Hu, Z.; Ramirez, D. J. E.; Cervera, B. E. H.; Oskam, G.; Searson, P. C. *J. Phys. Chem. B* **2005**, *109*, 11209.
(641) Oskam, G.; Nellore, A.; Penn, R. L.; Searson, P. C. *J. Phys. Chem. B* **2003**, *107*, 1734.
(642) Madani, A.; Nessark, B.; Brayner, R.; Elaissari, H.; Jouini, M.; Mangeney, C.; Chemini, M. M. *Polymer* **2010**, *51*, 2825.
(643) Furedi-Milhofer, H.; Babic-Ivancic, V.; Brecevic, L.; Filipovic-Vincekovic, N.; Kralj, D.; Komunjer, L.; Markovic, M.; Skrtic, D. *Colloids Surf.* **1990**, *48*, 219.
(644) Mafuné, F.; Kohno, J.-Y.; Takeda, Y.; Kondow, T.; Sawabe, H. *J. Phys. Chem. B* **2000**, *104*, 8333.
(645) Sugimoto, T.; Shiba, F. *Colloids Surf. A* **2000**, *164*, 205.
(646) Zhang, W.; Qiao, X.; Chen, J. *Mater. Chem. Phys.* **2008**, *109*, 411.
(647) Pal, T.; Sau, T. K.; Jana, N. R. *Langmuir* **1997**, *13*, 1481.
(648) Pawar, M. J.; Chaure, S. S. *Chalcogenide Lett.* **2009**, *6*, 689.
(649) Ghosh Chaudhuri, R.; Paria, S. *J. Colloid Interface Sci.* **2010**, *343*, 439.
(650) Lecommandoux, S.; Sandre, O.; Chécot, F.; Rodriguez-Hernandez, J.; Perzynski, R. *Adv. Mater.* **2005**, *17*, 712.
(651) Luque De Castro, M. D.; Priego-Capote, F. *Ultrason. Sonochem.* **2007**, *14*, 717.
(652) Hu, C. G.; Li, Y.; Liu, J. P.; Zhang, Y. Y.; Bao, G.; Buchine, B.; Wang, Z. L. *Chem. Phys. Lett.* **2006**, *428*, 343.
(653) Morel, A. L.; Nikitenko, S. I.; Gionnet, K.; Wattiaux, A.; Lai-Kee-Him, J.; Labrugere, C.; Chevalier, B.; Deleris, G.; Petibois, C.; Brisson, A.; Simonoff, M. *ACS Nano* **2008**, *2*, 847.
(654) Pol, V. G.; Resisfeld, R.; Gedanken, A. *Chem. Mater.* **2002**, *14*, 3920.
(655) Pol, V. G.; Srivastava, D. N.; Palchik, O.; Palchik, V.; Slifkin, M. A.; Weiss, A. M.; Gedanken, A. *Langmuir* **2002**, *18*, 3352.
(656) Wu, W.; He, Q.; Chen, H.; Tang, J.; Nie, L. *Nanotechnology* **2007**, *18*, No. 145609.
(657) Li, Q.; Li, H.; Pol, V. G.; Bruckental, I.; Koltypin, Y.; Calderon-Moreno, J.; Nowik, I.; Gedanken, A. *New J. Chem.* **2003**, *27*, 1194.
(658) Anandan, S.; Grieser, F.; Ashokkumar, M. *J. Phys. Chem. C* **2008**, *112*, 15102.
(659) Kan, C.; Cai, W.; Li, C.; Zhang, L.; Hofmeister, H. *J. Phys. D: Appl. Phys.* **2003**, *36*, 1609.
(660) Banerjee, S.; Roy, S.; Chen, J. W.; Chakravorty, D. *J. Magn. Magn. Mater.* **2000**, *219*, 45.
(661) Chipara, M.; Skomski, R.; Sellmyer, D. J. *Mater. Lett.* **2007**, *61*, 2412.
(662) Gorelikov, I.; Kumacheva, E. *Chem. Mater.* **2004**, *16*, 4122.
(663) Gorer, S.; Penner, R. M. *J. Phys. Chem. B* **1999**, *103*, 5750.
(664) Yu, J.; Liu, W.; Yu, H. *Cryst. Growth Des.* **2008**, *8*, 930.
(665) Qian, L.; Sha, Y.; Yang, X. *Thin Solid Films* **2006**, *515*, 1349.
(666) Lu, L.; Sun, G.; Zhang, H.; Wang, H.; Xi, S.; Hu, J.; Tian, Z.; Ray, C. *J. Mater. Chem.* **2004**, *14*, 1005.
(667) Chávez, J. L.; Wong, J. L.; Duran, R. S. *Langmuir* **2008**, *24*, 2064.
(668) Alayoglu, S.; Zavalij, P.; Eichhorn, B.; Wang, Q.; Frenkel, A. I.; Chupas, P. *ACS Nano* **2009**, *3*, 3127.
(669) Wang, L.; Chen, D. *Mater. Lett.* **2007**, *61*, 2113.
(670) Guchhait, A.; Rath, A. K.; Pal, A. J. *Chem. Mater.* **2009**, *21*, 5292.
(671) Cui, X.; Zhong, S.; Yan, J.; Wang, C.; Zhang, H.; Wang, H. *Colloids Surf. A* **2010**, *360*, 41.
(672) Karg, M.; Wellert, S.; Prevost, S.; Schweins, R.; Dewhurst, C.; Liz-marzán, L. M.; Hellweg, T. *Colloid Polym. Sci.* **2010**, 1.
(673) Kuo, K.; Chen, S.; Cheng, B.; Lin, C. *Thin Solid Films* **2008**, *517*, 1257.
(674) Goon, I. Y.; Lai, L. M. H.; Lim, M.; Munroe, P.; Gooding, J. J.; Amal, R. *Chem. Mater.* **2009**, *9*, 673.
(675) Grasset, F.; Labhsetwar, N.; Li, D.; Park, D. C.; Saito, N.; Haneda, H.; Cador, O.; Roisnel, T.; Mornet, S.; Duguet, E.; Portier, J.; Etourneau, J. *Langmuir* **2002**, *18*, 8209.
(676) Hellweg, T.; Dewhurst, C. D.; Eimer, W.; Kratz, K. *Langmuir* **2004**, *20*, 4330.
(677) Mang, J. T.; Hjelm, R. P.; Son, S. F.; Peterson, P. D.; Jorgensen, B. S. *J. Mater. Res.* **2007**, *22*, 1907.
(678) Riley, T.; Heald, C. R.; Stolnik, S.; Garnett, M. C.; Illum, L.; Davis, S. S.; King, S. M.; Heenan, R. K.; Purkiss, S. C.; Barlow, R. J.; Gellert, P. R.; Washington, C. *Langmuir* **2003**, *19*, 8428.
(679) Crowther, H. M.; Saunders, B. R.; Mears, S. J.; Cosgrove, T.; Vincent, B.; King, S. M.; Yu, G.-E. *Colloids Surf. A* **1999**, *152*, 327.
(680) Fernández-Barbero, A.; Fernández-Nieves, A.; Grillo, I.; López-Cabarcos, E. *Phys. Rev. E* **2002**, *66*, No. 051803.
(681) Kratz, K.; Hellweg, T.; Eimer, W. *Polymer* **2001**, *42*, 6631.
(682) Liu, R.; Li, Y.; Zhao, H.; Zhao, F.; Hu, Y. *Mater. Lett.* **2008**, *62*, 2593.
(683) Wang, K.; Tan, W.; He, X. *Conf. Proc.: Annu. Int. Conf. IEEE Eng. Med. Biol. Soc.* **2005**, *1*, 717.
(684) Bai, Y.; Teng, B.; Chen, S.; Chang, Y.; Li, Z. *Macromol. Rapid Commun.* **2006**, *27*, 2107.
(685) Balivada, S.; Rachkatla, R. S.; Wang, H.; Samarakoon, T. N.; Dani, R. K.; Pyle, M.; Kroh, F. O.; Walker, B.; Leaym, X.; Koper, O. B.;

Tamura, M.; Chikan, V.; Bossmann, S. H.; Troyer, D. L. *BMC Cancer* **2010**, *10*, 119.
(686) Jain, P. K.; Lee, K. S.; El-Sayed, I. H.; El-Sayed, M. A. *J. Phys. Chem. B* **2006**, *110*, 7238.
(687) McGill, S. L.; Cuylear, C. L.; Adolphi, N. L.; Osiński, M.; Smyth, H. D. C. *IEEE Trans. Nanobiosci.* **2009**, *8*, 33.
(688) Otsuka, H.; Nagasaki, Y.; Kataoka, K. *Adv. Drug Delivery Rev.* **2003**, *55*, 403.
(689) Vogt, C.; Toprak, M. S.; Muhammed, M.; Laurent, S.; Bridot, J. L.; Muller, R. N. *J. Nanopart. Res.* **2010**, *12*, 1137.
(690) Kircher, M. F.; Mahmood, U.; King, R. S.; Weissleder, R.; Josephson, L. *Cancer Res.* **2003**, *63*, 8122.
(691) Qiang, Y.; Antony, J.; Marino, M. G.; Pendyala, S. *IEEE Trans. Magn.* **2004**, *40*, 3538.
(692) Qiang, Y.; Antony, J.; Sharma, A.; Nutting, J.; Sikes, D.; Meyer, D. *J. Nanopart. Res.* **2005**, *8*, 489.
(693) Tan, W.; Wang, K.; He, X.; Zhao, X. J.; Drake, T.; Wang, L.; Bagwe, R. P. *Med. Res. Rev.* **2004**, *24*, 621.
(694) Nayak, S.; Lyon, L. A. *Angew. Chem., Int. Ed.* **2004**, *43*, 6706.
(695) Deng, S.; Pinagali, K. C.; Rockstraw, D. A. *IEEE Sens. J.* **2008**, *8*, 730.
(696) Katti, K. S. *Colloids Surf. B* **2004**, *39*, 133.
(697) Morley, K. S.; Webb, P. B.; Tokareva, N. V.; Krasnov, A. P.; Popov, V. K.; Zhang, J.; Roberts, C. J.; Howdle, S. M. *Eur. Polym. J.* **2007**, *43*, 307.
(698) Stanciu, L.; Won, Y.-H.; Ganesana, M.; Andreescu, S. *Sensors* **2009**, *9*, 2976.
(699) Vasir, J. K.; Reddy, Maram K.; Labhasetwar, V. D. *Curr. Nanosci.* **2005**, *1*, 47.
(700) Yakoyama, M. *J. Artif. Organs* **2005**, *8*, 77.
(701) Torchilin, V. P. *Handb. Exp. Pharmacol.* **2010**, *197*, 3.
(702) Chertok, B.; David, A. E.; Yang, V. C. *Biomaterials* **2010**, *31*, 6317.
(703) Crotts, G.; Park, T. G. *J. Controlled Release* **1995**, *35*, 91.
(704) Mahmud, A.; Xiong, X. B.; Aliabadi, H. M.; Lavasanifar, A. *J. Drug Targeting* **2007**, *15*, 553.
(705) Pathak, C.; Jaiswal, Y. K.; Vinayak, M. *Biosci. Rep.* **2008**, *28*, 73.
(706) Schellenberger, E. A.; Sosnovik, D.; Weissleder, R.; Josephson, L. *Bioconjugate Chem.* **2004**, *15*, 1062.
(707) Daneshvar, H.; Nelms, J.; Muhammad, O.; Jackson, H.; Tkach, J.; Davros, W.; Peterson, T.; Vogelbaum, M. A.; Bruchez, M. P.; Toms, S. A. *Nanomedicine* **2008**, *3*, 21.
(708) Law, W. C.; Yong, K. T.; Roy, H. D.; Ding, H.; Hu, R.; Zhao, W.; Prasad, P. N. *Small* **2009**, *5*, 1302.
(709) SalmanOgli, A.; Rostami, A. *J. Nanopart. Res.* **2010**, 1.
(710) Pinaud, F.; Michalet, X.; Bentolila, L. A.; Tsay, J. M.; Doose, S.; Li, J. J.; Iyer, G.; Weiss, S. *Biomaterials* **2006**, *27*, 1679.
(711) Wu, W.; Zhou, T.; Berliner, A.; Banerjee, P.; Zhou, S. *Chem. Mater.* **2010**, *22*, 1966.
(712) Yin, X. J.; Peng, K.; Hu, A. P.; Zhou, L. P.; Chen, J. H.; Du, Y. W. *J. Alloys Comp.* **2009**, *479*, 372.
(713) Campbell, J. L.; Arora, J.; Cowell, S. F.; Garg, A.; Eu, P.; Bhargava, S. K.; Bansal, V. *PLoS ONE* **2011**, *6*, No. e21857.
(714) Qiu, J. D.; Cui, S. G.; Deng, M. Q.; Liang, R. P. *J. Appl. Electrochem.* **2010**, *40*, 1651.
(715) Qiu, J. D.; Cui, S. G.; Liang, R. P. *Microchim. Acta.* **2010**, *171*, 333.
(716) Qiu, J. D.; Peng, H. P.; Liang, R. P.; Xia, X. H. *Biosens. Bioelectron.* **2010**, *25*, 1447.
(717) Ching-Lin, T. *Appl. Biomed. Eng. Commun.* **1994**, *6*, 110.
(718) Crowley, J.; Chalivendra, V. B. *Biomed. Mater. Eng.* **2008**, *18*, 149.
(719) Zhang, N.; Nichols, H. L.; Tylor, S.; Wen, X. *Mater. Sci. Eng., C* **2007**, *27*, 599.
(720) Carmona-Ribeiro, A. M. *Int. J. Nanomed.* **2010**, *5*, 249.
(721) Yao, L. H.; Li, Y. X.; Zhao, J.; Ji, W. J.; Au, C. T. *Catal. Today* **2010**, *158*, 401.
(722) Ferrando, R.; Jellinek, J.; Johnston, R. L. *Chem. Rev.* **2008**, *108*, 845.
(723) Wang, L.; Yamauchi, Y. *J. Am. Chem. Soc.* **2010**, *132*, 13636.
(724) Zhao, D.; Chen, X.; Liu, Y.; Wu, C.; Ma, R.; An, Y.; Shi, L. *J. Colloid Interface Sci.* **2009**, *331*, 104.
(725) Feng, L.; Gao, G.; Huang, P.; Wang, K.; Wang, X.; Luo, T.; Zhang, C. *Nano Biomed. Eng.* **2010**, *2*, 258.
(726) Fan, F.-R.; Liu, D.-Y.; Wu, Y.-F.; Duan, S.; Xie, Z.-X.; Jiang, Z.-Y.; Tian, Z.-Q. *J. Am. Chem. Soc.* **2008**, *130*, 6949.
(727) Habas, S. E.; Lee, H.; Radimilovic, V.; Somorjai, G. A.; Yang, P. *Nat. Mater.* **2007**, *6*, 629.
(728) Duan, J.; Feng, Y.; Yang, G.; Xu, W.; Li, X.; Liu, Y.; Zhao, J. *Ind. Eng. Chem. Res.* **2009**, *48*, 1468.
(729) Guchhait, A.; Pal, A. J. *J. Phys. Chem. C* **2010**, *114*, 19294.
(730) Phely-Bobin, T. S. University of Connecticut, 2001, Paper AAI3002674.
(731) White, M. A.; Maliakal, A.; Turro, N. J.; Koberstein, J. *Macromol. Rapid Commun.* **2008**, *29*, 1544.
(732) Guo, X. Y.; Wang, Y. N.; Gu, L. G.; He, Y. F.; Zhang, C. X.; Tang, Z. M.; Lu, Z. H. *Chem. J. Chin. Univ.* **2006**, *27*, 1725.
(733) Inagaki, M.; Kojin, F.; Tryba, B.; Toyoda, M. *Carbon* **2005**, *43*, 1652.
(734) Shanmugam, S.; Gabashvili, A.; Jacob, D. S.; Yu, J. C.; Gedanken, A. *Chem. Mater.* **2006**, *18*, 2275.
(735) Wang, Y.; Zhang, H. J.; Lu, L.; Stubbs, L. P.; Wong, C. C.; Lin, J. *ACS Nano* **2010**, *4*, 4753.
(736) Galakhov, V. R.; Shkvarin, A. S.; Semenova, A. S.; Uimin, M. A.; Mysik, A. A.; Shchegoleva, N. N.; Yermakov, A. Y.; Kurmaev, E. Z. *J. Phys. Chem. C* **2010**, *114*, 22413.
(737) Fitzgerald, J. J.; Landry, C. J. T.; Pochan, J. M. *Macromolecules* **1992**, *25*, 3715.
(738) Ogoshi, T.; Itoh, H.; Kim, K. M.; Chujo, Y. *Macromolecules* **2002**, *35*, 334.
(739) Chung, Y. S.; Lim, J. S.; Park, S. B.; Okuyama, K. *J. Chem. Eng. Jpn.* **2004**, *37*, 1099.
(740) Khanal, A.; Inoue, Y.; Yada, M.; Nakashima, K. *J. Am. Chem. Soc.* **2007**, *129*, 1534.
(741) Wan, Y.; Yu, S. H. *J. Phys. Chem. C* **2008**, *112*, 3641.
(742) van Bommel, K. J. C.; Jung, J. H.; Shinkai, S. *Adv. Mater.* **2001**, *13*, 1472.
(743) Le, Y.; Chen, J. F.; Wang, W. C. *Appl. Surf. Sci.* **2004**, *230*, 319.
(744) Liu, X.; Wu, H.; Ren, F.; Qiu, G.; Tang, M. *Mater. Chem. Phys.* **2008**, *109*, 5.
(745) Xu, X.; Asher, S. A. *J. Am. Chem. Soc.* **2004**, *126*, 7940.
(746) Chen, H. M.; Liu, R. S.; Lo, M. Y.; Chang, S. C.; Tsai, L. D.; Peng, Y. M.; Lee, J. F. *J. Phys. Chem. C* **2008**, *112*, 7522.
(747) Darbandi, M.; Thomann, R.; Nann, T. *Chem. Mater.* **2007**, *19*, 1700.
(748) Marinakos, S. M.; Shultz, D. A.; Feldheim, D. L. *Adv. Mater.* **1999**, *11*, 34.
(749) Peng, Z.; Wu, J.; Yang, H. *Chem. Mater.* **2010**, *22*, 1098.
(750) Park, K. H.; Im, S. H.; Park, O. O. *Nanotechnology* **2011**, *22*, No. 045602.
(751) Ghosh Chaudhuri, R.; Paria, S. *J. Colloid Interface Sci.* **2011**, in press; DOI: 10.1016/j.jcis.2011.11.064.
(752) Yao, T.; Lin, Q.; Zhang, K.; Zhao, D.; Lv, H.; Zhang, J.; Yang, B. *J. Colloid Interface Sci.* **2007**, *315*, 434.
(753) Weda, P.; Trzebicka, B.; Dworak, A.; Tsvetanov, C. B. *Polymer* **2008**, *49*, 1467.
(754) Wang, Z.; Chen, M.; Wu, L. *Chem. Mater.* **2008**, *20*, 3251.
(755) Yang, J.; Lee, J. Y.; Too, H. P.; Valiyaveettil, S. *J. Phys. Chem. B* **2006**, *110*, 125.